CIBA/TM SERIES NO.70/2026/10

केंखाजपाअसं
CIBA

HANDS ON TRAINING MANUAL ON

MOLECULAR DIAGNOSIS OF TRANSLUCENT POST LARVAE DISEASE (TPD) OF SHRIMP

4th – 8th May, 2026

National Referral Laboratory for Brackishwater Aquatic Animal Diseases
NABL Accredited Laboratory
Aquatic Animal Health and Environment Division
ICAR – Central Institute of Brackishwater Aquaculture
(ISO 9001:2015 certified)
75, Santhome High Road, MRC Nagar, Chennai 600 028, Tamil Nadu, India
www.ciba.res.in

CIBA/TM Series No.70/2026/10

Hands on Training Manual
on

Molecular Diagnosis of Translucent Post Larvae Disease (TPD) of Shrimp

4th – 8th May, 2026

National Referral Laboratory for Brackishwater Aquatic Animal Diseases
NABL Accredited Laboratory
Aquatic Animal Health and Environment Division
ICAR – Central Institute of Brackishwater Aquaculture
(ISO 9001:2015 certified)
75, Santhome High Road, MRC Nagar, Chennai 600 028, Tamil Nadu, India
www.ciba.res.in

CIBA/TM Series No.70/2026/10

Hands on training manual
on

Molecular Diagnosis of Translucent Post Larvae Disease (TPD) of Shrimp

Published by
Dr. Kuldeep Kumar Lal,
Director, ICAR – Central Institute of Brackishwater Aquaculture,
Chennai – 28.

Convener
Dr. Shashi Shekhar,
Principal Scientist and Head, Aquatic Animal Health and Environment Division (AAHED).

Course Director
Dr. Subhendhu Kumar Otta,
Principal Scientist, AAHED.

Course Co-ordinator
Dr. P. Ezhil Praveena, Principal Scientist, AAHED.
Dr. T. Bhuvaneswari, Senior Scientist, AAHED.

Resource Person
Dr. Sujeeth Kumar T, Dr. Ashok Kumar J, Dr. Sathish Kumar T, Ms. Mary Lini R and
Dr. Joseph Sahaya Rajan J.

Compiled and edited by
Dr. Subhendhu Kumar Otta, Dr. Ezhil Praveena P and Dr. Bhuvaneswari T.

Technical assistant
Mr. Gocula Velun R A, Mr. Sudama Swain and Mr. Karthirkaman V.

Cite as: Otta S.K., Praveena E.P. and Bhuvaneswari T. (2026) Hands on training manual on molecular diagnosis of translucent post larvae disease (TPD) of shrimp.
Training manual series No.70/2026/10 pp62.

1. Shrimp translucent post-larvae disease (TPD) – An emerging disease and a concern for shrimp industry

Disease is one of the major factors that hinders shrimp aquaculture sustainability and every year the industry faces huge loss due to existing and emerging disease outbreaks. All kinds of microorganisms have been found to be associated with shrimp disease and based on the virulence nature, the severity of the mortality is decided. Though virus are generally considered as highly virulent pathogens, during the recent times some of the specific bacterial strains carrying the virulent plasmids have reported to create havoc in the industry. One of such emerging diseases is translucent post-larvae disease (TPD). The same disease is also known in different names such as glass post-larval disease, bacterial vitrified syndrome, and highly lethal *Vibrio* disease (HLVD). Initially reported in Ecuador during 2015, this disease has further spread to China (2020) and Vietnam in 2023 (Zou et al., 2020; Vietnam Fisheries Magazine, 2023; Hong Tham, 2024). This disease started in large scale in Southern China during the early 2020 and caused large scale mortality. The effect was so high that it resulted closure of about 70-80% hatcheries and nurseries. It then spread rapidly to northern China causing similar scale problem.

1.1 Clinical signs

The disease is highly dangerous to post larvae and animals at nursery phage. Usually, PL5-PL7 larvae are most affected. The symptoms starts as early as 24 hours of infection and within 3 days, mortality can reach 80-90%. Juveniles when infected are reported to stop feeding and exhibit reduced vitality.

Hepatopancreas of infected larvae appears pale with empty stomach and mid-gut. TPD shrimps show pale and shrunken body. Affected larvae sink to the bottom due to reduced activity. The entire body colour from cephalothorax to tail looks completely transparent or semi-transparent. The disease is named on this basis.

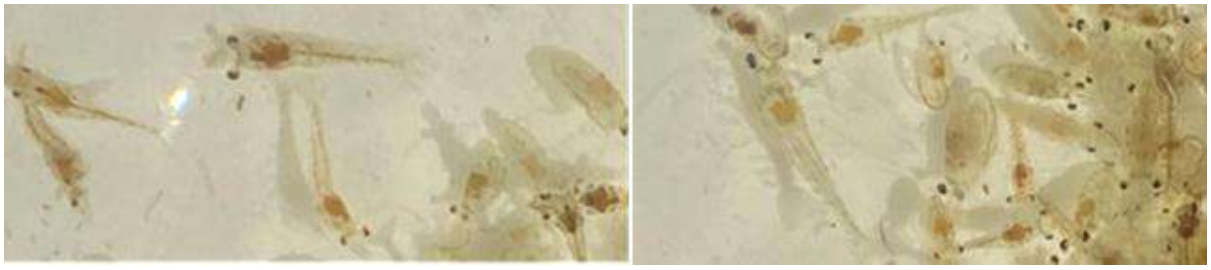

1.2 Causative agent

A highly virulent strain of *Vibrio parahaemolyticus* named as *Vibrio parahaemolyticus* causing TPD (VpTPD) was proved to be the causative agent. The toxin genes which are actually responsible for the virulence are located in 187,791 bp plasmid that the bacteria carry. Mainly 3 virulent proteins such as VhVp-1, VhVp-2 VhVp-3 are considered as virulent genes. These proteins have been found to be similar to Tc toxins, a class of insecticidal proteins produced by entomopathogenic bacterium *Photorhabdus luminescens.* Subsequently it was reported that even other vibrios such as *V. harveyi*, *V. campbelli* can also carry this plasmid and cause similar infection.

1.3 Host range

Initially it was found that P. vannamei is the shrimp which gets affected by TPD. Subsequently, through epidemiological study, it was found that even other shrimps like P. chinensis and P.japonicus can also get infected by this disease.

1.4 Diagnosis

This disease can be identified by various methods. The bacteria involved in this disease can be isolated and reinfected to healthy larvae for disease reproduction. Isolated bacteria can also be verified by molecular methods such as PCR. Histopatholgoically, it will be difficult to pinpoint for this disease as the findings are similar to EMS/AHPND. Molecular methods such as conventional PCR and real time PCR are available for the detection of this pathogen.

1.5 Disease management

Since TPD is caused by a bacteria which is highly virulent, even 1000 times more virulent than the AHPND bacteria, care should be taken first not to allow the spread. Infected tanks/ponds should be thoroughly disinfected and stocks should be destroyed. Disinfectants such as PHMB(Polyhexamethylene biguanide) has been found to be effective in controlling vibrios and therefore may help to control this disease. Some of the reports indicated Gallic acid (GA; 3,4,5-trihydroxybenzoic acid) to be effective in controlling TPD. Phage therapy can also be good strategy as it will be specific to kill the pathogens. The immunity of shrimps should be strengthened through the use of probiotics and immunostimulants. Brood stocks in hatcheries should be screened for the presence of this pathogen. Farmers should further test their larvae for TPD before stoking in the ponds. A strong biosecurity is essential both for hatcheries and farms.

1.6 Further reading

Jia T, Xu T, Xia J, Liu S, Li W, Xu RD, Kong J, Zhang QL (2023) Clinical protective effects of polyhexamethylene biguanide hydrochloride (PHMB) against Vibrio parahaemolyticus causing translucent post-larvae disease (VpTPD) in *Penaeus vannamei*. J Invertebr Pathol 201:108002.

Jia TC, Liu S, Yu XT, Xu TT, Xia JT, Zhao WX, Wang W, Kong J, Zhang QL (2024) Prevalence investigation of translucent post-larvae disease (TPD) in China. Aquaculture 583:740583.

Tham H (2024) Warning of new disease appearing on white leg shrimp. Vietnam Agriculture.

Vietnam Fisheries Magazine (n.d.) Zeigler Vietnam meets with customers on management of transparent post-larvae disease. Vietnam Fisheries Magazine.

Wang YG, Yu YX, Liu X (2021) Pathogens and histopathological characteristics of shrimp postlarvae bacterial vitrified syndrome (BVS) in *Litopenaeus vannamei*. J Fish China 45:1563–1573.

Yang F, Xu LM, Huang WZ, Li F (2022) Highly lethal *Vibrio parahaemolyticus* strains cause acute mortality in *Penaeus vannamei* post-larvae. Aquaculture 548:737605.

Yang F, You Y, Lai Q, Xu L, Li F (2023) *Vibrio parahaemolyticus* becomes highly virulent by producing Tc toxins. Aquaculture 739817.

Zhang Q, Liu S, Yang B, Feng D, Wan X, Zhang X, Xu T, Yu X, Wang W, Xie G (2025) Diagnostic method for shrimp translucent post-larva disease (TPD). Aquaculture Industry Standard of the People's Republic of China SC/T 7243-2025.

Zou Y, Xie G, Jia T, Xu T, Wang C, Wan X, Li Y, Luo K, Bian X, Wang X, Kong J, Zhang Q (2020) Determination of the infectious agent of translucent post-larva disease (TPD) in *Penaeus vannamei*. Pathogens 9:741.

2. Comprehensive diagnostic methods for translucent post-larval disease (TPD) in shrimp

Translucent Post-Larvae Disease (TPD), often called "Glass Post-Larvae Disease," is an emerging problem in *Penaeus vannamei* culture. First reported in China in March 2020, it has quickly become a major concern due to the heavy losses it causes, especially in early post-larval stages (PL4–PL7).

The disease is linked to a highly virulent strain of *Vibrio parahaemolyticus* (VpTPD), and its impact has been widespread, affecting around 70–80% of hatcheries and shrimp farmers. The disease can spread rapidly within just 2–3 days and can cause mortality up to 90%. Without timely management and accurate detection, this rapid progression can lead to severe production losses. Therefore, early, rapid, and accurate diagnostics are critically important for effective disease management.

This chapter presents the currently available diagnostic methods for the detection of TPD.

2.1 Clinical symptom–based diagnosis of TPD

Clinical observation is often the first step in identifying Translucent Post-Larval Disease (TPD) in shrimp hatcheries. Although it is not confirmatory, careful monitoring of early behavioural and physical changes can provide early warning signs and help initiate timely interventions.

In the early stage (6–12 hours post-infection), affected post-larvae show

- Reduced feeding activity
- Lethargic and weak swimming behavior
- Reduced responsiveness to stimuli
- Gills may appear pale yellow.

As the disease progresses, more pronounced signs develop within 24–48 hours.

- Hepatopancreas color changes from dark brown to light brown.
- Intestine becomes transparent like glass; empty stomach.
- Gills swollen, loose, and easily damaged.
- Hepatopancreas showing necrosis and pallor, reduced digestive function.
- Body becomes whitish and translucent; muscle atrophy observed.
- Rapid weakening followed by mass mortality if untreated.

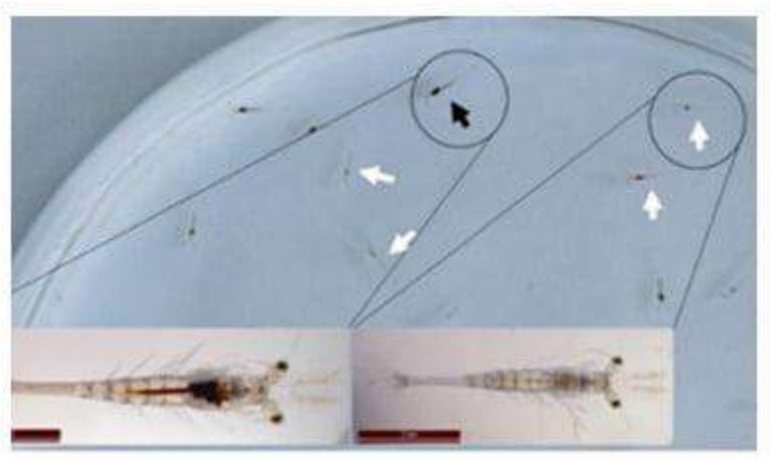

Fig.1. Clinical sign of TPD affected (white arrow) PL appeared pale and translucent with an empty gut, and the normal shrimp (black arrow) showed full gut. Source: QL Zhang

Externally, the post-larvae appears whitish and translucent, often accompanied by muscle atrophy. At this advanced stage, the PL weaken rapidly, and if untreated, the condition can lead to mass mortality within a short period.

2.2 Microbiological diagnostic methods for TPD

Microbiological diagnosis is a key component in the investigation of Translucent Post-Larval Disease (TPD), particularly for isolating the suspected causative agent, *Vibrio parahaemolyticus* (Vp-TPD). Although culture-based methods alone cannot confirm TPD, they are essential for obtaining pure bacterial isolates required for further molecular confirmation, virulence studies, and experimental validation.

The process begins with careful selection of moribund post-larvae (PL) exhibiting typical signs such as a glassy or translucent appearance. Samples are handled aseptically, surface-sterilized using 70% ethanol to remove contaminants. The hepatopancreas is then homogenized in sterile saline (1.5–3.0% NaCl) to prepare the sample for bacterial isolation. The homogenate is inoculated onto Thiosulfate-Citrate-Bile Salts-Sucrose (TCBS) agar, a selective medium for Vibrio species, and incubated at 28–30°C for 18–24 hours. Colonies are then examined, with *V. parahaemolyticus* typically producing green colonies. However, since colony morphology on TCBS is not specific, this step serves only as a preliminary indication of Vibrio presence. A critical step in diagnosis is verification using molecular tools, as microbiological methods alone are insufficient for confirming TPD. Techniques such as PCR or TaqMan-based qPCR targeting specific virulence genes (e.g., vhvp-1, vhvp-2, vhvp-3) are required for definitive identification.

In practice, microbiological diagnosis serves as a supporting tool—valuable for isolating pathogens and understanding bacterial load, but always requiring molecular confirmation. When integrated with advanced diagnostics, it plays an important role in accurate detection and effective management of TPD in shrimp hatcheries and farming systems.

2.3 Histopathological Detection

Histopathology provides valuable insights into the tissue-level damage caused by TPD, particularly in the hepatopancreas. In healthy shrimp, the hepatopancreas shows well-organized tubules with abundant lipid reserves. During early infection in TPD infected shrimp PL, mild changes such as tubular contraction and initial necrosis are observed. As the disease progresses, epithelial cell detachment and sloughing increase. In advanced stages, severe degeneration occurs, including complete loss of tubular structure, extensive necrosis, and heavy bacterial colonization (Fig 2). These changes reflect the progressive nature of the disease.

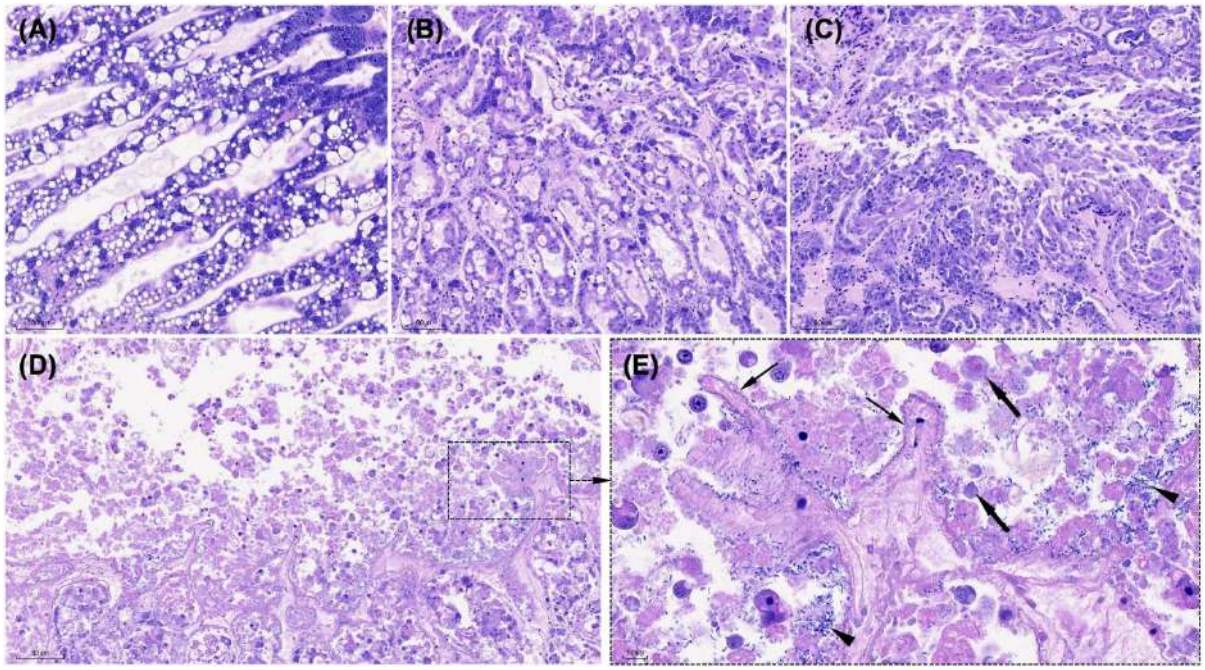

Fig 2 : Histopathological changes in hepatopancreas following infection.

The control group displayed normal histological architecture, with intact hepatopancreas tubule structure and abundant lipid deposits (A). In the early phase of infection, hepatopancreatic tubules exhibited contraction with mild necrosis (B). By the middle phase of infection, intestinal epithelial cells detached, and sloughing lesions intensified (C). In the later phase of infection, severe structural degradation of hepatopancreas tubule was evident

(D), with the complete loss of elliptical and circular luminal structures and extensive tubular necrosis (thin arrows in E), severe sloughing of epithelial cells and tissue debris (arrows), accompanied by massive rod-shaped bacterial colonization (arrowheads). Slides were stained with Mayer–Bennet hematoxylin and eosin-phloxine (H&E). Scale bars are included in the images (80 µm in panels A–D, except 10 µm in panel E). Source Hung et al., 2025.

2.4 Molecular diagnosis of TPD

Molecular diagnosis has become the most dependable way to detect *Vibrio parahaemolyticus* strains associated with Translucent Post-Larval Disease (TPD). Unlike microbiological methods, molecular tools focus on specific virulence genes such as vhvp-1, vhvp-2, and vhvp-3 that are linked to TPD-causing strains.

Molecular diagnosis with high sensitivity and specificity is considered extremely valuable for early detection, routine screening, and maintaining hatchery biosecurity.

2.5 Conventional PCR for TPD detection

Conventional PCR is widely used for laboratory confirmation of TPD. It involves amplification of target virulence genes using specific primers.

DNA is extracted from shrimp tissues or bacterial isolates, followed by PCR amplification. The products are then visualized using agarose gel electrophoresis. The presence of specific DNA bands indicates a positive result.

Primers	Sequences (5'-3')	Ta	Target region	Reference
VHVP-1-P -F	GAGGAGAGTGTTGACCGAAATC	58° C	362 bp	Jia et al., 2024).
VHVP-1-P -R	CTGCGCCAGTAGTAACGATAAG			
VHVP-2-P -F	GCTGGTCCGGACGGTGCC	60° C	864 bp	
VHVP-2-P -R	GTGATACATTAATACTTGTCTACAA			
VHVP-3-P -F	CCCGTATCACAGAGCGATTT	58° C	306 bp	
VHVP-3-P -R	CTTTGGTGTCGGTCGTAGTT			

Table 1. PCR primers for the detection of TPD.

2.6 Real-time PCR (qPCR) for TPD detection

Real-time PCR (qPCR) is currently considered the gold standard for TPD diagnosis, especially in well-equipped laboratories and hatchery screening programs. What makes qPCR particularly powerful is that it not only detects the pathogen but also measures the amount of bacterial DNA present in the sample. Using TaqMan-based assays (Table 2) targeting genes

like vhvp-1, vhvp-2, and vhvp-3, qPCR can detect extremely low levels of infection—down to about 10 copies per reaction. This makes it highly useful as an early warning tool, helping identify infections before they lead to visible symptoms or mass mortality. In real-world applications, qPCR is widely used for screening broodstock and post-larvae to ensure only healthy, pathogen-free stocks are used in farming systems. Its high sensitivity, specificity, and rapid turnaround time make it a critical tool for strengthening biosecurity and minimizing the risk of TPD outbreaks.

Methods	Primers/Probe	Sequences (5'-3')	Ta	Target region
TaqMan Qpcr (Zhang et al., 2025)	vhvp_SpvB-F1 vhvp_SpvB-R1 vhvp_SpvB-P1	AGTCGTTTGGAGTATTGGGTG GCCATCAGAGGTGTAGATCAC 6-FAM-TCTTCGAGTGCTGCGACCACTTT-TAMRA	59°C	72 bp
	vhvp_TcdB-F2 vhvp_TcdB-R2 vhvp_TcdB-P2	GTAATCGTTTGGTTAGCACCG ACCAAACCCACGGAACTC VIC-CACGGCCATCCCAGACTCCAT-BHQ1	59°C	77 bp
TaqMan qPCR (Jia *et al.*, 2024).	VHVP-F VHVP-R VHVP-P	AACTCCCGAAATCCGTCAAG ACACCCAATACTCCAAACGAC AGGCATGGACCGTAAAGCTCTCAC	55.7°C	119 bp

Table 2. qPCR primers and probes for the detection of TPD

2.7 Conclusion

A comprehensive and integrated diagnostic approach is essential for the accurate detection of Translucent Post-Larval Disease (TPD). Clinical observations serve as an initial warning, while microbiological methods help in isolating the suspected pathogen. Histopathological analysis provides insights into tissue-level damage, and molecular techniques such as PCR and qPCR offer definitive confirmation. Among the available methods, qPCR stands out as the most sensitive, specific, and reliable tool for early detection, making it highly valuable for effective disease management.

2.8 Further reading

Jia T, Xu T, Xia J, Liu S, Li W, Xu RD, Kong J, Zhang QL (2023) Clinical protective effects of polyhexamethylene biguanide hydrochloride (PHMB) against *Vibrio parahaemolyticus* causing translucent post-larvae disease (VpTPD) in *Penaeus vannamei*. J Invertebr Pathol 201:108002.

Jia TC, Liu S, Yu XT, Xu TT, Xia JT, Zhao WX, Wang W, Kong J, Zhang QL (2024) Prevalence investigation of translucent post-larvae disease (TPD) in China. Aquaculture 583:740583.

Tham H (2024) Warning of new disease appearing on white leg shrimp. Vietnam Agriculture.

Vietnam Fisheries Magazine (n.d.) Zeigler Vietnam meets with customers on management of transparent post-larvae disease. Vietnam Fisheries Magazine.

Wang YG, Yu YX, Liu X (2021) Pathogens and histopathological characteristics of shrimp postlarvae bacterial vitrified syndrome (BVS) in *Litopenaeus vannamei*. J Fish China 45:1563–1573.

Yang F, Xu LM, Huang WZ, Li F (2022) Highly lethal *Vibrio parahaemolyticus* strains cause acute mortality in *Penaeus vannamei* post-larvae. Aquaculture 548:737605.

Yang F, You Y, Lai Q, Xu L, Li F (2023) *Vibrio parahaemolyticus* becomes highly virulent by producing Tc toxins. Aquaculture 739817.

Zhang Q, Liu S, Yang B, Feng D, Wan X, Zhang X, Xu T, Yu X, Wang W, Xie G (2025) Diagnostic method for shrimp translucent post-larva disease (TPD). Aquaculture Industry Standard of the People's Republic of China SC/T 7243-2025.

Zou Y, Xie G, Jia T, Xu T, Wang C, Wan X, Li Y, Luo K, Bian X, Wang X, Kong J, Zhang Q (2020) Determination of the infectious agent of translucent post-larva disease (TPD) in *Penaeus vannamei*. Pathogens 9:741.

3. Mechanism of plasmid mediated virulence in vibrios

3.1 Introduction

Over the past decade, shrimp aquaculture has witnessed the emergence of several bacterial diseases that have caused substantial economic losses worldwide. Among these, Acute Hepatopancreatic Necrosis Disease (AHPND) has been one of the most devastating, particularly in South-East Asian countries where it leads to mass mortalities ranging from 40–100 % during the first 35 days of culture. The disease is primarily caused by specific strains of *Vibrio parahaemolyticus* carrying plasmid-borne *pirAB* toxin which are directly responsible for the severe hepatopancreatic damage observed in infected shrimp.

Even as the global aquaculture industry began to recover from AHPND outbreaks, another emerging disease, Translucent Post-Larval Disease (TPD), was reported in China. The disease is also associated with *V. parahaeomolyticus*, affects early post-larval stages and is characterized by rapid onset mortality and distinctive translucent appearance of infected shrimp. Within a few years of its emergence, TPD spread widely across shrimp farming regions in China and pose a significant threat, with concerns regarding its potential dissemination to other aquaculture producing countries.

A common feature linking these diseases is the central role of plasmid as carriers of virulence determinants. In both AHPND and TPD, key toxin genes are located on plasmids, enabling rapid dissemination of pathogenic traits through horizontal gene transfer. This mobility allows non-pathogenic or less virulent strains to acquire virulence factors and become highly pathogenic, thereby accelerating disease emergence and spread. Thus, plasmids represent a critical driver of pathogenic evolution in vibrios.

3.2 Plasmid structure and role in disease

Plasmids are extrachromosomal, self-replicating DNA molecules that exist independently of the bacterial chromosome. They typically range from a few kilobases to over 100 kb and often carry genes that enhance bacterial fitness. The key characteristics of a plasmid is

a. Origin of replication
b. Presence of mobility genes enabling conjugation and horizontal gene transfer
c. Carry virulence, antimicrobial resistance genes or other environmental fitness

Plasmids are highly dynamic as they are able to move from one bacterial cell to another makes them powerful agents of horizontal gene transfer (HGT). Plasmid facilitates rapid dissemination of virulence factors among *Vibrio* populations. This is mediated by conjugative

machinery of the plasmid. Such virulence factors include PirAB toxin genes in AHPND and VHVP genes in TPD. The aquatic environment is especially suitable for plasmid exchange due to high bacterial densities and environmental stressors. Importantly, plasmids can cross species barriers. Studies have shown that virulence plasmids such as pVA1 of AHPND can transfer between different *Vibrio* species and even to non-Vibrio bacteria making the disease prevention strategies more vulnerable.

3.3 Role of plasmid in spread of AHPND

Plasmid play a central role in the pathogenesis of AHPND, primarily through the carriage of toxin genes. AHPND-causing *Vibrio* strains harbor a highly conserved ~70 kb plasmid (pVA1-type) encoding the binary toxins PirA and PirB, which are directly responsible for shrimp mortality. Experimental studies have demonstrated that deletion of *pirAB* genes abolishes virulence, confirming their essential role in the disease causation. Notably, these plasmids exhibit remarkable genetic conservation (>99% sequence identity) across diverse *Vibrio* species, indicating a common evolutionary origin and strong selective pressure to maintain toxin-associated virulence traits. The defining feature of the pVA1-type plasmid is its horizontal transferability, which significantly contributes to the rapid emergence and spread of AHPND. The plasmid contains conjugative transfer genes, including components of Type IV secretion system (T4SS), enabling its movement between bacterial cells. In addition, the localization of *pirAB* within a mobile transposon (pirAB-Tn903) further enhances its mobility and dissemination. Experimental studies have shown that this plasmid can be transferred from pathogenic *V. parahaemolyticus* to other species such as *V. campbellii*, converting them into highly-virulent strains capable of causing 100% mortality in shrimp.

Initially AHPND outbreak was attributed primarily to *V. parahaemolyticus* strains carrying the pVA1 plasmid. However, subsequent studies have reported its presence in multiple *Vibrio* species, including *V. campbellii, V. owensii, V. harveyi* and *V. punensis*. This widespread distribution indicated that AHPND is plasmid-dependent rather than species-specific. The ability of non-pathogenic strains to acquire the pVA1 plasmid via conjugation and subsequently express PirAB toxins underscores the dynamic nature of plasmid-mediated virulence. These findings have important epidemiological implications, explaining the increasing number of *Vibrio* species associated with AHPND outbreaks and highlighting plasmid as key drivers in disease emergence.

The PirA and PirB toxins encoded on the pVA1 plasmid are homologous to insecticidal toxins produced by *Photorabdus* species. Functionally, PirA and PirB acts as a binary toxin, where PirB is believed to form pores in host cell membrane while PirA facilitates binding and enhanced toxicity. Together, the toxins lead to cell sloughing, tissue necrosis and rapid organ dysfunction, ultimately resulting in high mortality. Apart from encoding toxin, the plasmid acts as a mobile virulence platform, enabling rapid dissemination of virulence traits across bacterial population and environments. Thus pVA1-type plasmid played a pivotal role in the emergence, persistence and global spread of AHPND.

3.4 Role of plasmid in translucent post larval disease

Translucent post-larval disease (TPD) is an emerging condition affecting shrimp post-larvae, characterized by a transparent body, empty gut, and rapid onset of high mortality. Recent studies have linked TPD to *V. parahaemolyticus* strain harboring plasmid-borne toxin genes that are distinct from the PirAB toxin associated with AHPND. Although the precise pathogenic mechanisms are still being elucidated, plasmids are increasingly recognized to play a central role in TPD, acting as carrier of virulence factors responsible for the disease.

Unlike AHPND-causing strains that harbors the pVA1 plasmid encoding PirAB toxin, the TPD-associated strains possess a large virulence plasmid (~187 kb) encoding Vibrio High Virulent Proteins (VHVPs), particularly the *vhvp-2* gene. This gene has been identified as a key determinant of pathogenicity, as its presence correlates with high mortality in shrimp post-larvae, while its deletion significantly reduces virulence. The VHVP-2 toxin contains domains homologous to the *Salmonella* virulence plasmid B protein (SpvB) and insecticide toxin TcdB-like region, suggesting a cytotoxic mode of action involving disruption of host cellular processes. In addition, the presence of multiple virulence genes (*vhvp-1, vhvp-2, vhvp-3*) on the same plasmid indicates a coordinated virulence system, where plasmids act as integrated genetic units controlling multiple pathogenic traits.

Beyond encoding toxins, plasmids in TPD-associated vibrios also act as evolutionary reservoirs, facilitating the acquisition and co-localization of additional virulence factors and antimicrobial resistance (AMR) genes. This combination enhances bacterial fitness, persistence and adaptability in aquaculture environments. The mobility of such plasmids through horizontal gene transfer, coupled with the global trade of shrimp post-larvae in aquaculture, significantly increases the risk of rapid dissemination of TPD-causing strains. Thus, plasmids are not merely carriers of virulence genes but act as dynamic drivers of pathogenic evolution, playing a pivotal role in the emergence, spread and severity of TPD,

and highlighting the urgent need for surveillance strategies targeting plasmid-borne virulence genes.

3.5 Role of plasmid in the pathogenesis of *Vibrio anguillarum*

The role of plasmid in the virulence of *Vibrio* species was first understood in *V. anguillarum* where pJM1 plasmid plays a critical role in the development of hemorrhagic speticaemia in fish. This ~65 kb plasmid encodes a sophisticated iron acquisition system which is essential for bacterial survival and proliferation within the host. Since iron is tightly bound by host proteins such as transferrin and lactoferrin, its availability is severely limited during infection. The pJM1 plasmid enables the bacterium to overcome this limitation by mediating the biosynthesis and uptake of the siderophore anguibactin, thereby allowing efficient scavenging of iron from the host environment. The iron acquisition capability conferred by pJM1 plasmid is directly linked to virulence, as strains lacking this plasmid show significantly reduced pathogenicity. At the molecular level, the pJM1 plasmid harbors a cluster of genes responsible for biosynthesis and transport of the siderophore anguibactin, which plays critical role in iron scavenging under host-imposed iron limitation. This clusters includes several nonribosomal peptide synthetases (NRPS) involved in anguibactin synthesis as well as the fatDCBA operon, which encodes components of the transport system required for the uptake of ferric-anguibactin complex into the bacterial cell.

Comparative genomic analysis has shown that that while *V. anguillarum* possesses additional chromosomal virulence factors, the anguibactin system encoded on pJM1 plasmid remains one of the primary drivers of pathogenicity. Experimental evidence further supports as introduction of pJM1 plasmid or its functional gene clusters into low-virulence strains restores their ability to grow under iron limited condition and significantly enhance their virulence. Thus, the pJM1 plasmid functions as a critical virulence determinant by enabling efficient iron acquisition, promoting bacterial survival in the host, and facilitating the development of systemic infection in fish.

3.6 Conclusion

Apart from well-known examples of AHPND, TPD and pJM1-associated virulence, plasmids broadly play a crucial role in bacterial pathogenicity by serving as reservoirs of diverse virulence determinants. These includes genes for toxins, toxin delivery secretion systems, siderophore-mediated iron acquisition, adhesion and colonization factors, and other elements that enhance host invasion and survival. The impact of plasmid becomes even more significant when they simultaneously carry antimicrobial resistance (AMR) genes, thereby

conferring both pathogenic potential and environmental fitness. Such dual function plasmids enable bacteria to survive under selective pressures, including antibiotic exposure, while enhancing virulence. The situation is further exacerbated by the high mobility of plasmids, which are often transferrable across bacterial species and even genera through horizontal gene transfer mechanisms such as conjugation. This facilitates rapid dissemination of virulence and resistance traits leading to emergence of highly pathogenic and multidrug-resistant strains. Given their profound role in shaping bacterial pathogenicity, there is an urgent need to monitor the evolution, distribution and transfer dynamics of virulence-associated plasmids.

3.7 Further reading

Actis LA, Fish W, Crosa JH, Kellerman K, Ellenberger SR, Hauser FM, Sanders-Loehr J (1986) Characterization of anguibactin, a novel siderophore from *Vibrio anguillarum* 775 (pJM1). J Bacteriol 167:57–65.

Dinh-Hung N, Mai HN, Matthews M, Wright H, Dhar AK (2025) Isolation, characterization, and pathogenicity of a *Vibrio parahaemolyticus* strain causing translucent post-larvae disease in *Penaeus vannamei* outside China. PLoS One 20:e0331862.

Dong X, Chen J, Song J, Wang H, Wang W, Ren Y, Guo C, Wang X, Tang KFJ, Huang J (2019) Evidence of the horizontal transfer of pVA1-type plasmid from AHPND-causing *Vibrio campbellii* to non-AHPND *Vibrio owensii*. Aquaculture 503:396–402.

Han JE, Tang KFJ, Tran LH, Lightner DV (2015) Photorhabdus insect-related (Pir) toxin-like genes in a plasmid of *Vibrio parahaemolyticus*, the causative agent of acute hepatopancreatic necrosis disease (AHPND) of shrimp. Dis Aquat Organ 113:33–40.

Jia T, Liu S, Yu X, Xu T, Xia J, Zhao W, Wang W, Kong J, Zhang Q (2024) Prevalence investigation of translucent post-larvae disease (TPD) in China. Aquaculture 583:740583.

Kumar V, Roy S, Behera BK, Bossier P, Das BK (2021) Acute hepatopancreatic necrosis disease (AHPND): virulence, pathogenesis and mitigation strategies in shrimp aquaculture. Toxins (Basel) 13:524.

Lai HC, Ng TH, Ando M, Lee CT, Chen IT, Chuang JC, Mavichak R, Chang SH, Yeh MD, Chiang YA (2015) Pathogenesis of acute hepatopancreatic necrosis disease (AHPND) in shrimp. Fish Shellfish Immunol 47:1006–1014.

López CS, Crosa JH (2007) Characterization of ferric-anguibactin transport in *Vibrio anguillarum*. Biometals 20:393–403.

Wang HC, Lin SJ, Mohapatra A, Kumar R, Wang HC (2020) A review of the functional annotations of important genes in the AHPND-causing pVA1 plasmid. Microorganisms 8:996.

Zhang Y, Tan P, Liang X, Zhang Q, Yang M (2025) *Vibrio* plasmids harboring vhv gene associated with shrimp translucent post-larvae disease: Coexistence of two types of T4SS and multiple transposons. J Invertebr Pathol 211:108324.

Zhang Y, Tan P, Yang M (2024) Characteristics of vhvp-2 gene distribution and diversity within the *Vibrio* causing translucent post-larvae disease (TPD). J Invertebr Pathol 207:108228.

Zou Y, Xie G, Jia T, Xu T, Wang C, Wan X, Li Y, Luo K, Bian X, Wang X (2020) Determination of the infectious agent of translucent post-larva disease (TPD) in *Penaeus vannamei*. Pathogens 9:741.

4. Bioinformatics analysis for shrimp disease diagnosis

Shrimp aquaculture has become one of the fastest growing sectors in global food production and plays a central role in meeting rising protein demands. Disease outbreaks remain one of the most significant constraints affecting productivity and sustainability of this sector. Traditional diagnostic methods such as histopathology, pathogen culture and PCR techniques are widely used for diagnosis. Bioinformatics has emerged as a transformative approach, to address the limitations in traditional diagnosis, enabling precise, rapid, and large scale analysis of shrimp diseases at the molecular level.

Shrimp are susceptible to a wide range of pathogens, including viruses, bacteria, fungi, and parasites. Viral diseases like White Spot Syndrome can spread rapidly and cause heavy mortality, while bacterial infections such as Vibriosis are also a serious threat in th shrimp farming system. A significant parasitic disease is *Enterocytozoon hepatopenaei* (EHP) does not usually cause death but severely affects growth, resulting in stunted shrimp and economic losses. These diseases can spread rapidly in aquaculture systems due to high stocking densities and environmental stressors. Early detection is critical, but conventional diagnostic techniques often fail to identify infections before clinical symptoms appear. Bioinformatics addresses these challenges by analysing genetic and molecular data from both shrimp hosts and pathogens. It enables detection at the DNA, RNA, or protein level changes even before visible signs of disease occur.

4.1 Genomics in disease diagnosis

Genomics in disease diagnosis refers to the study of an organism's complete genetic material to identify the genetic basis of diseases and detect pathogens responsible for infections. Whole genome sequencing (WGS) of shrimp and their pathogens provides comprehensive datasets that can be analysed to identify disease-causing agents. By comparing genomic sequences from healthy and infected shrimp, genetic variations associated with diseases can be identified.

Sequencing viral or bacterial genomes allows for precise identification and classification of pathogens. Bioinformatic tools can align unknown sequences with reference databases to detect known pathogens or even discover novel ones.

Metagenomic sequencing can analyse all genetic material in a sample, enabling detection of multiple pathogens simultaneously without prior knowledge. The process involves extracting total DNA from a sample, like water, sediment, gut, or whole organism and sequencing it

using technologies like Next-Generation Sequencing, and then analysing the data using bioinformatics tools

4.2 Transcriptomics and gene expression analysis

While genomics provides stable genetic information, transcriptomics reveals dynamic changes in gene expression during infection. It studies the complete set of RNA transcripts produced by an organism at a given time under specific conditions. The main molecule studied in transcriptomics is messenger RNA (mRNA), which carries genetic information from DNA to produce proteins that carry out cellular functions.

RNA sequencing (RNA-Seq) is widely used to study how shrimp respond to pathogens at the molecular level. RNA-Seq data is processed by bioinformatics tools to identify differentially expressed genes and signaling pathways. Gene expression refers to the process by which information encoded in a gene is used to synthesize functional products, mainly proteins or functional RNA molecules. The level of gene expression determines how active a gene is in a particular cell or condition. Changes in gene expression can indicate normal biological processes or the presence of diseases

This information is valuable for diagnosis because specific gene expression patterns can serve as biomarkers of infection. For example, upregulation of immune-related genes may indicate early-stage infection. Machine learning models can be trained on transcriptomic data to classify samples as healthy or diseased with high accuracy.

4.3 Metagenomics and microbiome analysis

Shrimp health is closely linked to the community of microorganisms living in their gut and environment. The microbiome includes bacteria, viruses, fungi, and other microbes that interact with each other and their host influencing health and ecosystem balance. Disruptions in this microbial balance can lead to disease. Metagenomics is used for the study of all the genetic material from microorganisms present in shrimp gut and the environment in which they live, without needing to culture them in the lab. One of the major advantages of microbiome metagenomic analysis is its ability to detect both beneficial and harmful microorganisms simultaneously.

This approach is particularly useful for detecting opportunistic pathogens and understanding disease ecology. For example, shifts in bacterial populations may signal the onset of disease before clinical symptoms appear. Metagenomics also identifies beneficial microbes that improve digestion, immunity, and water quality, enabling farmers to use probiotics more effectively.

4.4 Proteomics and biomarker

Proteomics complements genomic and transcriptomic approaches by analysing proteins expressed during infection. Since proteins are the functional molecules in biological systems, their study provides direct insights into disease processes. Proteomic studies use technologies such as mass spectrometry and chromatography combined with advanced bioinformatics tools to analyse complex protein molecules.

Differences in protein expression between healthy and infected shrimp can reveal useful biomarkers for diagnosis. Biomarkers are measurable protein molecules which can show the differences during a disease. These biomarkers can then be used to develop rapid diagnostic kits.

4.5 Bioinformatic tools used in shrimp disease diagnosis

Bioinformatics tools are specialized software and algorithms used to analyse, interpret, and manage biological data such as DNA, RNA, and protein sequences. A wide range of bioinformatic tools are used in shrimp disease diagnostics.

Commonly used tools include BLAST, which helps find similarities between biological sequences and Clustal Omega which is used for aligning multiple sequences and to identify conserved regions. Genome assembly and analysis tools like SPAdes and Bowtie are widely used for processing large sequencing datasets generated through Next-Generation Sequencing. Visualization and annotation tools such as MEGA assist in phylogenetic analysis and evolutionary studies.

Databases play a crucial role in bioinformatics. Public repositories store genomic and proteomic data for shrimp and pathogens. Major databases like GenBank, EMBL-EBI, and DDBJ collect nucleotide sequences from researchers worldwide and enables data sharing. UniProt database provide detailed information about protein structure and function. Specialized databases like KEGG help in understanding biological pathways and metabolic networks. These databases are interconnected and frequently updated.

4.6 Bioinformatics approaches in ICAR- CIBA

ICAR–CIBA has developed steadily growing bioinformatics and genomics research programS focused on improving brackishwater aquaculture. One of the major contributions of ICAR–CIBA in this domain is genome sequencing and assembly of important brackishwater species like *Mugil cephalus* and *Penaeus indicus.* Whole genome sequencing was done for pathogens like *Vibrio campbelli* and *Vibrio parahaemolyticus.*

The institute also focus studies on nutrigenomics in shrimp, where gene expression responses to different feed formulations and environmental stressors are studied. Also transcriptomics studies are done on effect of environmental stressors like salinity and temperature on important brackishwater species. In disease diagnosis, computational tools are used to study viral and bacterial genomes, develop molecular diagnostic markers, and support PCR-based detection systems for viral and bacterial infections in shrimp farming systems.

Bioinformatics tools like Missing Region Finder, MRF tool, which rapidly tabulates and depicts complete and partial missing coding DNA and an open access SNP database dbVAST was developed.

4.7 Advantages of bioinformatic approaches

Bioinformatic analysis offers several advantages over traditional diagnostic methods in aquaculture and disease monitoring. It provides high sensitivity and specificity. It allows the detection of pathogens even at very low concentrations and improves the accuracy of diagnosis. It also enables early detection of infections before visible symptoms appear and gives farmers the opportunity to take preventive measures in time. Another key benefit is its ability to perform comprehensive analysis, where multiple pathogens can be identified simultaneously from a single sample. Advanced technologies like Next-Generation Sequencing, bioinformatic pipelines can deliver rapid results, often within a few hours. This approach also provides detailed insights that help in effective disease management.

4.8 Challenges in bioinformatics approach

High costs of sequencing and computational infrastructure can be a practical challenge. Also data analysis requires specialized expertise, and interpretation of results can be complex. Another challenge is the lack of comprehensive reference databases for shrimp pathogens. These limitations can be overcome through continuous technological advancements and skill development, making it a rapidly growing and promising scientific approach for shrimp disease diagnosis.

5. Shrimp vibriosis and its management in aquaculture

Shrimp aquaculture is a commodity having high risk of disease occurrence starting from the early larval stages to adults, due to changing aquaculture management practices cum environment stress. Understanding the pond ecology with regard to host pathogen interaction is more important for sustainable farming and culture without loss due to disease is the highest challenge put forth. Vibriosis is considered to be major bacterial problem in Indian shrimp culture system and co-incidence of both vibriosis and viral disease is found to cause high mortality in shrimp. The vibrios are highly abundant in marine, brackish and saline environment, there are about more than hundreds of species of vibrios are identified in the shrimp so far. Vibriosis is a major problem in shrimp hatcheries and culture ponds. The possible pathogenic species in brackish water are *V. campbelli*, *V. harveyi, V. parahaemolyticus, V. vulnificus, V. alginolyticus* and *V. mimicus*.

Luminescent disease of larval stages of shrimp in hatcheries were found to be infected with a luminescent *V. harveyi* species, the most devastating bacteria that causes extreme losses. The developmental stages from naupli to protozoea-3 exhibited greater susceptibility to these pathogens when compared to mysis to post larval stages with the larval rearing tank with luminescent glowing at night. All larval substages of *L. vannamei* were reported to be susceptible to *V. harveyi* with high mortality rates upto 80%. Gross signs of vibriosis are light or dark brown focal lesions and necrosis of appendage tips. The change of colour is the result of melanin produced by host hemocytes involved in the inflammatory process.

Robertson et al. (1998) reported that infection of *L. vannamei* larvae with V. harveyi at 10^5 cfu /ml produced a larval disease called Bolitas negricans and bioluminescence. The highest mortalities were recorded during the transition from zoea-3 to mysis. "Bolitas" is the Spanish name given to a syndrome involving the detachment of epithelial cells from the intestine and hepatopancreas, which appear as small spheres within the digestive tract. Development of bioluminescence reduced feeding and retarded development, sluggish swimming, reduced escape mechanisms, degeneration and formation of bundles of necrotic tissues within the hepatopancreas leading to death of infected larvae.

Vibriosis of juveniles and adult characterized with lethargy, reduced feeding, and swimming on the surface or edge of ponds. Clinical signs include reddish coloration, black spots/blisters on the carapace (melanization), tail necrosis, and pale and shrunken hepatopancreas. Large number of motile bacteria is visible in the hemolymph and hepatopancreas of moribund shrimp. Haemolymph of the affected shrimp does not clot or clot at very slow rate. Different

species of *Vibrio* can be isolated from haemolymph and hepatopancreas by plating on TCBS agar and Zobell marine agar. The luminescence can be demonstrated by preparing a smear from haemolymph and observation in dark. In case of heavy infection, the luminescence can be seen if the haemolymph is observed in dark.

Recently, it has been found that some specific strains of *V. parahaemolyticus* is associated with Acute hepatopancreatic necrosis disease (AHPND), currently the most important non-viral disease threat for cultured shrimp, characterized by mortality ranging from 40 -100 % during the first 35 days of culture. The disease was initially named early mortality syndrome (EMS). *V. parahaemolyticus* was first discovered by Tsunesaburo Fujino in 1950 as a causative agent of food borne disease following a large outbreak in Japan and it is the leading seafood-borne pathogen across the world. According to US-FDA, the allowable limit of 10000 cells per gram of seafood with zero tolerance of pathogenic strains harbouring virulence genes such as *tdh* and *trh*. *Vibrio parahaemolyticus* is found to be associated with number of diseases in fish and shellfish causing economic loss to the sector. Facultative aerobe gram negative curved rods, motile with single polar flagellum and lateral flagella for swimming and swarming and ability to produce capsule for strain survival in environment and host infection (Broberg et al., 2011). It can grow in 0.5 to 10% salinity with the optimal levels between 1-3% and the growth temperature ranges from 35^{o}C to 39^{o}C under culture conditions. The organism is a natural habitat of aquatic environment and most prevalent during warm summer season. It has the ability to tolerate and resist up to toxic levels of magnesium and the enhanced ability to use magnesium has increased the survivability under various conditions (Bhattacharya, 2000). The AHPND affected shrimp shows lethargy, reduced feed intake and growth rate, spiral swimming, empty stomach and empty or interrupted gut, finally sinks and die at the pond bottom, clinical symptoms include atrophy and pale discolouration of hepatopancreas, at times black discolouration as spots or streaks of hepatopancreas were reported. The target tissue of AHPND bacteria is hepatopancreas starting from proximal to distal part of the organ. It disrupt mitotic cell division of E-cells, dysfunction of R, B, F cells with massive cell rounding and sloughing of hepatopancreatic tubule epithelial cells. Lesions include haemocytic infiltration and formation of melanised granuloma with bacteria witnessing secondary bacterial infection.

Shell disease commonly affects the exoskeleton of shrimp larvae. It is also known as

chitinolytic bacterial disease, brown spot disease, black spot disease and rust disease. It is often associated with *Vibrio* spp, *Aeromonas*, and *Pseudomonas*. The shell disease is

identified by the presence of black spots and lesions on the exoskeleton and appendages. The progressive erosion of lesions leads to the aggressive multiplication of bacteria and pathogens in the affected region. Severe infection results in the loss of an affected appendage and the exoskeleton ultimately hampered the molting and locomotion. Thus, the affected larvae become susceptible, weak, and eventually, mortality occurs due to stress/ energy exhaustion. In tail necrosis the affected shrimp had necrosis of uropods and pleopods. In acute case of infection, the uropods were completely lost; the muscle in the distal portion of the abdomen became completely necrotic and began to decompose. The diseased shrimp lost their swimming ability and exhibited erratic gliding movements near the edge of ponds. There is no known treatment for shell disease. The management of shell disease can be achieved by maintaining organic load at a low level, by removing dead larvae, sediments, and debris, which may harbour a heavy load of bacteria. High stocking may be avoided, and good water quality and proper diet should be maintained.

Whitegut syndrome cannot be pinpointed to a single agent in provocating symptoms like stunted growth with reduced feed intake. The gut was found to be empty and appeared opaque. Gut filled with gas and feed intermittently. Signs are more visible when the shrimp reaches 3 gms and above. If the environmental conditions are favourable to infectious agent causing white gut, the shrimp will stop feeding and die with the development of loose shell. The white gut in many occasions is correlated with increase in pathogenic vibrios in the cultured pond. In some instances, the mortality has been recorded with the symptoms of stunted growth and opaque white gut visible through the transparent cuticle as a white streak. The feed consumed was released as white fluid material. Large number of motile bacteria is visible in the hemolymph and hepatopancreas of moribund shrimp. The possible main vibrio species are *V. parahemolyticus, V. vulnificus, V. alginolyticus* and *V. harveyi*. It has been reported that white gut affected samples had 0.2 x 10^5 cfu/mL of vibrio load in hemolymph (Jayashree *et.al.* 2006).

Bacterial pathogen management mainly involves preventing the entry of pathogen. However, if due to some reason, the pathogens enter the system, and then take necessary steps either to eliminate it completely or reduce the number substantially to prevent mortality. It is necessary to know the nature and virulence status of each pathogen and act accordingly. Many of the pathogens have reservoirs either as living organisms, water or inanimate objects. Therefore, one should be thorough with the nature of the pathogen and accordingly steps should be taken. Suitable environment and conditions for pathogen multiplication should be avoided.

Ponds should have proper fencing system to avoid pathogen reservoirs or passive carriers for disease spread. Obtaining good water is an important aspect of aquaculture practice. Water can be a primary source for the entry of pathogens. Wherever possible, it is advisable to go for recirculatory systems and thereby any pathogen entry can be avoided. Otherwise, it is necessary to go for adequate amounts of reservoir ponds where water can be stored initially, treated and finally matured before taking into culture ponds. Throughout the culture period, it is required to maintain good water quality and there by avoid stress. Along with feed and other management practices, the aquatic environment should always be maintained healthy.

6. Acute hepatopancreatic necrosis disease

6.1 Introduction

Vibrio parahaemolyticus is found to be associated with number of diseases in fish and shellfish acts as opportunistic or secondary pathogen that can cause mortality from a few to 100% in affected populations under stress. Recently, it has been found that unique strain of *Vibrio parahaemolyticus* is found to cause disease in shrimp leading to severe economic loss in culture practices named acute hepatopancreatic necrosis disease (AHPND), most important bacterial disease characterized by mass mortality during the first 35 days of culture, where affected shrimp show massive sloughing of hepatopancreatic epithelial cells followed by death. It was first reported from China in 2009, followed by Vietnam in 2010, Malaysia in 2011, and in Thailand since 2012. The disease was identified as early mortality syndrome (EMS) before identification of the causative agent.

The causative agent was identified in 2013 as a bacterial agent, *V. parahaemolyticus*, carrying a specific toxin on a specific extra-chromosomal DNA. AHPND-causing *V. parahaemolyticus* strains carry a conjugative plasmid (~ 63–70 kb, pVA1 type) encoding the binary toxins $PirA^{VP}$ and $PirB^{VP}$ that damage shrimp hepatopancreas cells. Recent studies have shown the $PirAB^{vp}$ binary toxin has been identified in other *Vibrio* species belonging to the *Harveyi* clade, such as *V. harveyi*, *V. campbellii*, and *V. owensii.* The presence of these genes in different bacterial species is a potential risk for the spread of emerging diseases. The clinical signs of shrimp affected with AHPND are a pale hepatopancreas, empty gut, anorexia, and lethargy accompanied by pathognomonic lesions: massive sloughing of tubule epithelial cells of the shrimp hepatopancreas. In addition, two variable regions have also been identified in the pVA1-type plasmids which have been linked to the geographical region of origin of the isolates. These regions correspond to a 4,243 bp *tn3*-like transposon and a 9 bp small sequence repetition (SSR). The presence of the *tn3*-like transposon has only been reported in *V. parahaemolyticus* isolates from Mexico, and a variation in the number of repeated units (RU) of SSR has been reported in isolates from different geographical origins, although no evidence has been reported linking those regions with the virulence capacity of the strain.

The differences in the virulence have been reported with variations in the mortality rate caused by different isolates of AHPND causing *V. parahaemolyticus* (VP_{AHPND}) in shrimp populations have been observed during disease outbreaks in various regions of the world, as well as when strains are used under experimental conditions during challenge tests. It is reported low virulence in

VP_{AHPND} strains due to a partial or total loss in the $PirAB^{vp}$ genes, but the disease could continue to occur. Therefore, there are other factors involved in the pathogenesis of AHPND. The differences in chromosomal and plasmid genes could be related to virulence factors associated with variations in pathogenicity. Secretion systems have major role in pathogenic pathways in *Vibrio* species, type 3 secretion systems (T3SS) and type 6 secretion systems (T6SS) are elements that have been studied and appear to be the most promising for explaining the virulence differences among *V. parahaemolyticus* strains. The involvement of genes related with transposases, DNA methyltransferases, anti-restriction proteins, post segregational killing systems, and secretion systems needs to be studied for their role in virulence mechanism of bacteria causing AHPND.

6.2 Transmission and host susceptibility

Horizontal transmission is the primary mode of spreading through contaminated water, feed and in-animate objects in the farm, the transmission also occurs due to cannibalism of infected dead shrimp, through infected carriers such as planktons, polychaetes, crabs and mollusks. Experimental studies have shown that *Vp* AHPND could not be transmitted via frozen infected shrimp as AHPND *V. parahaemolyticus* are known to be sensitive to freezing, refrigeration, heating and common disinfectants. *Penaeus vannamei* and *P. monodon* are highly susceptible when compared to *P. indicus* and *P. japonicus*. The post larvae life stages from PL 10 to PL 30 is highly susceptible than other life stages of shrimp, the susceptibility increase with high water temperature 28 to 32 ^{o}C, high salinity above 15 ppt, poor water quality, high stocking density and poor feed management.

6.3 Clinical signs and pathology

The infected shrimp were observed with lethargy, empty gut, soft shell, pale atrophied hepatopancreas, reduced feed intake and sudden mass mortality within 35 days of culture period. Black spots or streaks on the surface of hepatopancreas, does not squash easily between the thumb and forefinger (probably due to increased fibrous connective tissue and haemocytes.

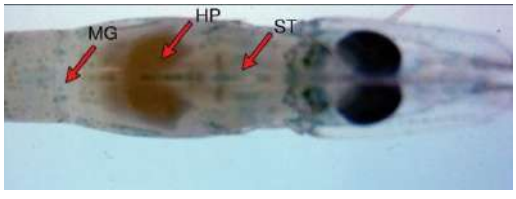

Pale and atrophied hepatopancreas

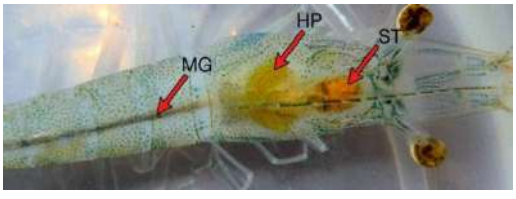

Normal size HP with dark orange color

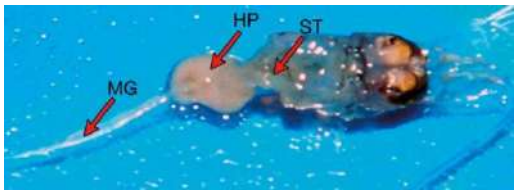

Empty stomach (ST) and midgut (MG)

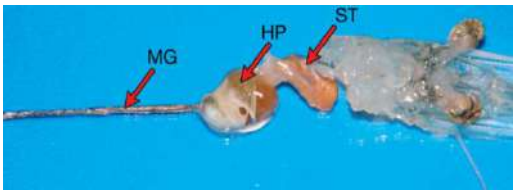

Full stomach and midgut

Histopathological findings include acute sloughing of the hepatopancreatic epithelial cells, tubular necrosis, the acute phase is characterised by a massive and progressive degeneration of the HP tubules from proximal to distal, with significant rounding and sloughing of HP tubule epithelial cells into the HP tubules, HP collecting ducts and posterior stomach. No B-, F- and R-cells are seen in the hepatopancreatic tubule and some nuclei of tubule epithelial cells are enlarged (karyomegaly). No significant bacterial involvement appears during this phase.

The terminal phase is characterised by marked intra-tubular haemocytic inflammation and development of massive secondary bacterial infections that occur in association with the necrotic and sloughed HP tubule cells. In *Penaeus vannamei* AHPND tolerant lines, the chronic phase is characterised by only a few tubules with epithelial necrosis with bacteria and inflammation.

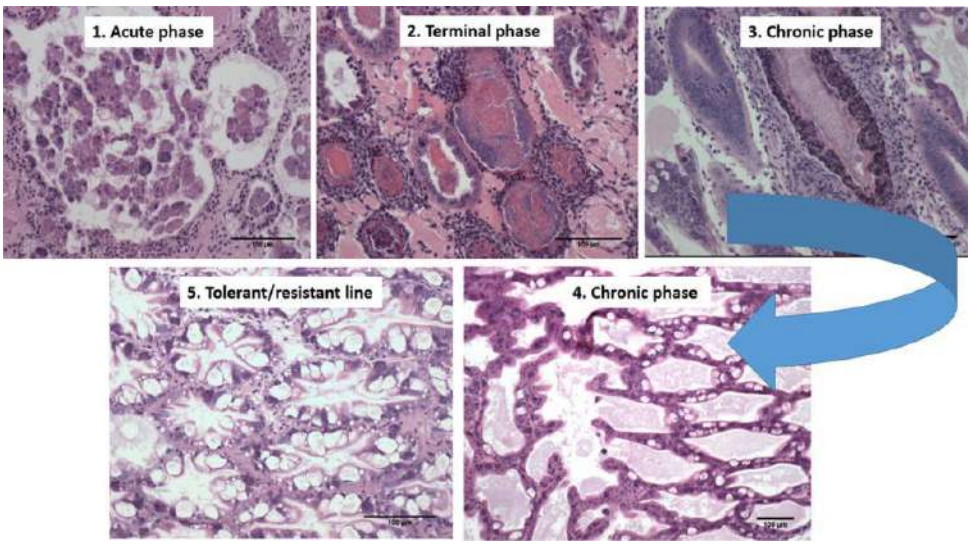

Evolution of the pathology of AHPND in Latin America, with microphotographs of the tubules of hepatopancreas of affected animals, from the acute phase (1), to the terminal phase, to the chronic phase, and eventually to the tolerant/resistant line. Courtesy: Luis Fernando Aranguren Caro, et.al. (2020)

6.4 PCR methodology

PCR methods have been developed that target the *Vp* AHPND toxin genes. Two one-step PCR methods (AP1 and AP2) are described here for detection of the pVA1 plasmid in enrichment broth cultures (Flegel & Lo, 2014). The AP3 method is a single-step PCR that targets the 12.7 kDa $PirA^{vp}$ gene (Sirikharin et al., 2015). Single-step PCRs such as the AP3 method and others, e.g. VpPirA-284, VpPirB-392 (Han et al., 2015a) and TUMSAT-Vp3 (Tinwongger et al., 2014), have relatively low sensitivity when used for detection of *Vp* AHPND at low levels (e.g. sub-clinical infections) or in environmental samples such as sediments and biofilms. Alternatively, a nested PCR method, AP4, has been developed with a 100% positive predictive value for *Vp* AHPND (Dangtip et al., 2015), and has greater sensitivity (1 fg of DNA extracted from *Vp* AHPND), allowing it to be used directly with tissue and environmental samples without an enrichment step. In addition, real-time PCR methods, for example the *Vp* AHPND-specific TaqMan real-time PCR developed by Han et al., 2015b, and an isothermal loop-mediated amplification protocol (LAMP) method developed by Koiwai et al., 2016 also have high sensitivity and can be used directly with tissue and environmental samples without an enrichment step.

6.5 Primers and probe for the real-time PCR method for detection of VpAHPND

Primer / Probe name	Sequence	Target gene	Reference
VpPirA-F	5'-TTG-GAC-TGT-CGA-ACC-AAA-CG-3'	pirA	Han et al., 2015b
VpPirA-R	5'-GCA-CCC-CAT-TGG-TAT-TGA-ATG-3'		
VpPirA Probe	5'-6FAM-AGA-CAG-CAA-ACA-TAC-ACC-TAT-CAT-CCC-GGA-TAMRA-3'		

6.6 PCR primer sequences

Method	Primers	Target gene	Expected Amplicon size	Reference
AP1	AP1F: 5'-CCT-TGG-GTG-TGC-TTA-GAG-GAT-G-3' AP1R: 5'-GCA-AAC-TAT-CGC-GCA-GAA-CAC-C-3'	*pVA1*	700 bp	Flegel & Lo, 2014
AP2	AP2F: 5'-TCA-CCC-GAA-TGC-TCG-CTT-GTG-G-3' AP2R: 5'-CGT-CGC-TAC-TGT-CTA-GCT-GAA-G-3'	*pVA1*	700 bp	
AP3	AP3-F: 5'-ATG-AGT-AAC-AAT-ATA-AAA-CAT-GAA-AC-3' AP3-R: 5'-GTG-GTA-ATA-GAT-TGT-ACA-GAA-3'	*pir*Avp	333 bp	Sirikharin *et al.*, 2014, 2015
TUMSAT-Vp3	TUMSAT-Vp3 F: 5'-GTG-TTG-CAT-AAT-TTT-GTG-CA-3' TUMSAT-Vp3 R: 5'-TTG-TAC-AGA-AAC-CAC-GAC-TA-3'	*pir*Avp	360 bp	Tinwongger *et al*., 2014
VpPirA-284	VpPirA-284F: 5'-TGA-CTA-TTC-TCA-CGA-TTG-GAC-TG-3' VpPirA-284R: 5'-CAC-GAC-TAG-CGC-CAT-TGT-TA-3'	*pir*Avp	284 bp	Han *et al.*, 2015a
VpPirB-392	VpPirB-392F: 5'-TGA-TGA-AGT-GAT-GGG-TGC-TC-3' VpPirB-392R: 5'-TGT-AAG-CGC-CGT-TTA-ACT-CA-3'	*pir*Avp	392 bp	
AP4 Step 1	AP4-F1: 5'-ATG-AGT-AAC-AAT-ATA-AAA-CAT-GAA-AC-3' AP4-R1: 5'-ACG-ATT-TCG-ACG-TTC-CCC-AA-3'		1269 bp	Dangtip *et al.*, 2015
AP4 Nested Step	AP4-F2: 5'-TTG-AGA-ATA-CGG-GAC-GTG-GG-3' AP4-R2: 5'- GTT-AGT-CAT-GTG-AGC-ACC-TTC-3'		230 bp	

6.7 Conclusion

PCR-based assays targeting the *pirA* and *pirB* toxin genes are the highly specific method for the detection of Acute Hepatopancreatic Necrosis Disease (AHPND) in shrimp. These methods enable identification of pathogenic strains, allowing timely implementation of management and biosecurity measures. Molecular diagnosis serves as a reliable tool for confirming AHPND outbreaks and monitoring the presence of virulent strains in hatcheries and grow-out systems.

6.8 Further reading

Dangtip S, Sirikharin R, Sanguanrut P, Thitamadee S, Sritunyalucksana K, Taengchaiyaphum S, Mavichak R, Proespraiwong P, Flegel TW (2015) AP4 method for two-tube nested PCR detection of AHPND isolates of *Vibrio parahaemolyticus*. Aquac Rep 2:158–163.

Flegel TW, Lo CF (2014) Free release of primers for specific detection of bacterial isolates that cause acute hepatopancreatic necrosis disease (AHPND). Network of Aquaculture Centres in Asia-Pacific, Bangkok.

Han JE, Tang KFJ, Tran LH, Lightner DV (2015a) Photorhabdus insect-related (Pir) toxin-like genes in a plasmid of *Vibrio parahaemolyticus*, the causative agent of acute hepatopancreatic necrosis disease (AHPND) of shrimp. Dis Aquat Org 113:33–40.

Han JE, Tang KFJ, Pantoja CR, White BL, Lightner DV (2015b) qPCR assay for detecting and quantifying a virulence plasmid in acute hepatopancreatic necrosis disease (AHPND) due to pathogenic *Vibrio parahaemolyticus*. Aquaculture 442:12–15.

Sirikharin R, Taengchaiyaphum S, Sanguanrut P, Chi TD, Mavichak R, Proespraiwong P, Nuangsaeng B, Thitamadee S, Flegel TW, Sritunyalucksana K (2015) Characterization and PCR detection of binary, Pir-like toxins from *Vibrio parahaemolyticus* isolates that cause acute hepatopancreatic necrosis disease (AHPND) in shrimp. PLoS One 10:e0126987. https://doi.org/10.1371/journal.pone.0126987

Tinwongger S, Proespraiwong P, Thawonsuwan J, Sriwanayos P, Kongkumnerd J, Chaweepack T, Mavichak R, Unajak S, Nozaki R, Kondo H, Hirono I (2014) Development of PCR diagnosis method for shrimp acute hepatopancreatic necrosis disease (AHPND) strain of *Vibrio parahaemolyticus*. Fish Pathol 49:159–164.

7. Major disease problems in shrimp aquaculture industry

7.1 Introduction

Shrimp aquaculture has emerged as a valuable economic resource in crustacean aquaculture sector, contributing substantially to food security, employment, and international trade. Over the past few decades, shrimp farming has expanded rapidly, particularly in tropical and subtropical regions, driven by increasing global demand for high-quality protein and export-oriented seafood products. Among all farmed shrimp species, the black tiger shrimp (*Penaeus monodon*) and the pacific white shrimp (*Penaeus vannamei*) contribute to more than 90-95% of the world production. In India, shrimp aquaculture has evolved into a key export industry, playing a crucial role in the national economy and supporting the livelihoods of millions of farmers, traders, and workers. Over the past few decades, there has been a rapid growth in penaeid shrimp aquaculture sector. Technological advancements in hatchery production, feed formulation, and farm management practices have significantly improved productivity and efficiency in recent years. This over-intensification, along with introduction of new varieties, climate variability, has resulted in an increased occurrence of emerging shrimp diseases. The World Organization of Animal Health (WOAH) recognizes certain diseases as the most significant, which were included in their list for penaeid shrimp diseases. Disease outbreaks over the last two decades, however, have led to dramatic declines in the shrimp output and challenges for the India claiming its place as a global shrimp leader. Penaeid shrimps, unlike vertebrates are vulnerable to diseases caused by viruses, bacteria, and other pathogens, lack adaptive immune system and separate lymphatic systems to protect themselves against invading pathogens; thus, increasing the risk of mortality within a few days of infection making health management a critical component of successful aquaculture operations. The major shrimp disease which is of greater concern are

7.2 White spot disease

White spot disease (WSD) caused by white spot syndrome virus (WSSV) that causes rapid death, affecting all stages of shrimp. The virus belongs to the genus Whispovirus, enveloped with double-stranded DNA (dsDNA) and a genome size of 290 to 305 Kbp on average. It is the important pathogen causing serious threats to the shrimp aquaculture. This restricted the import requirements for shrimp broodstocks in different countries with a ban on animal imports from regions with viral infection. Significant signs of acute WSD include a sudden drop in food intake, lethargy, and loosened cuticles with white spots 0.5 to 2.0 mm wide, visible beneath the carapace. In some cases, infected shrimp may exhibit a pink to reddish-

brown colour due to increased chromatophores. Additionally, white spots are occasionally observed in infected *P. vannamei* from America. This virus can infect mesodermal and ectodermal cells, such as the subcuticular epithelium, in various crustacean species, leading to inconsistent mortality rates. The virus spreads through vertical and horizontal transmission, including cannibalism of infected dead shrimp and water-borne pathways. Furthermore, vectors or reservoirs of WSSV include aquatic insect larvae, invertebrates, and copepods.

7.3 Infectious hypodermal and hematopoietic necrosis

Infectious hypodermal and hematopoietic necrosis (IHHN) is a viral disease affecting penaeid shrimp, caused by the Infectious hypodermal and hematopoietic necrosis virus, a member of the family *Parvoviridae*. This is the smallest known shrimp virus, measuring approximately 22 nm in diameter. It is a non-enveloped, icosahedral virus containing a single-stranded DNA (ssDNA) genome of about 3.9 kb. The pathogenicity varies with host species and developmental stage. In *P. stylirostris*, it can cause high mortality in juveniles, while adults typically exhibit low mortality but may show clinical signs such as reduced feeding, behavioural changes and stunted growth. In advanced stages, infected shrimp may develop a mottled bluish appearance with abdominal opacity. In *P. vannamei*, this infection is commonly associated with "Runt Deformity Syndrome" (RDS), characterized by reduced growth, cuticular deformities, bent rostrum, wrinkled antennae, rough exoskeleton, and formation of "bubble-head" structures. It targets ectodermal and mesodermal tissues, including the gills, hypodermis, connective tissues, nerve cord, lymphoid organ, and antennal gland. Transmission occurs both horizontally and vertically. Horizontal spread takes place through cannibalism of infected individuals and exposure to contaminated water, while vertical transmission occurs via infected broodstock passing the virus to their offspring through eggs.

7.4 Taura syndrome

Taura Syndrome caused by Taura Syndrome Virus (TSV), a member of the family *Dicistroviridae*, is a major viral pathogen affecting *P. vannamei* aquaculture. It is a small (≈32 nm), non-enveloped icosahedral virus with a positive-sense single-stranded RNA (+ssRNA) genome of about 10.2 kb. The whiteleg shrimp (*P. vannamei*) is highly susceptible, with mortality rates ranging from 40% to 90%, though several other penaeid shrimp species are also affected. Clinically, infection progresses through three phases *viz*., acute phase where in high mortality with symptoms like reddish discoloration, soft shell and empty gut seen, recovery phase characterized by melanized lesions and chronic phase with subclinical

persistent infection. The virus replicates in the cytoplasm and spreads mainly through horizontal transmission via contaminated water and cannibalism; vertical transmission is suspected but not yet confirmed. Certain aquatic insects, such as *Trichocorixa reticulata*, may act as vectors.

7.5 Infectious myonecrosis

Infectious myonecrosis (IMN) is an emerging viral disease of shrimp caused by the Infectious myonecrosis virus, a member of the family *Totiviridae*. It is a non-enveloped, icosahedral virus measuring approximately 40 nm in diameter, possessing a single double-stranded RNA (dsRNA) genome of about 7,560 base pairs. This disease can result in cumulative mortality rates ranging from 40% to 70%, particularly affecting juvenile and subadult shrimp. Clinically, infected shrimp exhibits lethargy, reduced feeding and loss of coordination. A characteristic feature of the disease is the presence of necrotic areas in the striated muscles, which appear as whitish to reddish regions, often making the shrimp visible near the water surface during daylight hours. The primary target tissues include striated muscles, hemocytes, lymphoid organ parenchyma and connective tissues. Transmission occurs mainly through horizontal routes including cannibalism of infected shrimp and exposure to virus-contaminated water facilitating rapid spread within culture systems.

7.6 Monodon baculovirus disease

Monodon baculovirus disease (MBD) is a viral infection in shrimp caused by the Monodon baculovirus, a rod-shaped, enveloped virus belonging to the family *Baculoviridae*. The virus contains a circular double-stranded DNA (dsDNA) of approximately 80 to 160 kbp. Although *P. monodon* is the primary host, infections have been reported in a wide range of crustaceans, including *Penaeus vannamei* and several other penaeid species. Although all developmental stages can be affected, the most susceptible to infection are the larval and juvenile shrimp. Infected shrimp exhibit reduced feed intake, stunted growth, lethargy and fouling of the body surface, often accompanied by a darkened appearance and are invariably smaller in size compared to healthy counterparts. It primarily infects the anterior midgut and hepatopancreas, leading to digestive abnormalities thereby reduced nutrient absorption. Transmission occurs mainly through horizontal routes, facilitating the spread of infection within culture systems.

7.7 Decapod iridescent virus 1 disease

Decapod iridescent virus 1 disease caused by Decapod iridescent virus 1 (DIV1), classified under the family *Iridoviridae* and genus *Decapodiridovirus*, is an emerging and highly pathogenic virus affecting a wide range of crustaceans. DIV1 is an enveloped, icosahedral double-stranded DNA (dsDNA) virus measuring approximately 150–158 nm, with a genome size of ~166 kb and at least 30 identified structural proteins. DIV1 has a remarkably broad host range, infecting multiple shrimp, prawn, crab, and crayfish species, with both natural and experimental infections reported. Clinically, infected crustaceans commonly exhibit empty gut, empty stomach, and pale hepatopancreas, along with signs such as soft shell, reddish discoloration, or characteristic white lesions. Mortality rates can reach up to 100% in susceptible species like *P. vannamei*. Transmission occurs horizontally, and its persistence in environmental conditions increases the risk of dissemination through contaminated feed and polyculture systems.

7.8 *Penaeus vannamei* solinvivirus disease

Penaeus vannamei solinvivirus (PvSV) is a recently described virus possesses a positive-sense RNA genome of approximately 10.4 kb. The virus shows broad tissue tropism, infecting hepatopancreas, gastrointestinal tract, lymphoid organ, and muscle. This disease was seen when shrimps were with 20-40 days of culture (DOC) weighing about 2 – 4 gm. Farmers observe graded mortality of about 4-5 piece in the morning and by the evening about 40-50 shrimps come to pond sides. Mortalities were usually observed after two to three days of post moult. As the mortality incidence, increases, farmers harvest the shrimp in fear of losing the crop. The genomic organization of PvSV closely resembles members of the family *Solinviviridae*. These findings suggest that PvSV represents an important addition to the emerging group of solinviviruses infecting shrimp, with potential implications for shrimp health and aquaculture biosecurity.

7.9 Vibriosis

This is one of the most important bacterial disease affecting shrimp aquaculture, contributing to substantial mortality in cultured shrimp populations. The disease is caused by Gram-negative bacteria belonging to the family *Vibrionaceae*, with several species like *Vibrio harveyi, Vibrio alginolyticus*, and *Vibrio parahaemolyticus*. The emergence and prevalence of vibriosis are often linked to over-intensification of shrimp farming practices, which can create stressful environmental conditions that favour bacterial proliferation and disease outbreaks. Clinically, vibriosis is characterized by reduced growth, lethargy and the presence

of opaque or whitish musculature. Additional signs include necrosis of appendages, empty gut, chromatophore expansion and the appearance of patches on the body surface.

7.10 Acute hepatopancreatic necrosis disease

Acute hepatopancreatic necrosis disease (AHPND), is a highly destructive bacterial disease that poses a serious threat to global shrimp aquaculture, leading to significant economic loss. It is caused by virulent strains of *V. parahaemolyticus*, a Gram-negative bacterium belonging to the family *Vibrionaceae*. The virulence of these strains is primarily attributed to the presence of plasmid, which harbours genes encoding binary toxins (PirA and PirB), along with transposons and conjugative transfer elements. This genetic makeup facilitates the horizontal transfer of virulence factors to other bacterial strains or species, raising concerns about the rapid dissemination of pathogenic traits. Infection is initiated when the bacteria colonize the shrimp gut, followed by the expression of plasmid-encoded toxins that specifically target the hepatopancreas. These toxins cause sloughing of the epithelial lining of hepatopancreatic tubules, resulting in tissue degeneration and the characteristic pale and atrophied appearance of the organ. Clinically, infected shrimp show reduced feed intake, empty gut, lethargy, sluggish or erratic (often spiral) swimming behaviour and a shrunken, pale hepatopancreas. Mortality is typically rapid and often occurs within the first 20–30 days of culture. Transmission of AHPND occurs horizontally through cohabitation with infected shrimp, ingestion of contaminated materials and exposure to pathogen-contaminated water.

7.11 Hepatopancreatic microsporidiosis

Hepatopancreatic Microsporidiosis is caused by the microsporidian parasite, *Ecytonucleospora hepatopenaei* (EHP) which infects the hepatopancreas of shrimp, particularly *Penaeus vannamei* and *Penaeus monodon*. Unlike many viral diseases, EHP does not usually cause high mortality, but it significantly affects growth, leading to severe stunting and size variation within cultured populations, resulting in economic losses. The primary target of this parasite is the epithelial cells of the hepatopancreas, impairing digestion and nutrient absorption. Infected shrimp often show poor growth rates, uneven sizes and reduced feed efficiency, with no obvious external clinical signs. Transmission occurs horizontally through ingestion of spores present in contaminated feed, faeces or infected shrimp tissues.

7.12 Running mortality syndrome (RMS) in shrimp:

Running Mortality Syndrome (RMS) is an emerging health condition reported mainly in *Penaeus vannamei* aquaculture, characterized by continuous, unexplained daily mortalities over an extended period rather than sudden mass die-offs. Farmers often describe it as

"running" mortality because deaths occur persistently day after day, leading to significant cumulative losses. The exact cause of RMS is not fully understood, but it is considered a multifactorial syndrome. Several studies suggest an association with viral agents, environmental stressors such as poor water quality, temperature fluctuations, high stocking density, and secondary bacterial infections (e.g., *Vibrio* spp.) may play a crucial role in triggering or exacerbating the condition. Clinical signs include gradual, continuous mortality (rather than acute outbreaks), lethargy and reduced feeding, empty gut and poor growth, occasionally pale or weak shrimp without clear gross lesions. Transmission mainly by horizontal via water and cohabitation and possible association with carrier shrimp or subclinical infections. RMS is not a single disease but a syndrome likely driven by viral associations and environmental stress, making integrated health management essential for its control in shrimp farming.

7.13 Management strategies

Biosecurity Measures

Biosecurity in shrimp aquaculture refers to a set of preventive measures aimed at excluding pathogens and reducing the risk of disease outbreaks. Key farm-level practices include proper pond preparation through drying and sun exposure, filtration and disinfection of water and regular monitoring of water quality. Physical barriers like fences and bird nets prevent the entry of potential carriers, while treatment of farm effluents minimizes environmental contamination. Routine health surveillance, including diagnostic methods, supports early detection of infections. Larger semi-intensive farms typically maintain higher biosecurity standards due to better infrastructure, controlled broodstock sourcing, and reduced reliance on antibiotics. In contrast, small-scale farms often face limitations in resources and technical expertise. To overcome these challenges, Better Management Practices (BMPs) have been developed as affordable and practical guidelines to improve disease control, enhance productivity, and promote environmentally sustainable shrimp farming. In recent years, Artificial Intelligence and Machine Learning, along with sensor and imaging technologies, are enhancing early disease detection and enabling more precise and efficient shrimp farming.

Specific pathogen free stocks

Specific Pathogen-Free (SPF) stocks are an important biosecurity tool in shrimp aquaculture, helps to reduce disease risks and improve productivity. The shrimp are produced under strict quarantine and screening to ensure they are free from specific high-risk pathogens such as White spot syndrome virus, Yellow head virus, Infectious hypodermal and hematopoietic

necrosis virus, Taura syndrome virus, and Infectious myonecrosis virus. Currently, large-scale SPF production is mainly available for *Penaeus vannamei*. However, SPF shrimp are not disease-resistant; they are only free from listed pathogens at the time of certification and may still be vulnerable to other or emerging infections.

Specific pathogen resistant stocks

Specific Pathogen-Resistant (SPR) stocks are shrimp genetically bred to resist specific pathogens, often showing minimal or no disease symptoms upon exposure. SPR reflects inherited disease resistance. Notably, *Penaeus vannamei* has shown strong resistance to TSV, while progress against WSSV remains moderate. Overall, SPR stocks are a key long-term solution for disease management, especially when combined with SPF stocks and strong biosecurity practices.

Probiotics

Probiotic use in shrimp aquaculture is an effective and sustainable alternative to antibiotics. Probiotics are beneficial live microorganisms added through feed or water to improve gut microbiota balance and enhance shrimp health. They help strengthen the immune response and reduce the prevalence of harmful bacteria. Studies show that healthy shrimp possess beneficial microbial communities, whereas diseased shrimp often harbour pathogenic microbes. Although probiotics have shown promising results in improving disease resistance, their effectiveness may vary depending on shrimp developmental stages and gut microbiota composition. Therefore, stage-specific probiotic application is recommended for optimal results in shrimp health management.

7.14 Diagnostic strategies for disease management in shrimp aquaculture

Shrimp disease diagnostics range from conventional methods like histopathology and microscopy to advanced molecular tools. Techniques such as PCR and RT-PCR provide highly sensitive detection of pathogens like White spot syndrome virus, while ELISA and lateral flow tests offer rapid, field-level diagnosis. To overcome limitations of cost and expertise, simple point-of-care methods like LAMP have been developed. Emerging technologies including CRISPR-based assays, biosensors, nanotechnology and AI-based analysis are further improving the speed, accuracy and on-site applicability of shrimp disease detection.

7.15 Further reading

Bateman KS, Stentiford GD (2017) A taxonomic review of viruses infecting crustaceans with an emphasis on wild hosts. *J Invertebr Pathol* 147:86–110.

Flegel TW (2012) Historic emergence, impact and current status of shrimp pathogens in Asia. *J Invertebr Pathol* 110:166–173.

Lee D, Yu YB, Choi JH, Jo AH, Hong SM, Kang JC, Kim JH (2022) Viral shrimp diseases listed by the OIE: A review. *Viruses* 14:585.

Shinn AP, Pratoomyot J, Griffiths D, Trong TQ, Vu NT, Jiravanichpaisal P, Briggs M (2018) Asian shrimp production and the economic costs of diseases. *Asian Fish Sci* 31:29–58.

Walker PJ, Mohan CV (2009) Viral disease emergence in shrimp aquaculture: Origins, impact and the effectiveness of health management strategies. *Rev Aquac* 1:125–154.

PRACTICAL

1. Tissue preservation for molecular analysis

1.1 Introduction

Collection, storage and archiving of specimens and tissue samples are prerequisites for the successful acquisition of molecular data for any systematic study. This chapter reviews the important practical aspects of the sampling and storage: 1) selection of appropriate tissues for nucleic acid extraction 2) storage of freshly collected tissues in the field 3) transportation, long-term storage and archiving of tissue samples.

1.2 Tissue samples

Sampling must ensure an accurate representation of the health status of the population or individual. The healthy animals should also be tested along with the diseased animals during sampling.

1.3 Tissue tropism

Tissue Tropism is the cells and tissues of a host which support growth of a particular virus. Some viruses have a broad tissue tropism and can infect many types of cells and tissues. Other viruses may infect primarily a single tissue. For example White Spot Syndrome Virus (WSSV) infects ectodermal and mesodermal origin tissues such as epidermis, gills, pleopod and hemolymph. But Monodon Baculovirus(MBV) infects only endodermal origin tissue hepatpancreas. So the selection of particular tissue type is mandatory in the accurate diagnosis of viral infection. The selected tissue of the organism should be relatively free of compounds potentially damaging to the nucleic acid or interfere with PCR. For example, Eye balls are known to contain PCR inhibitors.

1.4 Preservation of tissue

Fresh material from live animals consistently provides the highest yield and quality of DNA for amplification. The live animals or moribund animals can be frozen in dry ice and rapidly placed in the cold and away from light. The tissues should be packed in plastic cryotubes or Ziploc bags excluding as much air as possible to avoid cross contamination.

The tissue samples can routinely stored and transported in 95– 100% ethanol at ambient temperature for molecular studies. The larger size or exoskeleton of the animal does not allow the penetration of ethanol of the tissue and causes degradation of the tissues. These samples should be injected with ethanol, dissected into smaller pieces to allow the ethanol to diffuse directly into the internal tissues. There should be about 10 volumes of ethanol to 1volume of sample for the

proper preservation of the sample. Ethanol should be replaced after the initial fixation and periodically at a regular interval.

Long-term storage conditions should minimise variation in temperature. The animal tissues will remain indefinitely stable for extraction of nucleic acids at –70–80 °C.

This will allow the archiving of samples for reanalysis. There are also several commercial preservative available specifically to preserve nucleic acid in tissue.

1.5 Steps to avoid contamination

The investigator should be aware of the importance of keeping their instruments, containers and reagents clean in order to prevent cross-contamination. The individual tissue samples should be stored in separate containers. The investigator should Label and document all materials they collect with the details such as date of collection, collector, voucher number, etc with the permanent ink markers.

1.6 Target organ of DNA, RNA viruses, bacteria and fungus infecting shrimp

DNA Viruses	**Abbreviation**	**Target organ**	**Genome**
White spot syndrome virus	WSSV	Post larvae, Pleopod, gill, hypodermis , hemocytes	dsDNA
Infectious hypodermal haeamtopoietic necrosis virus	IHHNV	Post larvae, Pleopod, gill, hypodermis,haematopoietic tissues, lymphoid organ	ssDNA
Decapod iridescent virus 1	DIV 1	Post larvae, Hepatopancreas, stomach, gut	dsDNA
RNA Viruses	**Abbreviation**	**Target organ**	**Genome**
Yellow head virus	YHV	Post larvae, gill, gut, gonads, pleopod,hemocytes, lympoid organ	(+)ssRNA
Taura syndrome virus	TSV	Post larvae, gill, gut, striated muscle, pleopod, hypodermis, lympoid organ	(+)ssRNA
Infectious myonecrosis virus	IMNV	Post larvae, Skletal muscles, lympoid organ, hemocytes	(+)ssRNA
Bacteria	**Abbreviation**	**Target organ**	**Genome**
Acute Hepatopancreatic Necrosis Disease	AHPND	Post larvae, Hepatopancreas, gut	Plasmid
Necrotising Hepatopancreatitis bacterium	NHPB	Post larvae, Hepatopancreas, gut	dsDNA
Translucent Post larval Disease	TPD	Post larvae, Hepatopancreas, gut, Faeces	dsDNA
Fungi	**Abbreviation**	**Targer organ**	**Genome**
Enterocytozoon hepatopenaei	EHP	Post larvae, Hepatopancreas	ds DNA

2 Extraction of nucleic acid from shrimp tissue

2.1 Introduction

The extraction of DNA, RNA, and protein, is the most crucial method used in molecular biology. These biomolecules can be isolated from any biological material for subsequent downstream processes, analytical, or preparative purposes. In the past, the process of extraction and purification of nucleic acids used to be complicated, time-consuming, labour-intensive. Currently, there are many specialized methods that can be used to extract nucleic acids, such as solution-based and column-based protocols. Manual method has certainly come a long way over time with various commercial offerings. Automated systems designed for medium-to-large laboratories have grown in demand over recent years. It is an alternative to labor-intensive manual methods. The technology should allow a high throughput of samples; the yield, purity, reproducibility, and scalability of the biomolecules as well as the speed, accuracy, and reliability of the assay should be maximal, while minimizing the risk of cross-contamination.

2.2 Components

The role various components of nucleic acid extraction protocol is as follows:

A. The extraction buffer: It includes a detergent such as SDS which disrupts the cell membranes, a chelating agent such as EDTA which chelates the magnesium ions required for DNase activity, a buffer which is almost always Tris at pH 8 and a salt such as sodium chloride which aids in precipitation by neutralizing the negative charges on the DNA so that the molecules can come together.

B. Precipitation of nucleic acids: Alcohol precipitation is the most commonly used method for nucleic acid precipitation. This requires diluting the nucleic acid with a monovalent salt, adding alcohol to it and mixing gently. The nucleic acid precipitated spontaneously. Ethanol (twice the volume) or isopropanol (two thirds volume) are the standard alcohols used for nucleic acid precipitation.

C. Elution of nucleic acid: The nucleic acid pellet can be resuspended in either sterile distilled water or TE (10 mM Tris:1mM EDTA)

2.3 Protocol for isolation and purification of DNA using silica membrane spin column

Lysis: Transfer 0.2ml the lysis buffer in to a fresh micro centrifuge tube and take 20 to 100mg tissue sample and homogenize. Make up to 0.5ml with lysis buffer.

⇩

Incubate the sample at 95°C for 10 minutes.

⇩

Centrifuge the sample at 8,000 rpm for 5 min.

⇩

Take out 250µl of clear supernatant without disturbing the pellet in to a fresh tube and add 350µl neutralisation or binding buffer.

⇩

Centrifuge the sample at 8,000 rpm for 5 min.

⇩

Take out 350µl clear supernatant and add 350µl 100% isopropanol and mix thoroughly.

⇩

Apply the supernatant to the column and centrifuge at 8000 rpm for 1 min.

⇩

Wash the spin column with 700µl wash buffer 1.

⇩

Wash the spin column with 700µl wash buffer 2.

⇩

Discard the flow through and spin the column at 8000 rpm for 2 mins to dry the membrane completely.

⇩

Elute the DNA with 50µl water or TE buffer and quantity the DNA using Nano spectrophotometer.

2.4 Buffer Recipe

2.4.1 Tissue lysis buffer

Tris base (pH 8 – 8.5)	-	100mM
Sodium chloride	-	200mM
Sodium dodecyl sulfate	-	0.2%
EDTA	-	5mM

It can be stored at 4° C for up to 12 months.

2.4.2 Neutralisation buffer or binding buffer

5M guanidine hydrochloride	(477.65 gms)
0.5M Potassium acetate	(49.09 gms)

Dissolved the content in 500 ml distilled water. Adjust the pH of the solution to more or less 4.2 with acetic acid and make up the solution to 1000ml with distilled water and filter sterilise and store indefinitely at 4°C.

2.4.3 Wash buffer 1

Tris base (pH7.5)	-	2mM
Sodium chloride	-	20mM
EDTA	-	0.1mM

In 90 % ethanol

2.4.4 Wash buffer 2

Tris base (pH7.5)	-	2mM
Sodium chloride	-	20mM

In 70 % ethanol

2.4.5 Elution buffer

Tris base (pH 8)	-	10mM
EDTA	-	1mM

2.5 Protocol for isolation and purification of RNA using silica membrane spin column

Lysis: Transfer 0.2ml the TRIZOL reagent in to a fresh micro centrifuge tube and take 20 to 100mg tissue sample and homogenize. Make up to 0.5ml with TRIZOL reagent.

⇩

Incubate the homogenized sample for 5 minutes at room temperature to permit the complete dissociation of nucleoprotein complexes.

⇩

Add 0.2 ml of chloroform to the supernatant. Vortex samples vigorously for 15 seconds and incubate them at room temperature for 2 to 3 minutes.

⇩

Centrifuge the samples at 12,000 x g for 15 minutes at 2 to 4°C.

⇩

Take out 250µl of clear supernatant without disturbing the interphase in to a fresh tube and add 350µl neutralisation or binding buffer.

⇩

Centrifuge the sample at 8,000 rpm for 5 min.

⇩

Take out 350µl clear supernatant and add 350µl 100% isopropanol and mix thoroughly.

⇩

Apply the supernatant to the column and centrifuge at 8000 rpm for 1 min.

⇩

Wash the spin column with 700µl wash buffer 1.

⇩

Discard the flow through and spin the column at 8000 rpm for 2 mins to dry the membrane completely.

⇩

Discard the flow through and spin the column at 8000 rpm for 2 mins to dry the membrane completely.

⇩

Elute the RNA with 50µl water or TE buffer and quantity the RNA using Nano spectrophotometer.

2.6 Nucleic acid quantification

S. No.	Sample Code	DNA/RNA Code	Quantity in ng / µl	A260/280
1				
2				
3				
4				
5				
6				
7				
8				
9				
10				

3. Fractionation of nucleic acid by gel electrophoresis

3.1 Agarose electrophoresis

Agarose gel electrophoresis is a method of gel electrophoresis used in molecular biology to separate nucleic acids based on their size and charge. These gels are easy to cast and are widely used in laboratories. An agarose is a polysaccharide polymer material, generally extracted from seaweed. It is a linear polymer made up of the repeating unit of agarobiose, which is a disaccharide made up of D-galactose and 3,6-anhydro-L-galactopyranose. The melting temperature of agarose is 85-95 °C and gelling temperature of 35-42 °C. The nucleic acids have a net negative charge due to its phosphate back bone so they migrate towards the positive electrode in an electric field. The migration of nucleic acids affected by several factors like pore size of the gel, size of DNA being electrophoresed, the voltage used the ionic strength of the buffer, and the concentration of intercalating dye such as ethidium bromide.

3.2 Agarose gel preparations

3.2.1 To prepare a gel required quantities of agarose weighed and add in to the wide mouth glass conical flask with 1x TAE buffer and melt the mixture in the microwave oven, until it becomes clear without any gel particle.

3.2.2 Cool down the clear agarose gel under room temperature and add 1 µl ethidium bromide (10mg/ml) and slowly pour the gel into the gel mould. The volume of the gel varies from the size of the gel mould. The height of agarose gel only has to go above the bottom of the gel comb for about 0.3~0.5 cm, and thickness is suggested to be no less than 0.8 cm.

3.2.3 When agarose gel is completely solidified. Carefully remove blockers at both sides of the gel mould and place it in the gel tank containing 1x TAE buffer. After few minutes the comb will loosen up in the gel and can be carefully removed without damaging the wells. This agarose gel is ready for electrophoresis.

3.3 Electrophoresis

3.3.1 Add 1X TAE buffer over the gel box until the buffer level submerge the gel.

3.3.2 Load 5 µl each of the “PCR product-loading dye mixture” into each well. The mixture will sink to the bottom of the wells because its density is higher than

buffer. This step should be carefully handled in order to avoid cross contamination between the adjacent wells.

3.3.3 5 ul of DNA marker is loaded at the extreme end of the gel. The DNA molecular weight marker is served as reference to predict the size of the PCR product.

3.3.4 After loading of all the samples, the gel was electrophoresed at constant voltage between 70V~100V.

3.3.5 The loading dye in the kit contains 2 colorants: Bromphenol Blue gives deep blue color; Xylene Cyanol gives light blue color. When the dark blue dye approaches 1/2 to 2/3 of the gel, stop the electrophoresis. Then, remove the gel from the gel box to proceed with the EtBr staining procedures.

3.3.6 To avoid contamination, DO NOT re-use the gel electrophoresis buffer unless several gels will be used in the same day. When the electrophoresis is finished, wash the gel box with plenty of water.

3.4 Staining and visualization

The ethidium bromide intercalates into the major grooves of the DNA and fluoresces under UV light. So the gel can be viewed under trans-illuminator (254nm) to observe DNA bands. The exposure of DNA to UV radiation for as little as 45 seconds can produce damage to DNA and affect subsequent procedures such as cloning, *in vitro* transcription, and PCR. The exposure of the DNA to UV radiation therefore should be limited. The use of a higher wavelength of 365 nm UV light causes lesser damage to the DNA. The trans-illuminator apparatus fitted with image capture devices, such as a digital or polaroid camera allow an image of the gel to be stored in a computer or printed.

4. Translucent post larvae disease (TPD) - Taqman assay

4.1 Objective

The aim of this procedure is to provide guidance to detect the pathogenic agent Translucent Post larval Disease (TPD) in aquatic animals (Crustacean, Polychaetes, Faecal, Mollusc, Algae, Copepod, Artemia and Artemia Products, Post Larvae, Live/Frozen Shrimp and Crab, Feed, Feed additives for Aquaculture and selectively enriched culture) using Real-Time PCR (RT-PCR)

4.2 Definitions

4.2.1 Cycle threshold (Ct) – The cycle number at which the fluorescence passes a determined threshold

4.2.2 Positive control (PC) – The PC typically consists of the plasmid construct with respective target sequence. The successful performance of this control (Ct value falls within pre-defined ranges) set indicates that the PCR reaction was properly performed and all components of master mix are working properly

4.2.3 No template control (NTC) – The successful performance of this control (Ct value undetermined or zero) indicates that contamination did not occur during the PCR master mix setup protocol. Nuclease-free water serves as the NTC, as the NTC does not contain template

4.2.4 Method control (MC) - Successful performance of this control (Ct value undetermined or zero) indicates that contamination did not occur during the PCR template and positive control addition protocol. Nuclease-free water serves as the NTC, as it does not contain template

4.3 Materials required

- PCR stripes or plates
- TaqMan probe master mix
- Primers and probe
- Sterile water

4.4 Equipment required

- Micro Pipette (2.5µl, 10µl, 20µl, 100µl, 200µl)
- Real-Time –PCR thermal cycler

4.5 Storage of kit components

- Primer Probe mix – store -20°C and protect from light
- Mastermix – store at -20°C for long term storage. Avoid repeated freeze thawing may reduce the sensitivity of the assay.
- Lysis buffer can be stored at room temperature

4.6 Primer

Pathogen/ Target gene	Primer Name	Primer/probe (5'–3')
TPD	VHVP-F	5'-ACA-CCC-AAT-ACT-CCA-AAC-GAC-3'
	VHVP-R	5'-AAC-TCC-CGA-AAT-CCG-TCA-AG-3'
	VHVP-P	6FAM- 5'-AGG-CAT-GGA-CCG-TAA-AGC-TCT-CAC-3'-BHQ- 3
House keeping gene	EF94 F	5'-CAAGATCTGTAAGCTCTCGGT-3'
	EF94 R	5'-CTTGCCAGAGTCTACGTG-3'
	EF94 Probe	6 HEX 5'- TGGATCTTCTCCTTGCCCATGGTTG -BHQ- 3'

4.7 Samples

- Specimens for testing for infection with WSSV are aquatic animals (Crustacean, Polychaetes, Faecal, Mollusc, Algae, Copepod, Artemia and Artemia Products, Post Larvae, Live/Frozen Shrimp and Crab, Feed and Feed additives for Aquaculture)
- Samples such as pleopods, gills, haemolymph, stomach and abdominal muscle of crustacean are recommended for submission
- Haemolymph, faeces or excised pleopods may be collected and used when non-lethal testing of valuable broodstock is necessary
- Selective enrichment of *Vibrio parahaemolyticus* (Vp_{TPD})
- This bacterium grows rapidly in high levels of bile salts and alkaline conditions. Therefore, alkaline peptone water (APW) supplemented with 1.5–2.5% of sodium chloride (NaCl). The target organ such as hepatopancreas, gut and faeces were aseptically dissected out and inoculated into the broth and incubated at 37°C for 18 hrs. The medium will become turbid due to growth of the bacterium. The bacterial culture was centrifuged at 5000 rpm for 5 minutes. The supernatant was discarded and the bacterial pellet will be used for extraction of DNA.

4.8. Procedure

4.8.1 PCR reaction

- Wear disposable powder free gloves and at all times when handling plates / strips/tubes. Avoid contaminating plates with tissue lint etc. Determine the number of reaction (N) to set up per assay in addition include positive, negative and method control in the test
- Prepare one excess reaction cocktail for every 10 reactions to account for pipetting error, if no. of samples (n)including controls =1 to 10, then N = n + 1
- Prepare the master mix in PCR work station in the reagent preparation room by following the table below:

Reagents	Volume 1x Reaction (10µl)
Sterile water	3.6µl
2X Taq Master mix	5.0 µl
WSSV Primer probe mix	0.2 µl
EF 94 primer probe mix	0.2 µl
DNA Template (100 to 200ng)	1.0 µl
Total	10.0 µl

- A master mix is prepared in a tube by combining a 2X master mix reagent and primer and probe mix with water (protect from light)
- After mixing thoroughly 9 µl volumes of the master mix are quickly dispensed into the plate / strips/ tubes
- Before moving to template addition PCR work station, Add 2 µl of the sterile water into NTC (negative control) tube
- In the template addition UV cabinet add 1 µl of sterile water to method control tube. Add
- 1 µl of each DNA sample to respective well as per plate/strips/tubes set up
- Finally add 1 µl of positive plasmid template into positive control tubes in positive control UV cabinet
- Centrifuge the tubes for 10 sec to remove bubbles trapped in the reaction tubes
- Amplification is performed with the Real time PCR thermal cycler. The cycling profile is as follows

Cycling steps	Temperature	Time	No. of cycles
Step 1	95° C	30 sec	1
Step 2	95° C	5 sec	40
	60° C	31 sec	

4.9 Data analysis

After completion of the amplification reaction, amplification plots must be critically assessed. The baseline and the threshold can be set either automatically or manually. The threshold should be placed above the background fluorescence noise, across the exponential phase of all the amplification curves. The PTC with a known target concentration can act as a calibrator to enable standardization of data analysis and an approximate estimation of the viral load.

The test reliability is assured by analyzing the results of the controls. If the controls did not yield the expected results the causative reason must be investigated and corrective must be taken,

Controls	Expected results	Corrective action to be taken
Positive control	Positive, there must be an increase in fluorescence from the FAM fluorophore yielding a sigmoidal amplification curve at the expected Ct value	Repeat the test from the nucleic acids extraction and check the positive control stock
Negative control	Negative, i.e. absence of fluorescence increase from the FAM fluorophore, with no sigmoidal amplification curve	Repeat the test from the nucleic acids extraction and check all the nucleic acid extraction reagents and disinfect the nucleic acid extraction, template addition chambers.
Method control	Negative, i.e. absence of fluorescence increase from the FAM fluorophore, with no sigmoidal amplification curve	Repeat the test from the nucleic acids extraction, check or change all the PCR reagents.

4.10 Interpretation of results

The following criteria must be followed for data interpretation of diagnostic samples.

Results	Interpretation
Increase in fluorescence from the FAM fluorophore yielding an amplification curve with Ct ≤ 37th cycle.	Positive
Absence of fluorescence increase from the FAM fluorophore, with no sigmoidal amplification curve	Negative
Weak increase in fluorescence from the FAM Fluorophore yielding a sigmoidal amplification curve with Ct between 38th and 40th cycle.	Inconclusive, repeat the test from the nucleic acids extraction

Plate display

	1	2	3	4	5	6	7	8	9	10	11	12
A												
B												
C												
D												
E												
F												
G												
H												

5. Translucent post larvae disease (TPD) - PCR assay

5.1 Objective

The aim of this procedure is to provide guidance to detect the pathogenic agent Translucent Post larval Disease (TPD) in aquatic animals (Crustacean, Polychaetes, Faecal, Mollusc, Algae, Copepod, Artemia and Artemia Products, Post Larvae, Live/Frozen Shrimp and Crab, Feed and Feed additives for Aquaculture) using PCR.

5.2 Definitions

5.2.1 Positive control (PC) – The PC typically consists of the plasmid construct with respective target sequence. The successful performance of this control (Ct value falls within pre-defined ranges) set indicates that the PCR reaction was properly performed and all components of master mix are working properly

5.2.2 No template control (NTC) – The successful performance of this control (Ct value undetermined or zero) indicates that contamination did not occur during the PCR master mix setup protocol. Nuclease-free water serves as the NTC, as the NTC does not contain template

5.2.3 Method control (MC)- Successful performance of this control (Ct value undetermined or zero) indicates that contamination did not occur during the PCR template and positive control addition protocol. Nuclease-free water serves as the NTC, as it does not contain template

5.3 Equipment / Instruments

- Autoclave
- Micropipettes (2.5, 10, 100, 200, 1000 µL)
- Spectrophotometer
- Refrigerated centrifuge
- Thermal cycler
- Gel electrophoresis system
- Gel doc or UV transilluminator with desk top PC

5.4 Reagents

- 2x PCR master Mix (Taq DNA Reaction Mix)
- primers
- WSSV positive control
- Ladder - 100 bp

- Agarose
- 6x gel loading dye
- Green R DNA Gel stain
- 1x TAE buffer (0.4M Tris-acetate, 1 mM EDTA)

5.5 Storage of kit components

- 2x PCR master Mix, Primers & DNA ladder – store -20°C
- Positive control – store at -20°C in a separate refrigerator.

5.6 Primers

Oligonulceotide	Sequence (5'- 3')	Amplicon size	Reference
vhvp-2 F1	GGAGTATTGGTGGGCTGAAA	351 bp	Tianchang Jia et al. (2024), Aquaculture 583 (2024) 740583
vhvp-2 R1	GGTAGGCATGGACCGTAAAG		

5.7 Samples

- Specimens for testing for infection with WSSV are aquatic animals (Crustacean, Faecal, Post Larvae, Live/Frozen Shrimp and Crab, Feed and Feed additives for Aquaculture)
- Samples such as pleopods, gills, haemolymph, stomach and abdominal muscle of crustacean are recommended for submission
- Haemolymph, faeces or excised pleopods may be collected and used when non-lethal testing of valuable broodstock is necessary

5.8 Selective enrichment of *Vibrio parahaemolyticus* (Vp_{TPD})

This bacterium grows rapidly in high levels of bile salts and alkaline conditions. Therefore, alkaline peptone water (APW) supplemented with 1.5–2.5% of sodium chloride (NaCl). The target organ such as hepatopancreas, gut and faeces were aseptically dissected out and inoculated into the broth and incubated at 37°C for 18 hrs. The medium will become turbid due to growth of the bacterium. The bacterial culture was centrifuged at 5000 rpm for 5 minutes. The supernatant was discarded and the bacterial pellet will be used for extraction of DNA.

5.9 Procedure

5.9.1 Isolation of DNA

- Nucleic acid extraction performed according to the DNA Extraction in the nucleic acid extraction room.

5.9.2 PCR reaction

- Perform PCR reaction with the given primers for WSSV gene Determine the number of reactions (N) to set up per assay In addition include Negative control and Positive control in the test
- Prepare excess reaction cocktail to account for pipetting error If number of samples (n) including controls = 1 to 10, then N=n+1
- In the clean reagent preparation room prepare the master mix: Prepare the reaction mix with the following amount of each reagent and the primer set

Component	Volume (µl)
Nuclease free water	8.5
Taq DNA reaction mix	12.5
Forward primer	1.0
Reverse primer	1.0
Template DNA	2.0
Total	25.0

- Mix reaction mixtures by pipetting up and down Do not vortex
- Centrifuge for 5-6 seconds to collect contents at bottom of the tube, and then place the tube in cold rack
- Set up reaction tubes in PCR rack
- Dispense 23 µl of each master mix into each PCR tubes
- Before moving to nucleic acid handling area Add 2 µl of the nuclease free water in to NTC (No template control) tubes Cap NTC tubes
- In the Pre-PCR room, add 2 µl of each sample to respective tubes as per the set up
- Cap the PCR tubes to which the samples have been added
- Finally, pipette 2 µl of positive plasmid template control into positive template control (PTC) tubes in positive control addition area Cap PTC tubes Centrifuge the tubes for 10 seconds Make sure that bubbles are eliminated from the bottom of the reaction tubes
- The reaction volume is 25 µl Program schedule as follows:

Cycling steps	Temperature	Time	No. of cycles
Step 1	95° C	5 min	1
Step 3	95° C	30 sec	35
	60° C	30 sec	
	72° C	1 min	
Step 3	72° C	5 min	1
Step 4	4° C	Infinite hold	

- After completion PCR run, analyse the amplified product by agarose gel electrophoresis in Post - PCR room
- After completion of PCR, either it can be preserved in 4°C for further analysis

10. Data analysis

- The amplified product should be resolved through an agarose gel electrophoresis with appropriate DNA ladder to find out the exact size of the amplified PCR amplicon in post-PCR room.
- The test reliability is assured by analyzing the results of the controls. If the controls did not yield the expected results the causative reason must be investigated and corrective must be taken,

Controls	Expected results	Corrective action to be taken
Positive control	Positive, there must be an amplicon of 351bp length.	Repeat the test from the nucleic acids extraction and check the positive control stock
Negative control	Negative, there should be any amplification	Repeat the test from the nucleic acids extraction and check all the nucleic acid extraction reagents and disinfect the nucleic acid extraction, template addition chambers.
Method control	Negative, there should be any amplification	Repeat the test from the nucleic acids extraction, check or change all the PCR reagents.

10.1 Interpretation of results

The following criteria must be followed for data interpretation of diagnostic samples.

Results	Interpretation
Clear DNA band of 351bp length	Positive
Absence of any clear band at around 351bp length	Negative
Weak DNA band at the range of around 351bp length	Inconclusive, repeat the test from the nucleic acids extraction

NOTES

NOTES

NOTES

NOTES

NOTES

NOTES

Aquaculture 583 (2024) 740583

Contents lists available at ScienceDirect

Aquaculture

journal homepage: www.elsevier.com/locate/aquaculture

Prevalence investigation of translucent post-larvae disease (TPD) in China

Tianchang Jia [a,b], Shuang Liu [a], Xingtong Yu [a], Tingting Xu [a], Jitao Xia [a], Wenxiu Zhao [a], Wei Wang [a], Jie Kong [a,b], Qingli Zhang [a,b,*]

[a] State Key Laboratory of Mariculture Biobreeding and Sustainable Goods; Key Laboratory of Maricultural Organism Disease Control, Ministry of Agriculture; Qingdao Key Laboratory of Mariculture Epidemiology and Biosecurity; Yellow Sea Fisheries Research Institute, Chinese Academy of Fishery Sciences, Qingdao, Shandong 266071, China

[b] Laboratory for Marine Fisheries Science and Food Production Processes, Laoshan Laboratory, Qingdao, Shandong 266237, China

ARTICLE INFO

Keywords:
Shrimp
Translucent post-larvae disease (TPD)
Clinical epidemiological investigation
Pathogenic strain diversity

ABSTRACT

In early 2020, the shrimp farming in China suffered a severe setback due to an outbreak of the translucent post-larvae disease (TPD) in *Penaeus vannamei*. The emerging disease was caused by a hypervirulent strain of *Vibrio parahaemolyticus* (Vp_{TPD}). Although some progress has been made in understanding virulence factors of Vp_{TPD}, the diversity and prevalence of TPD pathogen are still unclear. Therefore, this study was undertaken to systematically investigate the epidemiology of TPD in China. In this study, potentially pathogenic bacteria present in naturally infected shrimp samples were isolated, identified, and preserved firstly. The further investigation showed that different *Vibrio* species carrying the key virulence genes of Vp_{TPD} can infect post-larvae of *P. vannamei* and cause TPD, revealing the diversity of TPD pathogens, and the pathogenic *Vibrio* strains has been temporarily named as *Vibrio* causing TPD (V_{TPD}). In addition, epidemiological surveillance based on TaqMan qPCR detection and histopathology techniques analysis showed that V_{TPD} positive samples were detected in most shrimp aquaculture ponds in different shrimp aquaculture provinces of China, with prevalence rate exceeding 50% in some areas. And seawater cultured species such as *P. vannamei* and *P. japonicus* were more sensitive to V_{TPD} and were more likely to be infected or carry it. Freshwater cultured shrimp such as *Macrobrachium rosenbergii* and *Procambarus clarkii* may not be affected by V_{TPD}. However, shrimp bait organisms are still at risk of carrying or being infected with V_{TPD}. The result suggests that V_{TPD} is still prevalent and spreading in coastal shrimp farming areas in China, with a high risk of transmission. This effort of present study provided a basic epidemiological understanding as well as important technical insights for prevention and management of emerging shrimp diseases.

1. Introduction

In early 2020, a disease called "translucent post-larvae disease" (TPD) emerged on a large scale in the major shrimp farming areas of southern China. This disease primarily affected the post-larval stages P_5-P_7 of *Penaeus vannamei*, with a short outbreak duration and high mortality rates (He, 2020; Huang, 2020; Zou et al., 2020). Within three days of symptom onset, morbidity and mortality rates could reach up to 90%. The disease was highly infectious, causing affected *P. vannamei* juveniles to stop feeding and exhibit reduced vitality. The hepatopancreas appeared pale, and the midgut and stomach were empty. The body colour changed from the cephalothorax to the abdominal segments, becoming transparent or semi-transparent. The disease then spread rapidly to the coastal aquaculture areas of northern China, showing a rapidly epidemic trend (Harkell, 2020a; Harkell, 2020b). A new and highly virulent strain of *Vibrio parahaemolyticus*, known as *V. parahaemolyticus* causing TPD (Vp_{TPD}), was found to be responsible for the disease (Zou et al., 2020).

By pathogenicity analysis of different molecular weight proteins of Vp_{TPD} on the post-larvae of *P. vannamei*, combining with mass spectrometry analyses, comparative genomic analysis, epidemiological investigation and challenge test of Vp_{TPD}, Liu Shuang et al. identified the novel virulence protein, *vibrio* high virulent protein (VHVP), as the potential key virulence factors of Vp_{TPD}. VHVP-2, encoded by the virulence genes *vhvp-2* located on a 187, 791 bp plasmid, was identified as the key virulence factor of Vp_{TPD} and indispensability for the lethal virulence of *V. parahaemolyticus* to shrimp post-larvae (Liu et al., 2023). Actually, further analysis of this plasmid based on comparative genomics and

* Corresponding author at: Yellow Sea Fisheries Research Institute, Chinese Academy of Fishery Sciences, Qingdao, Shandong 266071, China.
E-mail address: zhangql@ysfri.ac.cn (Q. Zhang).

https://doi.org/10.1016/j.aquaculture.2024.740583
Received 25 October 2023; Received in revised form 1 January 2024; Accepted 14 January 2024
Available online 16 January 2024

mass spectrometry, we found except the key virulence gene of *vhvp-2* encoding the VHVP-2 protein (containing the conserved toxin domains SpvB and TcdB), there are two other potential virulence genes of *vhvp-1*encoding the VHVP-1 protein (molecular weights (MWs) > 100 kDa) and *vhvp-3* encoding the potential virulent protein (MWs about 100 kDa) in the virulence 187, 791 bp plasmid. Although vhvp-1 and vhvp-3 were not proved to be the key virulence gene of Vp_{TPD} in the previous study, their function in the lethal virulence to post-larvae shrimp is worth of exploring further.

According to the prediction result of the encoding genes in 187, 791 bp plasmid by using the online Conserved Domain Search Service (CD Search) in NCBI, the potential virulent factor VHVP-1 possessed the conserved domains of Tc toxin complex TcA related domain, neuraminidase-like domain and *Salmonella* virulence plasmid 28.1 kDa A protein, while the potential virulent factor VHVP-3 possessed the conserved TccC related domain. Considering the TcA and TccC domains are important component of toxin (Lyerly et al., 1982; Zhan et al., 2016), the function in the lethal virulence to post-larvae shrimp of their related genes in the Vp_{TPD} 187, 791 bp plasmid are interesting and worth in-depth study.

From 2021 to 2022, we conducted the isolation, identification and pathogenicity analysis of bacterial pathogens potentially responsible for TPD infections in shrimp collected from different provinces in China for understanding the basic biological characteristics of this pathogen. Meanwhile, to determine the prevalence of this disease in major shrimp farming species and different shrimp farming regions in China, this study conducted a molecular epidemiological investigation of TPD from 2021 to 2022, based on molecular biological analysis (PCR and real-time PCR) and histopathological analysis.

2. Materials and methods

2.1. Sample collection and experiment shrimp

Between March 2021 and December 2022, a total of 694 samples were collected from ten different provinces across China. For shrimp, the shrimp samples were promptly and accurately segmented into cephalothorax and abdominal portions along the central axis of the shrimp body. One portion, including a fraction of the hepatopancreas, a piece of abdominal muscle, and an eyestalk, was placed in a fixative solution containing 4% PFA-PBS (Sinopharm, Beijing, China) for tissue pathology analysis (Fig. 4a). The remaining hepatopancreas, gills, muscles, appendages, and other tissues were minced and mixed together. Then, 30 mg of the issue mixtures were extracted and placed in 95% ethanol for nucleic acid extraction (Zhang et al., 2017), and some tissue mixtures are used for the isolation of potential pathogens (2.3 for details). For post-larvae, 3–5 prawns were mixed and preserved in 95% ethanol for DNA extraction; another 2–3 individuals were cut transversely and fixed in 4%PFA for subsequent histopathological observation. To avoid cross-contamination, disposable gloves, blades, culture dishes, and other tools should be changed before collecting the next sample to avoid cross-contamination.

Specific pathogen free post-larvae shrimp (P_5-P_7, body length 7–9 mm) were obtained from a shrimp farm situated in Weifang, Shandong Province, and reared for two days before being used in the challenge test.

2.2. DNA extraction and real-time qPCR detection of Vp_{TPD}

Tissue genomic DNA was extracted using the TIANamp Bacteria DNA Kit (TIANGEN BIOTECH, Beijing, China).

The Vp_{TPD} real-time qPCR was performed using a BIORAD CFX96 Touch Real-Time PCR Detection System (BIORAD, Hercules, CA, USA) following the Roche® FastStart Essential DNA Probes Master instructions. Reaction parameters included an initial denaturation at a temperature of 95 °C for 1 min, followed by 40 cycles of denaturation at 95 °C for 10 s, and annealing and extension at a temperature of 55.7 °C for 25 s. The 20 μL reaction mixture contained 8 μL of FastStart Essential DNA Probes Master (2×), 8.6 μL of FastStart Essential DNA Probes Master (H_2O), 0.8 μL of primers and probe (0.4 μM each), and 1 μL of genomic DNA (Wang, 2022).

2.3. Bacteria isolation

The diseased shrimp in the feeding tank were disinfected with 75% alcohol, and then washed three times with PBS buffer. Then, part of the hepatopancreas, intestines and muscles were removed and mixed, and 30 mg tissue mixtures were homogenized with 0.5 mL sterile PBS buffer. 30-50 μL tissue solution was uniformly spread over TSA medium (for mariculture shrimp) or LB solid medium (for freshwater shrimp) and incubated at 28 °C (TSA medium) or 37 °C (LB solid medium) for 18–24 h. Individual colonies were selected from the colony-filled medium and inoculated onto fresh TSA or LB medium. Incubation was carried out at the above-mentioned temperature for 18–24 h. The purified single colony was then inoculated into TSB medium or LB liquid medium, and incubated in a shaker at 28 °C (TSB medium) or 37 °C (LB liquid medium) with a rotation speed of 180 r/min for 18–24 h to prepare bacterial suspension. Isolated bacteria were stored in broth containing 20% glycerol at −80 °C (Fig. 2a).

2.4. PCR amplification and sequencing of specific genes of bacteria

In order to better understand the prevalence and function of the potentially virulent related genes in the Vp_{TPD} 187, 791 bp plasmid (Fig. 1a), the PCR primer sets were designed targeting the related gene sequence encoding the TcA related domain in the *vhvp-1* gene, targeting the related gene sequence encoding the SpvB related domains in the *vhvp-2* gene, and targeting the related gene sequence encoding the TccC related domain in the *vhvp-3* gene (Fig. 1b). PCR amplification of various genes in bacterial strains was performed according to the instructions of Premix Ex Taq Version 2.0 (TaKaRa, Dalian). These genes included 16S rRNA and VHVP-1-P, VHVP-2-P, and VHVP-3-P, which are associated with Vp_{TPD} pathogenicity. Primers listed in Table 1 were used in this study.

A 25 μL PCR reaction mixture contained 12.5 μL of Premix Ex Taq, 0.5 μL of each forward and reverse primer (10 μM), 1 μL of template DNA, and 10.5 μL of ddH_2O. The amplification conditions were as follows: initial denaturation at 95 °C for 5 min; denaturation at 95 °C for 30 s, appropriate annealing temperature for 30 s, extension at 72 °C for a specified time, for 35 cycles; final extension at 72 °C for 10 min.

For the 16S rRNA gene, the annealing temperature was 54 °C, and the extension at 72 °C was for 90 s (Yi-Lin et al., 2015; Miller et al., 2013). For VHVP-1-P and VHVP-3-P, the annealing temperature was 58 °C, and the extension at 72 °C was for 30 s. For VHVP-2-P, the annealing temperature was 60 °C, and the extension at 72 °C was for 1 min.

The PCR products were separated using 2% agarose gel electrophoresis, purified using a gel recovery kit (OMEGA, USA), and then ligated into the pMD18-T vector (TaKaRa, Dalian, China) for transformation. Positive clones were sent to Sangon Biotech (Shanghai, China) for sequencing. The nucleotide sequences were compared and analyzed using the BLAST tool in NCBI.

2.5. Experimental challenge by immersion

Prior to the experiment, the experimental strains were cultured in Tryptic Soy Broth (TSB+) supplemented with additional NaCl and incubated overnight at 28 °C. The resulting bacteria were centrifuged at 6000 rpm/min for 10 min, washed with sterile seawater, and resuspended in sterile seawater three times. The cell density was measured by spectrophotometry at a wavelength of 600 nm and adjusted to 1.0, corresponding to approximately 1×10^9 cells/mL. The value obtained

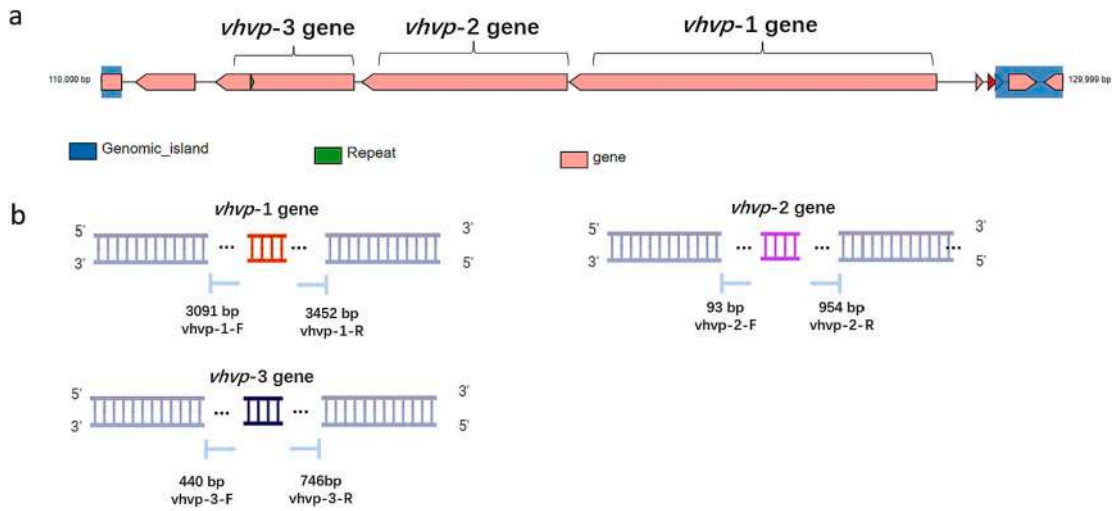

Fig. 1. The virulence 187, 791 bp plasmid contains three potential virulence genes (*vhvp*-1, *vhvp*-2 and *vhvp*-3). (a) The loci of *vhvp*-1, *vhvp*-2 and *vhvp*-3 genes in the virulence 187, 791 bp plasmid. (b) Three potential virulence genes (*vhvp*-1, *vhvp*-2 and *vhvp*-3) and the detection primers targeting the vhvp genes.

Table 1
Primers sequences of 16S rRNA, VHVP-1-P, VHVP-2-P, VHVP-3-P, *rct*B, *rpo*D and *tox*R for PCR.

Gene	Primer	Primer Sequences (5′-3′)
qPCR	VHVP-F	AGGCATGGACCGTAAAGCTCTCAC
	VHVP-R	AACTCCCGAAATCCGTCAAG
	Probe	ACACCCAATACTCCAAACGAC
16S rRNA	27F	*AGAGTTTGATCCTGGCTCAG*
	1492R	*GGTTACCTTGTTACGACTT*
VHVP-1-P	**VHVP-1-P -F**	ACGACTGACCCGGTACGCATGTAYATGMGNGARATGGGNACNGT
	VHVP-1-P -R	ATAGAAATAACCAGACGTAAGTTNGCYTCNACCATYTCYTTYT
VHVP-2-P	**VHVP-2-P -F**	GGAGTATTGGTGGGCTGAAA
	VHVP-2-P -R	GGTAGGCATGGACCGTAAAG
VHVP-3-P	**VHVP-3-P -F**	AGAGTTTGATCMTGGCTCAG
	VHVP-3-P -R	GGYTACCTTGTTACGACTT
*rpo*D	*rpo*D-F	ACGACTGACCCGGTACGCATGTAYATGMGNGARATGGGNACNGT
	*rpo*D-R	ATAGAAATAACCAGACGTAAGTTNGCYTCNACCATYTCYTTYT
*rct*B	*rct*B-F	ATHGARTTYACNGAYTTYCARYTNCAY
	*rct*B-R	YTTNCTYTGHATNGGYTCRAAYTCNCCRTC
*tox*R	*tox*R-F	GANCARGGNTTYGARGTNGAYGAYTC
	*tox*R-R	TTDKKTTGNCCNCYNGTVGCDATNAC

was then confirmed using the plate count dilution method as described by Bogosian et al. (2000). Finally, the bacteria were diluted in sterile seawater to a concentration of 1×10^4 CFU/mL.

The concentration of the artificial infection bacterial suspension was set at 1×10^4 CFU/mL to study the pathogenicity of different strains on shrimp larvae. Healthy shrimp larvae were randomly selected and placed in groups of 20 individuals in a 1 L beaker, each group receiving a different bacterial suspension. At the same time, a positive control group (inoculated with *Vp*-JS20200428004–2) and a negative control group (inoculated with sterile seawater only) were set up. Each group had three replicates and was aerated for 24 h, with normal feeding twice a day. Disease development and mortality rate were recorded every eight hours, and the median lethal time (LT_{50}) was then calculated. Dead shrimps were immediately removed, fixed in 4% paraformaldehyde solution, and subjected to tissue pathology analysis. Additionally, some moribund shrimps were isolated, cultured, purified, and identified to confirm whether the pathogenic bacteria were virulent strains.

2.6. Bacteria identification

After identifying the genus-level classification of the bacterial strain by analyzing the 16S rRNA gene sequence, we subjected the strains selected from the artificial infection experiments to strain identification using Multiple Locus Sequence Analysis (MLSA). The approach of Pascual et al. was followed, in which three protein-coding genes (*rct*B, *rpo*D, and *tox*R) were analyzed (Javier et al., 2010). The sequences of the three genes were concatenated and aligned, and the resulting concatenated sequences were used to construct a phylogenetic tree through the neighbor-joining algorithm with bootstrap analysis (1000 replicates) in MEGA7.

The various genes of the strains, including 16S rRNA and the three protein-coding genes (*rct*B, *rpo*D, and *tox*R), were amplified using the boiled bacterial supernatant as a template according to the instructions of Premix Ex Taq Version2.0 (TaKaRa, Dalian). According to previous reports, the conserved *rct*B and *rpo*D gene sequences were obtained through a thermal program: (i) 95 °C for 5 min; (ii) 10 cycles of 95 °C for 1 min, 54 °C for 2 min, and 72 °C for 1 min 15 s; (iii) 25 cycles of 95 °C for 35 s, 54 °C for 2 min, and 72 °C for 1 min 15 s; (iv) extension step at 72 °C for 10 min. The amplification of the *tox*R fragment was performed by the touchdown PCR method: (i) 95 °C for 5 min; (ii) 8 cycles of 95 °C for 1 min, 62 °C for 2 min, and 72 °C for 1 min 15 s, with 1 °C dropper cycle; (iii) 27 cycles of 95 °C for 35 s, 54 °C for 2 min, and 72 °C for 1 min 15 s; (iv) extension step at 72 °C for 7 min (Javier et al., 2010).

2.7. Histopathological section

The samples of cephalothorax and abdominal muscles were incubated in a 4% paraformaldehyde fixative for 24 h, followed by transfer

to 70% ethanol. Paraffin sections were prepared and stained with H&E using the histological methods outlined by Lightner (1996). Afterwards, the histological sections were examined and imaged using a light microscopy system (Nikon Eclipse E80i, Nikon Co., Tokyo, Japan).

3. Result

3.1. Isolation and detection results of potential pathogens

A total of 448 potentially pathogenic bacteria strains were isolated, purified and identified from shrimp samples collected from different provinces and cities. The most common bacteria specie was *Vibrio* spp. which accounted for 53.79% (241/448) of the total. Subsequently, 9 strains carrying potential virulence genes of Vp_{TPD} were selected from the aforementioned 448 bacteria using PCR detection method, and the sequence analysis of 16S rRNA gene showed that all the 9 strains belonged to *Vibrio*. Among these 9 potentially pathogenic bacteria strains, 2 strains carried three suspected virulence genes (*vhvp*-1, *vhvp*-2 and *vhvp*-3), 4 strains carried two suspected virulence genes, and 3 strains carried a single suspected virulence gene (Table 2.).

3.2. Pathogenicity of the strains carrying virulence gene of Vp_{TPD} determined by the challenge test

Following immersion infection with corresponding bacterial strains, all at a concentration of 10^4 CFU/mL, the positive control group of shrimps (*Vp*-JS20200428004-2) experienced mortality within 64 h, showing typical clinical symptoms of TPD. In contrast, the blank control group showed no obvious symptoms or mortality throughout the entire experiment, with the shrimp remaining healthy. Among the bacterial strains tested, the experimental groups of 20220614001-2, 20220614004-1, and 20220614009-1 showed a clear cumulative mortality curve that was similar to the positive control group (*Vp*-JS20200428004-2) (Fig. 2b). Additionally, these three experimental groups of shrimps showed typical clinical signs of TPD in the early, middle, and late stages of infection (Fig. 2c). Histopathological results of the tissue sections were consistent with those of naturally diseased shrimp groups. Other groups showed no significant mortality or only a few shrimp deaths without showing typical TPD symptoms.

Subsequently, IBM SPSS Statistics 27 was then used to calculate the median lethal time (LT_{50}) and 95% confidence intervals. The results of *Vp*-JS20200428004-2 and the three strains (20220614001-2, 20220614004-1, and 20220614009-1) at a concentration of 10^4 CFU/mL on post-larvae of *P. vannamei* were as follows: 32.3 h (29.0—35.5), 37.0 h (33.4—40.5), 34.8 h (31.1—38.5), and 20220614009–1: 43.5 h (39.6—47.4).

Histopathological examination showed that the post-larvae in the experimental group (20220614001-2, 20220614004-1, 20220614009-1), similar to the positive control group (*Vp*-JS20200428004-2), showed partial necrosis and sloughing of the epithelial cells in both hepatopancreatic tubules and midgut. In the early stage of infection, the epithelial cells of the hepatopancreatic tubules and midgut were slightly sloughed off and bacteria accumulated in the lumen. In the middle stage, there was more severe necrosis and partial sloughing (black arrow) of the epithelial cells in the hepatopancreatic tubules and midgut (Fig. 2d). At the late stage, there was severe necrosis and sloughing of the hepatopancreatic tubules and midgut tissue, with a large number of bacteria colonizing the lumen (red arrow). In contrast, healthy post larvae shrimp showed no significant histopathological changes in the hepatopancreatic tubules and midgut (Fig. 2d).

3.3. Bacterial identification

The 16S rRNA gene sequence analysis results showed that the strains 20220614001-2, 20220614004-1, and 20220614009-1 all belonged to the genus *Vibrio*. A multi-gene concatenation analysis of three protein-coding genes (*rct*B, *rpo*D, and *tox*R) was then performed to analyze the concatenated gene sequences of these three strains and construct the corresponding phylogenetic tree (Fig. 3). The results indicated that strain 20220614001-2 belonged to *V. natriegens*, strain 20220614004-1 clustered with *V. parahaemolyticus*, and strain 20220614009-1 clustered with *V. campbellii*.

Based on the results of the bacterial identification and the artificial infection experiment, it was observed that different *Vibrio* strains carrying the key virulence genes of Vp_{TPD} could infect post-larvae of *P. vannamei* and cause TPD. This revealed the diversity of pathogenic *Vibrio* strains associated with TPD, and the pathogenic Vibrio strains was temporarily named as *Vibrio* causing TPD (V_{TPD}).

3.4. Detection of V_{TPD} by TaqMan qPCR and PCR

In 2021 and 2022, we carried out an epidemiological survey of TPD in *P. vannamei* and other aquatic species in China. A total of 694 biological samples were collected from different provinces, including Tianjin, Hebei, Shandong, Jiangsu, Hunan, Hubei, Zhejiang, Guangxi, Hainan, and Xinjiang. Using TaqMan qPCR to detect the key virulence genes of V_{TPD} in the samples, we found that the positive rate of V_{TPD} was 23.1% (160/694). In the *P. vannamei* samples, the positive rate was 29.1% (135/463), while in the *P. japonicus* samples, the positive rate was 18.3% (11/60). No positive results were found in the samples of *Macrobrachium rosenbergii* and *Procambarus clarkii*. Additionally, the positive rate of V_{TPD} was 22.9% (14/61) in squid and silkworm samples, but no positive results were found in *Margarya melanoide* (wild) samples (Fig. 4b).

V_{TPD} positive samples were found in aquaculture ponds in most coastal provinces of China, but there were regional differences in their prevalence (Fig. 4d). The highest V_{TPD} infection rate was found in Xinjiang Province with 93.33% (14/15), followed by Guangxi Province

Table 2
Pathogenicity analysis of the suspected V_{TPD} strains.

Group	PCR			Cumulative mortality		LT_{50}
	VHVP-1-P	VHVP-2-P	VHVP-3-P	40 h	80 h	
***Vp*-JS20200428004-2**	+	+	+	75%	100%	**32.3 h(29.0-35.5)**
20210807003-1	+	-	-	0%	15%	/
20210919010-2	-	+	-	10%	15%	/
20211213001-2	+	-	+	0%	0%	/
20211213002-3	+	-	-	0%	0%	/
20220531102-1	+	+	-	0%	10%	/
20220614001-2	+	+	+	70%	100%	**37.0 h(33.4-40.5)**
20220614004-1	-	+	+	70%	100%	**34.8 h(31.1-38.5)**
20220614009-1	+	+	+	60%	95%	**43.5 h(39.6-47.4)**
20220614011-1	+	-	+	0%	10%	/
Control				0%	0%	/

Note: "+" means positive, "-" means negative.

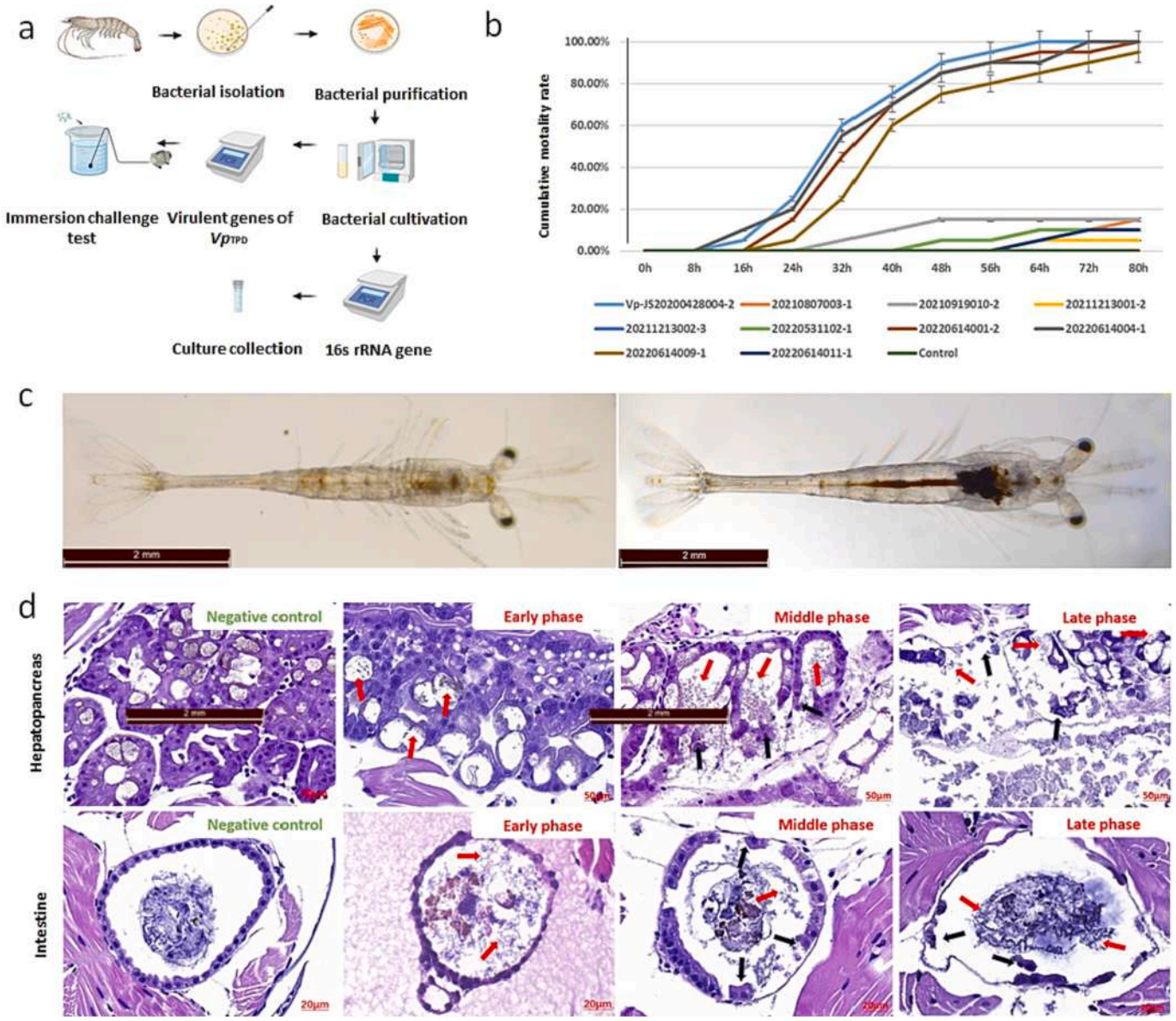

Fig. 2. Pathogenicity analysis of the strains carrying virulence gene of Vp_{TPD} determined by the challenge test. (a) Schematic diagram of isolation, detection and pathogenicity analysis of bacterial pathogens potentially responsible for TPD infections in shrimps. (b) The cumulative mortality rates of shrimp infected by different strains. (c) Clinical signs of the *Penaeus vannamei* post-larvae infected by Vp_{TPD}. The diseased individual (the left one) demonstrated syndromes of an empty digestive tract and a pale or colorless hepatopancreas. The right individual is a healthy post-larva. The scale bar = 2 mm. (d) Histopathological photos of hepatopancreas and intestine of *P. vannamei* post-larvae from V_{TPD} challenged group at different stages post infection (including early phase, middle phase, late phase). The black arrow indicates detached hepatopancreatic or intestinal epithelial cells; the red arrow indicates clustered V_{TPD} bacterial masses. (For interpretation of the references to colour in this figure legend, the reader is referred to the web version of this article.)

with 52.90% (18/34) and Hunan Province with42.9% (3/7), respectively. The largest number of samples came from Shandong Province and Hainan Provinces, with V_{TPD} prevalence rates of 25% (64/256) and 28.66% (45/157), respectively. However, no V_{TPD} positive samples were detected in Zhejiang Province and Hubei Provinces (Fig. 4c).

Histopathological analysis of samples positive for V_{TPD} in TaqMan qPCR showed that in the early stage of V_{TPD} infection (Fig. 5a, b), the infected *P. vannamei* hepatopancreatic epithelial cells were significantly contracted, and bacteria accumulated in the lumen. In the later stages of the infection (Fig. 5c, d), the structure of the hepatopancreas of infected *P. vannamei* was severely damaged. The elliptical or circular luminal structures of the intact hepatopancreatic tubules were basically not observed. The epithelial cells of the hepatopancreatic tubules were necrotic and apparently detached (black arrow). At the same time, a large number of bacteria can be observed colonizing in the lumen (red arrow). Then in the middle stage of the infection (Fig. 5e), the intestinal epithelial cells begin to detach (black arrow), and a large number of bacteria aggregate and settle in the lumen (red arrow). As the infection progresses, the severity of the midgut lesions worsens. In the later stages of the infection (Fig. 5f), the midgut structure is severely damaged, and almost all epithelial cells have been sloughed off (black arrow). The entire intestinal tissue is reduced to only the basal lamina.

4. Discussion

In early 2020, TPD in *P. vannamei* started rapidly spread in Southern China, resulting in the closure of 70–80% of hatcheries and nurseries in the coastal shrimp farming provinces. This had a severe impact on China's shrimp farming industry, resulting in significant losses. Initial research suggested that a new highly virulent strain of *Vibrio*

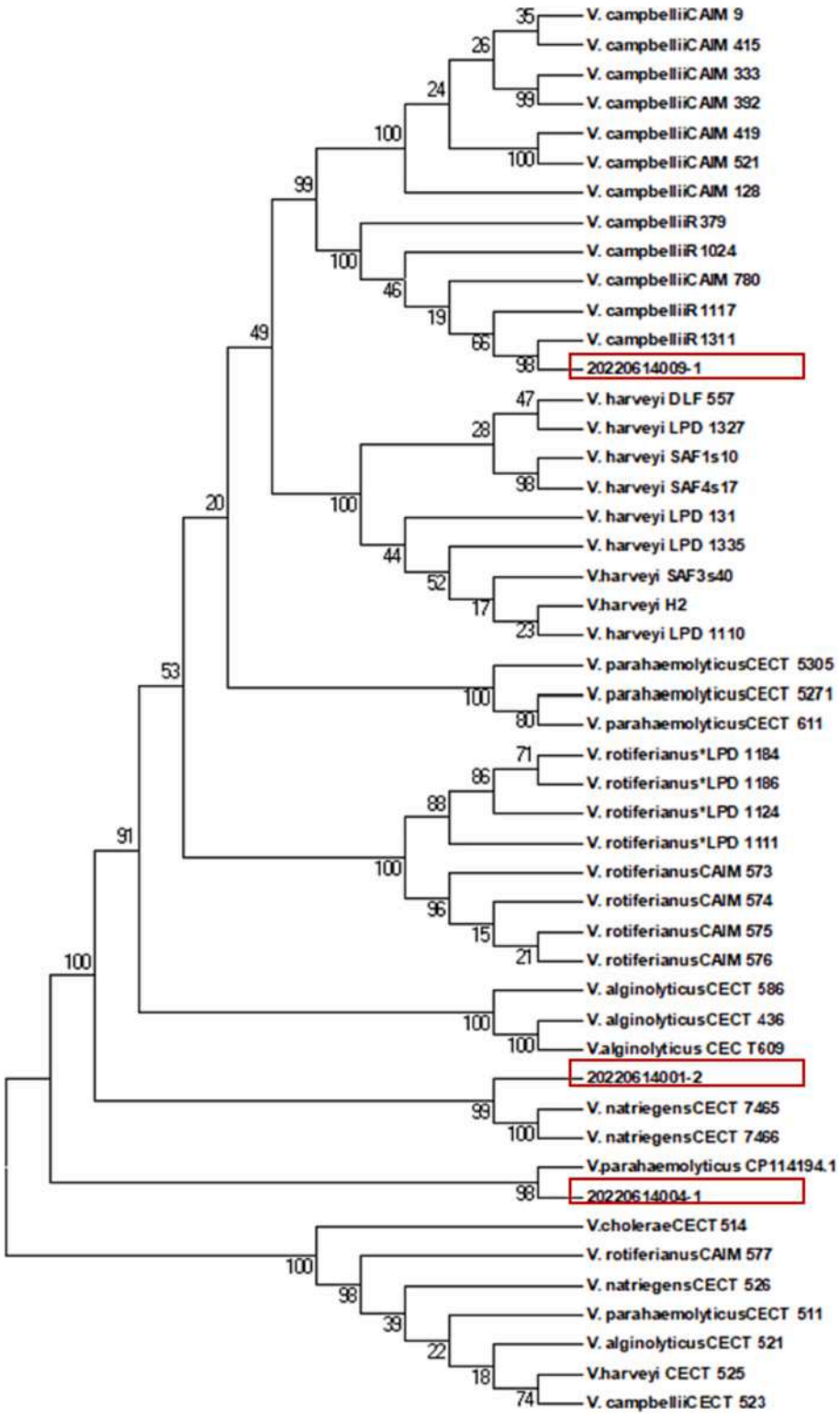

Fig. 3. Phylogenetic reconstruction based on concatenated *rpo*D, *rct*B, and *tox*R sequences. Percentage bootstrap values (1000 replicates). The reference sequences were as alignment as described by Pascual et al.

parahaemolyticus (Vp_{TPD}) was responsible for the pathogen causing TPD (Zou et al., 2020). In 2022, this finding was further confirmed by Yang Feng (Yang et al., 2022). By analyzing the pathogenicity of different molecular weight protein products from Vp_{TPD} on the post-larvae of *Penaeus vannamei* and combining the predicted virulence genes of Vp_{TPD} genome, Liu Shuang et al. identified three novel potential virulence proteins (vibrio high virulent protein, VHVP-1, VHVP-2, and VHVP-3) as suspected key virulence factors of Vp_{TPD} (Liu et al., 2023). Although some progress has been made in the study of TPD pathogens, their diversity and prevalence still require further investigation. In this study, a molecular epidemiological survey and pathogen research were conducted on shrimp causing TPD in different provinces of China from 2021 to 2022. The potential pathogenic bacteria isolated from diseased shrimp were molecularly identified, and PCR detection of the

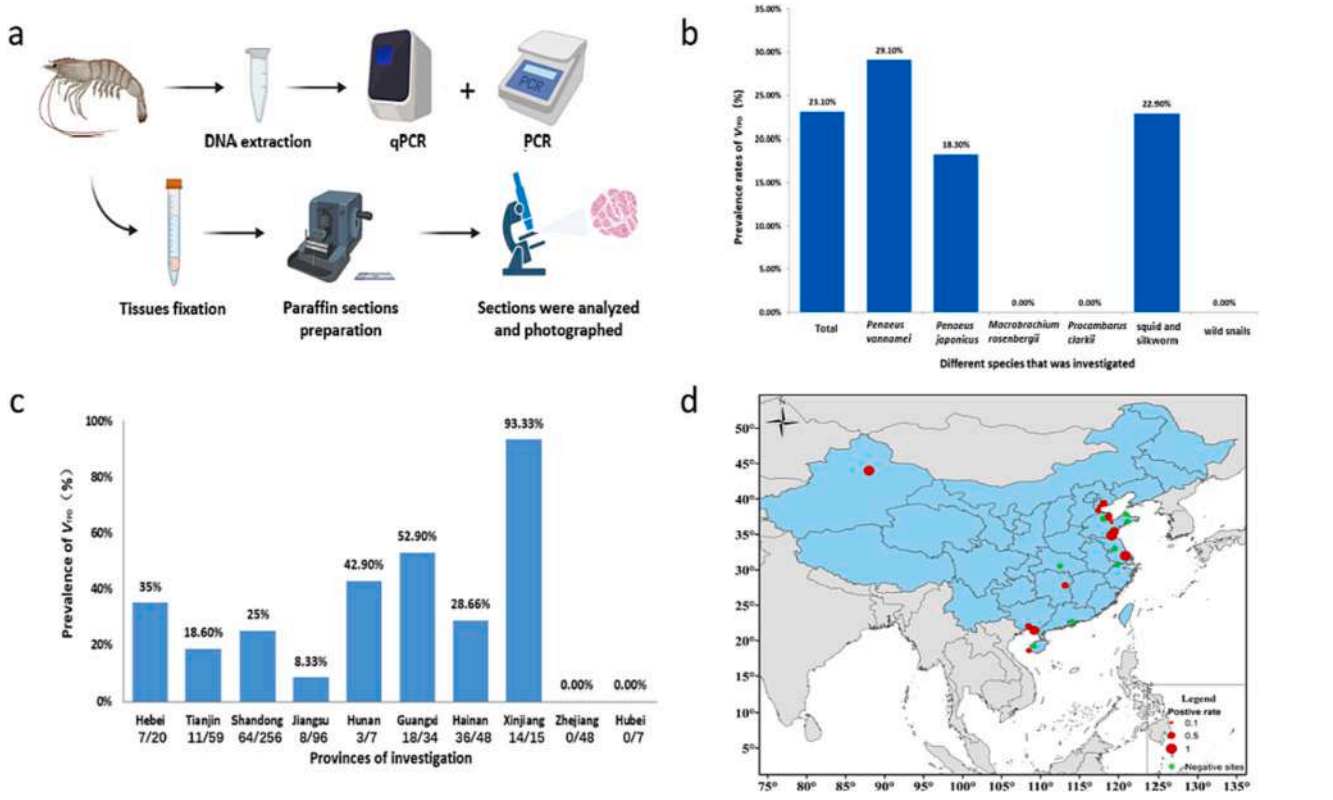

Fig. 4. Molecular epidemiology investigation of V_{TPD}. (a) Schematic diagram of molecular epidemiology investigation of V_{TPD}. (b) V_{TPD} positive rate in samples (2021−2022) of different species based on TaqMan qPCR. (c) Prevalence of V_{TPD} in the samples (2021–2022) from different provinces in China. (d) V_{TPD} prevalence in different shrimp aquaculture regions with different prevalence rates.

corresponding virulence protein genes of Vp_{TPD} was performed, aiming to understand the basic biological characteristics of this pathogen.

In this study, 448 potentially pathogenic bacteria were isolated, purified, and identified from natural disease samples from 2021 to 2022. Among them, the *Vibrio* genus had the highest proportion, accounting for 53.79% (241/448), indicating that the *Vibrio* genus plays an important role in the pathogenic bacteria of cultured shrimp. The *Vibrio* genus includes a wide range of species, a significant number of which are widely found in aquaculture environments and in the bodies of cultured animals. At the same time, they also act as opportunistic pathogens (Vandenberghe et al., 2003; Möller et al., 2020; Lee et al., 2015; Li et al., 2019). In the context of shrimp aquaculture, different species of *Vibrio* show varying degrees of pathogenicity towards shrimp (Moriarty, 1998; Arunkumar et al., 2020). Research indicates that the majority of pathogenic *Vibrio* species proliferate and cause vibriosis in shrimp only under adverse environmental conditions or when the physiological resistance of the shrimp is compromised (Kong et al., 1998; Saulnier et al., 2000). It's worth noting, however, that certain Vibrio species have the potential to cause disease, even at low levels. For example, the causative strains of AHPND, although present in minimal numbers, can cause disease in shrimp (Phiwsaiya et al., 2017; Han et al., 2015).

Conventional PCR was then used to detect the key virulence protein coding genes of Vp_{TPD} in the 448 dominant strains. Nine potentially pathogenic bacteria strains carried the suspected key virulence genes of Vp_{TPD}. Among these 9 potential pathogenic bacterial strains, 2 strains carried three suspected virulence genes (*vhvp*-1, *vhvp*-2, *vhvp*-3), 4 strains carried two suspected virulence genes, and 3 strains carried a single suspected virulence gene. Nine of the potentially pathogenic bacteria were then selected for an artificial infection experiment to analyze their pathogenicity to *P. vannamei* larvae. The results showed that three of the 9 selected strains (including 20220614001-2, 20220614004-1, 20220614009-1) were pathogenic bacteria of translucent post-larvae disease. The results of multi-gene tandem analysis (MLSA) based on three conserved protein-coding genes (*rct*B, *rpo*D and *tox*R) showed that strain 20220614001-2 was *V. natriegens*, strain 20220614004-1 was *V. parahemolyticus*, and strain 20220614009-1 was *V. campbellii*. These results confirmed that different *Vibrio* bacteria carrying key virulence genes of Vp_{TPD} can infect post-larvae of *P. vannamei* and cause TPD, and revealed the characteristics of the diversity of TPD pathogenic bacteria. The pathogenic *Vibrio* strains has been temporarily named as *Vibrio* causing TPD (V_{TPD}). Wang et al. analyzed the dominant pathogens causing TPD and found that the pathogens causing TPD have higher similarity with *V. alginolyticus*, *V. harveyi*, and *V. parahaemolyticus* (Wang et al., 2021). Yang et al. found that the causative agent of TPD was a strain of *V. parahaemolyticus* (Yang et al., 2022). The results of these two research teams not only confirm our previous identification of TPD pathogens but also suggest that the types of TPD pathogens may be diverse, which is consistent with the preliminary results of the results of this study.

It is interesting to note that all the currently discovered V_{TPD} belong to the *Harveyi* clade. The *Harveyi* clade includes a total of 11 species, namely *V. alginolyticus*, *V. parahaemolyticus*, *V. harveyi*, *V. azureus*, *V. sagamiensis*, *V. campbellii*, *V. owensii*, *V. natriegens*, *V. costicola*, *V. jasicida*, and *V. mytili*. However, certain members of the *Harveyi* clade, including *V. harveyi*, *V. campbellii*, and *V. parahaemolyticus*, have been reported to play significant roles as pathogens in aquatic organisms (Darshanee Ruwandeepika et al., 2012; Thompson et al., 2004; Darshanee Ruwandeepika et al., 2012). This highlights the variation in pathogenic potential within the same species and underscores the importance of strain-specific characteristics in determining their impact on aquatic organisms. Therefore, understanding these strain-specific traits is critical for effective disease management and the development of targeted strategies to mitigate the adverse effects of pathogenic Vibrio bacteria in aquatic environments. In particular, pathogenicity appears to

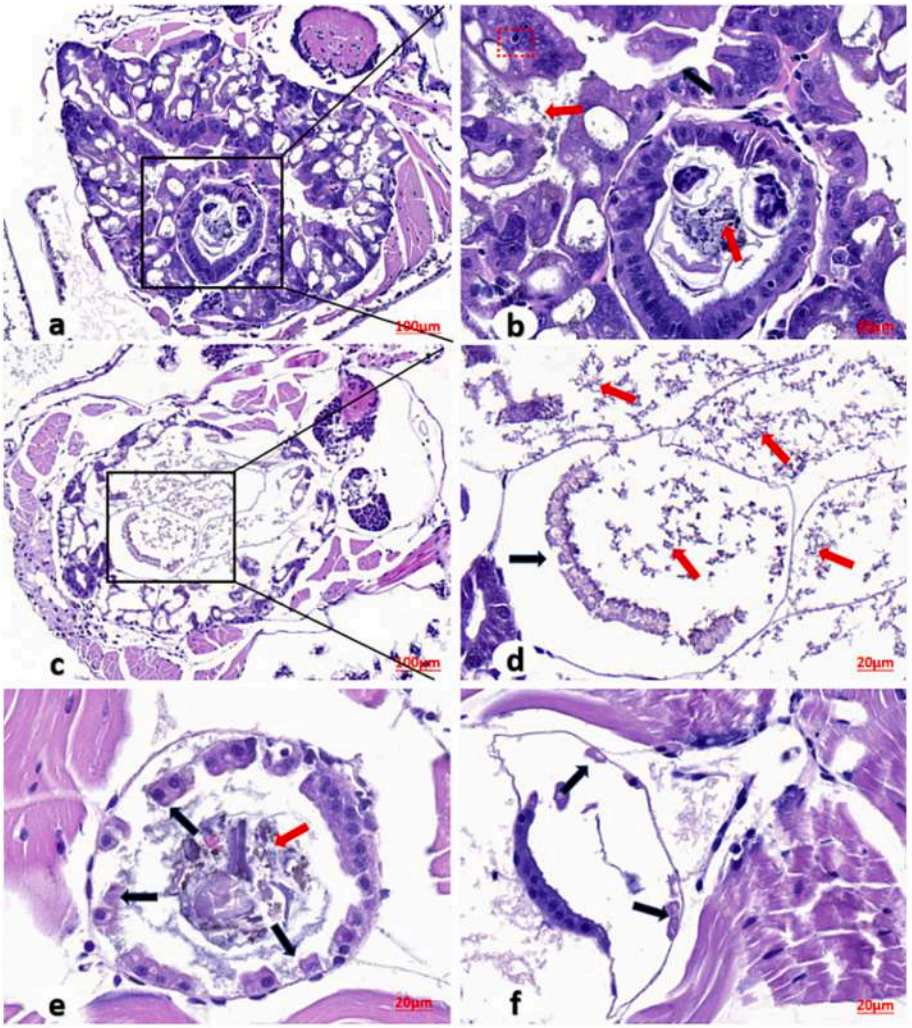

Fig. 5. Histopathological results of *P. vannamei* artificially infected with TPD. (a) and (b) are H&E staining microscopic photographs of hepatopancreas tissues from infected *P. vannamei* at early or middle stage, (c) and (d) are H&E staining microscopic photographs of hepatopancreas tissues from infected *P. vannamei* at late stage, (e) is H&E staining microscopic photograph of intestinal tissue of *P. vannamei* at early or middle stage, (f) is H&E staining microscopic photograph of intestinal tissue of *P. vannamei* at late stage. The red arrow indicates necrotic hepatopancreatic or intestinal epithelial cells; the black arrow indicates detached hepatopancreatic or intestinal epithelial cells; the white arrow indicates clustered V_{TPD} bacterial masses. (b) and (d) are enlarged pictures of (a) and (c), with scale: (b), (d), (e) and (f) are 20 μm, (a) and (c) are 100 μm. (For interpretation of the references to colour in this figure legend, the reader is referred to the web version of this article.)

be species-independent and is instead a characteristic of individual bacterial strains. This means that certain strains within a specific species may possess pathogenic traits, while others remain non-pathogenic. Furthermore, there may be variation in the degree of pathogenicity among these strains (Austin and Zhang, 2006; Ruwandeepika et al., 2010).

Considering the diversity of TPD strains, we aimed to gain further insight into their pathogenic mechanisms by using the results of PCR analysis utilizing three sets of primers. The strains 20220614001-2, 20220614004-1, and 20220614009-1 all tested positive for *vhvp*-2 gene and *vhvp*-3 gene with strong positivity. However, strain 20220614004-1 did not carry the *vhvp*-1 gene. Meanwhile strains 20210807003-1 (carrying only the *vhvp*-1 gene) and strains 20211213001-2 (carrying both the *vhvp*-1 and *vhvp*-3 genes) remained non-pathogenic. These results show that the existence of the suspected virulence gene *vhvp*-1 alone or the co-existence of *vhvp*-1 and *vhvp*-3 genes does not cause the super virulence of Vp_{TPD}, which further confirms our previous results that *vhvp*-2 is the key virulence gene of Vp_{TPD} (Liu et al., 2023). According to our research and the findings of Liu et al. (2023), there is no doubt that *vhvp*-2 is a key virulence gene of V_{TPD}. However, Table 2 shows that the virulent strains contained at least two positive PCR for *vhvp*-2 and *vhvp*-3 genes. Based on these findings, we hypothesize that the combination of the *vhvp*-2 and *vhvp*-3 genes is the main factor leading to the high pathogenicity of V_{TPD}. That is, the regulatory control of virulence gene expression is also likely to be a key factor influencing pathogenicity. According to the prediction result of the encoding genes in 187, 791 bp plasmid by using the online Conserved Domain Search Service (CD Search) in NCBI, the potential virulent factor of VHVP-2 was found to contain the conserved domains of *Salmonella* virulence plasmid 65 kDa B protein (SpvB), insecticide toxin TcdB middle/C-terminal region, and insecticide toxin TcdB middle/N-terminal region domain; and the potential virulent factor of VHVP-3 possessed the conserved domains of the conserved domains of Tc toxin complex Tcc related domain. The Spv protein had been considered one of the most important virulence factors during *Salmonella* infection, and the SpvB protein played an important role in the pathogenesis of bacteria (Aguilera et al., 2012; Lesnick et al., 2001; Kurita et al., 2003). It could be directly secreted into the cytoplasm and mediate host cell actin ribosylation, inhibiting the polymerization and rearrangement of the actin cytoskeleton, causing actin filament fragmentation, disrupting the cell skeleton structure, leading to host cell apoptosis and exacerbating cell damage. Further studies have found that

the proline residues connecting the C-terminus and N-terminus are indispensable for the toxicity of the virulence protein during its translocation from bacteria to host cells (Libby et al., 2000; Barth and Aktories, 2011; Harterink et al., 2017). A high molecular weight insecticidal toxin complex (Tcs) was identified for the first time in *Photorhabdus luminescens* W14, which includes four toxin complex loci (tca, tcb, tcc, and tcd) (Lyerly et al., 1982; Zhan et al., 2016). Among these Tcs, it has been reported that tca may be involved in binding and translocation to membrane receptors, tcc may participate in self-translocation to the target cell membrane through the endocytic pathway, and tcb acts as a functional connector between tca and tcc (Meusch et al., 2014; Roderer and Raunser, 2019). Meanwhile, Yang et al. inferred that the production of Tcs toxin by V_{TPD} may be the main reason for its high pathogenicity (Yang et al., 2023). Based on our above research results of VHVP-1, VHVP-2 and VHVP-3, as well as Professor Yang's report, we speculate that VHVP-3 containing the conserved domain of TccC may play an auxiliary role in the super virulence of Vp_{TPD}. It is crucial to determine whether the *vhvp*-3 gene play a subservient role in the process of *vhvp*-2 gene functioning as high virulence gene. To this end, future epidemiological studies and artificial infection experiments using key virulence gene-deleted strains and complemented strains can be conducted to determine the effect of multiple virulence protein genes on pathogenicity.

In this study, we also conducted an epidemiological survey of TPD in 2021 and 2022, and collected 694 biological samples from different provinces in China. The results of TaqMan qPCR (*vhvp*-2 gene) and PCR (both *vhvp*-2 and *vhvp*-3) detection in the above samples showed that the positive rate of V_{TPD} in the samples was 23.1% (160/694), and the positive rate of V_{TPD} in the *P. vannamei* samples was 29.1% (135/463). The positive rate of V_{TPD} in *P. japonicus samples* was 18.3% (11/60), but no positive rate was found in *M. rosenbergii* and *Procambarus clarkii*. The positive rate of V_{TPD} in squid and silkworm samples was 22.9% (14/61). No positive results were found in wild snails. These results suggest that cultured species such as *P. vannamei* and *P. japonicus* are more sensitive to V_{TPD} and are more likely to be infected or carry it. Freshwater cultured shrimp such as *M. rosenbergii* and *Procambarus clarkii* may not be affected by V_{TPD}. Shrimp bait organisms are at risk of carrying or being infected with V_{TPD}. V_{TPD} positive samples have been found in aquaculture ponds in most coastal provinces of China, but there are regional differences in their prevalence. The highest V_{TPD} infection rate was found in Xinjiang Province with 93.33% (14/15), followed by Guangxi Province with 52.90% (18/34) and Hunan Province with 42.9% (3/7). The largest number of samples came from Shandong Province and Hainan Provinces, with V_{TPD} prevalence rates of 25% (64/256) and 28.66% (45/157), respectively. However, no V_{TPD} positive samples were detected in Zhejiang Province and Hubei Province. From 2021 to 2022, due to the influence of COVID-19, the sampling size of some provinces is not very large, which may make our prevalence results have some limitations. Positive samples were detected in most shrimp aquaculture ponds in different regions of China, with some areas showing a positive detection rate of >50%. This suggests that V_{TPD} is still prevalent and spreading in coastal shrimp farming areas in China, with a high risk of transmission and spread.

In conclusion, this study not only reveals the prevalence of TPD in major shrimp aquaculture species in China and investigates its pathogenic diversity, but also explores the relationship between the virulence genes carried by V_{TPD}s from different sources and their pathogenicity. Understanding the complex interplay between these virulence genes and their regulatory mechanisms is crucial to understanding the mechanisms underlying the enhanced pathogenicity in V_{TPD} infections. This knowledge could potentially lead to targeted strategies to mitigate the effects of these virulence factors and enhance our ability to manage and control diseases caused by V_{TPD} in aquatic environments.

Author contributions

QL Zhang, S Liu, TT Xu, TC Jia carried out the field investigation, sampling and pre-processing. TC Jia performed the laboratory analyses and documented the results. S Liu screened the potential virulence genes location in the genome. WX Zhao, W Wang and XT Yu performed the qPCR of the clinical sample. Jie Kong supplied the SPF shrimp post-larvae. TC Jia and TT Xu prefer the histopathological analysis. TC Jia drafted the manuscript, and QL Zhang revised the manuscript and all the authors approved the final version.

CRediT authorship contribution statement

Tianchang Jia: Methodology, Investigation, Formal analysis. **Shuang Liu:** Resources, Investigation, Funding acquisition, Formal analysis. **Xingtong Yu:** Investigation, Formal analysis. **Tingting Xu:** Resources, Investigation. **Jitao Xia:** Investigation. **Wenxiu Zhao:** Investigation. **Wei Wang:** Methodology, Investigation. **Jie Kong:** Resources, Conceptualization. **Qingli Zhang:** Writing – review & editing, Supervision, Resources, Project administration, Investigation, Funding acquisition, Formal analysis, Data curation, Conceptualization.

Declaration of competing interest

The authors have declared no conflict of interest.

Data availability

No data was used for the research described in the article.

Acknowledgments

This work was supported by Central Public-interest Scientific Institution Basal Research Fund, CAFS (No. 2020TD39; 2021XT0602; 2023TD42), Projects of marine fishery biological resources collection and preservation, Ministry of Agriculture and Rural Affairs of China, China Agriculture Research System of MARA (CARS-48), and Central Public-interest Scientific Institution Basal Research Fund, YSFRI, CAFS (No. 20603022021012; 20603022022024; 20603022022020; 20603022023009).

References

Aguilera, M.O., Berón, W., Colombo, M.I., 2012. The actin cytoskeleton participates in the early events of autophagosome formation upon starvation induced autophagy. Autophagy 8 (11), 1590–1603.

Arunkumar, M., LewisOscar, F., Thajuddin, N., Pugazhendhi, A., Nithya, C., 2020. In vitro and in vivo biofilm forming Vibrio spp: a significant threat in aquaculture. Process Biochem. 94, 213–223.

Austin, B., Zhang, X.H., 2006. Vibrio harveyi: a significant pathogen of marine vertebrates and invertebrates. Lett. Appl. Microbiol. 43, 119–124.

Barth, H., Aktories, K., 2011. New insights into the mode of action of the actin ADP-ribosylating virulence factors Salmonella enterica SpvB and Clostridium botulinum C2 toxin. Eur. J. Cell Biol. 90 (11), 944–950.

Bogosian, G., Aardema, N.D., Bourneuf, E.V., Morris, P.J., O'Neil, J.P., 2000. Recovery of hydrogen peroxide-sensitive culturable cells of Vibrio vulnificus gives the appearance of resuscitation from a viable but nonculturable state. J. Bacter. 182 (18), 5070–5075.

Darshanee Ruwandeepika, H.A., Sanjeewa Prasad Jayaweera, T., Paban Bhowmick, P., Karunasagar, I., Bossier, P., Defoirdt, T., 2012. Pathogenesis, virulence factors and virulence regulation of vibrios belonging to the Harveyi clade. Reviews in Aquaculture *4* (2), 59–74.

Han, J.E., Tang, K.F., Tran, L.H., Lightner, D.V., 2015. Photorhabdus insect-related (Pir) toxin-like genes in a plasmid of Vibrio parahaemolyticus, the causative agent of acute hepatopancreatic necrosis disease (AHPND) of shrimp. Dis. Aquat. Org. 113, 33–40.

Harkell, L., 2020a. Shrimp Hatcheries in China Hit by 'Glass Post-Larvae'. Undercurrentnews, 2020-4-22. Available online: https://www.undercurrentnews.com/2020/04/22/shrimp-hatcheries-in-china-hit-by-glass-post-larvae/ (accessed on 23 April 2020).

Harkell, L., 2020b. Chinese Scientists Confirm New Virus Causes Shrimp 'Glass Post-Larvae'. 2020-5-8. Available online: https://www.undercurrentnews.com/2020/05/

08/Chinese-scientists-confirm-new-virus-causes-shrimp-glass-post-larvae/ (accessed on 8 May 2020).
Harterink, M., da Silva, M.E., Will, L., Turan, J., Ibrahim, A., Lang, A.E., van Battum, E. Y., Pasterkamp, R.J., Kapitein, L.C., Kudryashov, D., Barres, B.A., Hoogenraad, C.C., Zuchero, J.B., 2017. DeActs: genetically encoded tools for perturbing the actin cytoskeleton in single cells. Nat. Methods 14, 479–482. https://doi.org/10.1038/nmeth.4257.
He, H., 2020. 4.13. Da Kao Yan! "Bo Li Miao" Cheng Zai, Raoping 9 Cheng Miao Chang Shou Ying Xiang! Ye Zhe: Bing Fei Guai Bing, Ke Fang Ke Kong, Yang Hu Bu Bi Kong Huang [A Great challenge! The outbreak of "glass post-larvae disease". Over 90% of the hatcheries in Raoping are hit!]. Shui Chan Qian Yan [Fisheries Adcance Magazine]. Avaliable online. https://mp.weixin.qq.com/s/eaqGJs1m22b_r3YzPmZcYg.
Huang, Y., 2020. 5.17. Nan Mei Bai Dui Xia "Bo Li Miao" Bu Rong Le Guan, Fang Fan Cuo Shi Xu Qiang Hua [The glass post-larvae disease is a serious problem for Penaeus vannamei. The strategies for disease prevention should be strengthen.]. Shui Chan Qian Yan [Fisheries Advance Magazine]. Avaliable online. https://mp.weixin.qq.com/s/W3kdpV6qx7Whon0GuQHZ9A.
Javier, Pascual, Carmen, Macián M., Arahal David, R., Pujalte María, J., 2010. Multilocus sequence analysis of the central clade of the genus Vibrio by using the 16S rRNA, recA, pyrH, rpoD, gyrB, rctB and toxR genes. Int. J. Syst. Evol. Microbiol. (Pt 1) https://doi.org/10.1099/ijs.0.010702-0.
Kong, Fan-jun, Kai, Zhou, Zheng, Guo-xing, 1998. Experiments of the acute lethal dose of three kinds of vibrios on cultivating of Penaeus chinensis. Mar. Sci. 04, 06–08, 1998.
Kurita, A.I., Gotoh, H., Eguchi, M., Okada, N., Matsuura, S., Matsui, H., Kikuchi, Y., 2003. Intracellular expression of the Salmonella plasmid virulence protein, SpvB, causes apoptotic cell death in eukaryotic cells. Microb. Pathog. 35 (1), 43–48.
Lee, Chung-Te, Chen, I-Tung, Yang, Yi-Ting, Ko, Tzu-Ping, Huang, Yun-Tzu, Huang, Jiun-Yan, Lo, Chu-Fang, 2015. The opportunistic marine pathogen Vibrio parahaemolyticus becomes virulent by acquiring a plasmid that expresses a deadly toxin (vol 112, pg 10798, 2015). Proc. Natl. Acad. Sci. U. S. A. 39.
Lesnick, M.L., Reiner, N.E., Fierer, J., Guiney, D.G., 2001. The Salmonella spvB virulence gene encodes an enzyme that ADP-ribosylates actin and destabilizes the cytoskeleton of eukaryotic cells. Mol. Microbiol. 39 (6), 1464–1470.
Li, L., Meng, H., Gu, D., Li, Y., Jia, M., 2019. Molecular mechanisms of Vibrio parahaemolyticus pathogenesis. Microbiol. Res. 222, 43–51.
Libby, S.J., Lesnick, M., Hasegawa, P., Weidenhammer, E., Guiney, D.G., 2000. The Salmonella virulence plasmid spv genes are required for cytopathology in human monocyte-derived macrophages. Cell. Microbiol. 2 (1), 49–58.
Lightner, D., 1996. A Handbook of Shrimp Pathology and Diagnostic Procedures for Diseases of Cultured Penaeid Shrimp.
Liu, S., Wang, W., Jia, T., 2023. Vibrio parahaemolyticus becomes lethal to post-larvae shrimp via acquiring novel virulence factors. Microbiol. Spectrum. 11 (6), e00492–23.
Lyerly, D.M., Lockwood, D.E., Richardson, S.H., Wilkins, T.D., 1982. Biological activities of toxins a and B of Clostridium difficile. Infect. Immun. 35 (3), 1147–1150.
Meusch, D., Gatsogiannis, C., Efremov, R.G., Lang, A.E., Hofnagel, O., Vetter, I.R., Raunser, S., 2014. Mechanism of Tc toxin action revealed in molecular detail. Nature 508 (7494), 61–65.
Miller Christopher, S., Handley Kim, M., Wrighton Kelly, C., Banfield Jillian, F., 2013. Short-read assembly of full-length 16S amplicons reveals bacterial diversity in subsurface sediments. PLoS One 2. https://doi.org/10.1371/journal.pone.0056018.
Möller, L., Kreikemeyer, B., Luo, Z.-H., Jost, G., Labrenz, M., 2020. Impact of coastal aquaculture operation systems in Hainan island (China) on the relative abundance and community structure of Vibrio in adjacent coastal systems. Estuar. Coast. Shelf Sci. 233, 106542.
Moriarty, D.J.W., 1998. Control of luminous Vibrio species in penaeid aquaculture ponds. Aquaculture 164 (1–4), 351–358.
Phiwsaiya, K., Charoensapsri, W., Taengphu, S., Dong, H.T., Sangsuriya, P., Nguyen, G. T., Taengchaiyaphum, S., 2017. A natural Vibrio parahaemolyticus Δ pirA Vp pirB Vp+ mutant kills shrimp but produces neither Pir Vp toxins nor acute hepatopancreatic necrosis disease lesions. Appl. Environ. Microbiol. 83 (16) e00680–00617.
Roderer, D., Raunser, S., 2019. Tc toxin complexes: assembly, membrane permeation, and protein translocation. Annu. Rev. Microbiol. 73, 247–265.
Ruwandeepika, H.A.D., Defoirdt, T., Bhowmick, P.P., Shekar, M., Bossier, P., Karunasagar, I., 2010. Presence of typical andatypical virulence genes in vibrio isolates belonging to the Harveyi clade. J. Appl. Microbiol. 109, 888–899.
Saulnier, D., Avarre, J.C., Le Moullac, G., Ansquer, D., Levy, P., Vonau, V., 2000. Rapid and sensitive PCR detection of Vibrio penaeicida, the putative etiological agent of syndrome 93 in New Caledonia. Dis. Aquat. Org. 40 (2), 109–115.
Thompson, F.L., Iida, T., Swings, J., 2004. Biodiversity of Vibrios. Microbiol. Mol. Biol. Rev. 68, 403–431.
Vandenberghe, J., Thompson, F., Gomez-Gil, B., Swings, J., 2003. Phenotypic Diversity amongst Vibrio Isolates from Marine Aquaculture Systems.
Wang, W., 2022. Preliminary Study on Application for New Veterinary Drug Certificate of Fluorescence Quantitative PCR Detection Kit for Two Shrimp Pathogens. Shanghai Ocean University.
Wang, Y., Yu, Y.X., Xiao, Liu, Yonggang, Zhang, Zheng, Zhang, Meijie, Liao, Luo, K., 2021. Pathogenic and pathological analysis of bacterial vitriosis (BVS) in *Penaeus vannamei*. J. Fish. China 09, 1563–1573.
Yang, F., Xu, L., Huang, W., Li, F., 2022. Highly lethal Vibrio parahaemolyticus strains cause acute mortality in Penaeus vannamei post-larvae. Aquaculture 548. https://doi.org/10.1016/j.aquaculture.2021.737605.
Yang, F., You, Y., Lai, Q., Xu, L., Li, F., 2023. Vibrio parahaemolyticus becomes highly virulent by producing Tc toxins. Aquaculture 739817.
Yi-Lin, Chen, Chuan-Chun, Lee, Ya-Lan, Lin, Tsunglin, Liu, 2015. Obtaining long 16S rDNA sequences using multiple primers and its application on dioxin-containing samples. BMC Bioinform. S18 https://doi.org/10.1186/1471-2105-16-S18-S13.
Zhan, Z., Qiu, X., Han, R., 2016. Horizontal transfer of the C-termini of tccC genes in Photorhabdus and Xenorhabdus. Genes Genom. 38, 685–692.
Zhang, Q., Xu, T., Wan, X., Liu, S., Wang, X., Li, X., Huang, J., 2017. Prevalence and distribution of covert mortality nodavirus (CMNV) in cultured crustacean. Virus Res. 233, 113–119.
Zou, Y., Xie, G., Jia, T., Xu, T., Wang, C., Wan, X., Zhang, Q., 2020. Determination of the infectious agent of translucent post-larva disease (TPD) in Penaeus vannamei. Pathogens 9 (9). https://doi.org/10.3390/pathogens9090741. Retrieved from https://www.ncbi.nlm.nih.gov/pubmed/32927617.

Update

Aquaculture

Volume 596, Issue P1, 15 February 2025, Page

DOI: https://doi.org/10.1016/j.aquaculture.2024.741792

Aquaculture 596 (2025) 741792

Contents lists available at ScienceDirect

Aquaculture

journal homepage: www.elsevier.com/locate/aquaculture

Corrigendum to "Prevalence investigation of translucent post-larvae disease (TPD) in China" [Aquaculture Volume 583, 30 March 2024, 740583]

Tianchang Jia [a,b], Shuang Liu [a], Xingtong Yu [a], Tingting Xu [a], Jitao Xia [a], Wenxiu Zhao [a], Wei Wang [a], Jie Kong [a,b], Qingli Zhang [a,b,*]

[a] State Key Laboratory of Mariculture Biobreeding and Sustainable Goods; Key Laboratory of Maricultural Organism Disease Control, Ministry of Agriculture; Qingdao Key Laboratory of Mariculture Epidemiology and Biosecurity; Yellow Sea Fisheries Research Institute, Chinese Academy of Fishery Sciences, Qingdao, Shandong 266071, China

[b] Laboratory for Marine Fisheries Science and Food Production Processes, Laoshan Laboratory, Qingdao, Shandong 266237, China

The authors deeply regret the errors that occurred in the primer information presented in Table 1. These errors will not significantly impact the overall results and conclusions of the paper.

The revised Table 1 is as follows:

Gene	Primer	Primer Sequences (5′-3′)
qPCR	VHVP-F	ACACCCAATACTCCAAACGAC
	VHVP-R	AACTCCCGAAATCCGTCAAG
	Probe	AGGCATGGACCGTAAAGCTCTCAC
16S rRNA	27F	AGAGTTTGATCCTGGCTCAG
	1492R	GGTTACCTTGTTACGACTT
VHVP-1-P	VHVP-1-P -F	GAGGAGAGTGTTGACCGAAATC
	VHVP-1-P -R	CTGCGCCAGTAGTAACGATAAG
VHVP-2-P	VHVP-2-P -F	GCTGGTCCGGACGGTGCC
	VHVP-2-P -R	GTGATACATTAATACTTGTCTACAA
VHVP-3-P	VHVP-3-P -F	CCCGTATCACAGAGCGATTT
	VHVP-3-P -R	CTTTGGTGTCGGTCGTAGTT
*rpo*D	*rpo*D-F	ACGACTGACCCGGTACGCATGTAYATGMGNGARATGGGNACNGT
	*rpo*D-R	ATAGAAATAACCAGACGTAAGTTNGCYTCNACCATYTCYTTYT
*rct*B	*rct*B-F	ATHGARTTYACNGAYTTYCARYTNCAY
	*rct*B-R	YTTNCTYTGHATNGGYTCRAAYTCNCCRTC
*tox*R	*tox*R-F	GANCARGGNTTYGARGTNGAYGAYTC
	*tox*R-R	TTDKKTTGNCCNCYNGTVGCDATNAC

(continued on next column)

(continued)

The authors would like to apologise for any inconvenience caused.

DOI of original article: https://doi.org/10.1016/j.aquaculture.2024.740583.

* Corresponding author.
E-mail address: zhangql@ysfri.ac.cn (Q. Zhang).

https://doi.org/10.1016/j.aquaculture.2024.741792

Available online 28 October 2024

Journal of Invertebrate Pathology 214 (2026) 108499

Contents lists available at ScienceDirect

Journal of Invertebrate Pathology

journal homepage: www.elsevier.com/locate/jip

Protective effects of gallic acid against *Vibrio parahaemolyticus*-induced translucent post-larvae disease in *Litopenaeus vannamei*: insights into antibacterial and anti-virulence mechanisms

Man-Hong Ye [a,b,1], Qian-Nan Han [a,1], Chuang Meng [a,b], Feng Ji [c], Bin Zhou [d,*]

[a] College of Bioscience and Biotechnology, Yangzhou University, Yangzhou 225009, China
[b] Jiangsu Key Laboratory of Zoonosis, Yangzhou University, Yangzhou 225009, China
[c] Institute of Animal Husbandry and Veterinary Medicine, Beijing Academy of Agriculture and Forestry Sciences, Beijing 100089, China
[d] College of Animal Science and Technology, Yangzhou University, Yangzhou 225009, China

ARTICLE INFO

Keywords:
Litopenaeus vannamei
Translucent post-larvae disease
Vibrio parahaemolyticus
Gallic acid
Whole-genome sequencing

ABSTRACT

Translucent post-larvae disease (TPD) is a lethal syndrome causing high mortality in post-larvae of *Litopenaeus vannamei*. This study investigated the protective efficacy of gallic acid (GA), a non-antibiotic compound, against TPD induced by a field isolate *Vibrio parahaemolyticus* TS-GE (*V. para.* TS-GE). Immersion challenge assays confirmed the high virulence of *V. para.* TS-GE, as it caused 100 % mortality in post-larvae within 24 h at 2.82×10^7 CFU/mL. Whole-genome sequencing revealed its genome comprised two chromosomes (3.50 Mb and 1.92 Mb) and three plasmids (69.7 kb, 60.7 kb, 60.5 kb). The 69.7-kb plasmid harbored TPD-associated virulence genes vhvp1 and vhvp2, while chromosomal genes encoded 40 type III secretion system components and thermolabile hemolysin. Pangenome analysis revealed the open genome nature of *V. parahaemolyticus* strains. Multilocus sequence typing identified *V. para.* TS-GE as ST2621. *In vitro*, GA exhibited growth-inhibitory activity against *V. para.* TS-GE. *In vivo*, 200 μg/mL GA significantly reduced cumulative mortality ($P < 0.01$) from 100 % to 18.3 %, preserving hepatopancreatic epithelium and midgut structure in *V. para.* TS-GE infected post-larvae. Mechanistic investigations revealed GA disrupted bacterial cell wall/membrane integrity, inhibited swimming motility, and suppressed biofilm formation. Molecular docking simulations predicted favorable binding of GA to virulence proteins VHVP1 (−6.3 kcal/mol) and VHVP2 (−7.8 kcal/mol), suggesting dual antibacterial and anti-virulence activities. These findings highlight GA as a promising antibiotic alternative for TPD control. Genomic data provide insights into the pathogenic adaptation of *V. para.* TS-GE in aquaculture.

1. Introduction

The Pacific white shrimp (*Litopenaeus vannamei*), responsible for over 50 % of global crustacean aquaculture production (FAO, 2022), is the world's most economically significant farmed shrimp species, with China being its largest producer and primary market. Since late 2019, a highly lethal translucent post-larvae disease (TPD) has rapidly spread across shrimp hatcheries in China. Its high mortality rates have inflicted significant economic losses on China's *L. vannamei* aquaculture sector (Zou et al., 2020).

TPD was initially identified in *L. vannamei* post-larvae. Typical symptoms of TPD included empty intestine, pale or colorless hepatopancreas (Yang et al., 2022). It is also known by multiple names, including glass post-larval disease, bacterial vitrified syndrome, and highly lethal *Vibrio* disease (HLVD), which are all based on the clinically translucent diseased features.

Studies have identified highly virulent *Vibrio parahaemolyticus* as the primary etiological agent of TPD (Yang et al., 2022; Zou et al., 2020). TPD-associated *V. parahaemolyticus* strains, designated as Vp_{HLVD} (Yang et al., 2023) or Vp_{TPD} (Jia et al., 2023), are specifically named to distinguish it from Vp_{AHPND}, namely *V. parahaemolyticus* strains causing acute hepatopancreatic necrosis disease (AHPND), thereby clarifying its unique pathogenicity and epidemiological profile.

Clinically and histologically, TPD exhibited remarkable pathological parallels to AHPND. Both TPD and AHPND can cause necrosis and shedding of epithelial cells in the hepatopancreas and midgut, and

* Corresponding author.
E-mail address: bzhou@yzu.edu.cn (B. Zhou).
[1] These authors contributed equally to this work.

https://doi.org/10.1016/j.jip.2025.108499
Received 25 August 2025; Received in revised form 25 September 2025; Accepted 18 November 2025
Available online 19 November 2025

ultimately result in high mortality rates among *L. vannamei* post-larvae (Yu et al., 2022). However, these two diseases affect *L. vannamei* at different developmental stages. TPD is highly lethal to post-larvae aged 4–7 days, while AHPND targets older shrimps and occurs approximately within 35 days after stocking of shrimp ponds (Zou et al., 2020). In terms of virulence, previous research findings have proposed that the pathogenicity of Vp_{TPD} was caused by a heat-labile bacterial toxin(s) that was not secreted into the culture environment (Yang et al., 2022) and its following studies narrowed the toxin to be the large protein complex toxin complex (Tc) which consisted of three subunits (TcA, TcB, and TcC) (Yang et al., 2023). The key virulence genes of Vp_{TPD} were identified as *vhvp2* (TcB/C unit) and *vhvp1* (TcA subunit) (Liu et al., 2023), located tandemly on plasmids. In contrast, the plasmid-borne genes ($pirA^{vp}$ and $pirB^{vp}$) encoding homologs of the *Photorhabdus* insect-related (Pir) toxins (PirA and PirB) were responsible for virulence in AHPND causative V_{pAHPND} strains (Lee et al., 2015; Phiwsaiya et al., 2017).

In shrimp aquaculture, antibiotic therapy remains the primary approach for controlling bacterial infections, including TPD. Antibiotics are frequently administered prophylactically to mitigate outbreak risks. However, long-term use of antibiotics has given rise to multiple problems, including the emergence of antimicrobial resistance (AMR) in target pathogens (Thornber et al., 2020), the potential horizontal transfer of antibiotic resistant genes among non-target bacteria, the persistence of antibiotic residues in shrimp products and aquatic environments (Hossain et al., 2022; Okeke et al., 2022), the disturbance of microorganism communities and the weakened immune system of shrimps (Chi et al., 2024). For example, the global emergence of antibiotic resistance in *Vibrio* spp. has been documented across multiple geographic regions and antimicrobial classes (Onohuean et al., 2022). Particularly, over the past decade, *V. parahaemolyticus* isolates from aquaculture and seafood systems exhibited high resistance rates to β-lactams (e.g., ampicillin, amoxicillin, penicillin G), vancomycin, and streptomycin (Hu and Chen, 2016; Zhao et al., 2018; Amalina et al., 2019; Jin et al., 2021). This resistance pattern not only limits treatment efficacy but also drives increased antibiotic doses, with some strains demonstrating complete therapeutic failure in standard regimens, underscoring the urgency of developing non-antibiotic alternatives for pathogen control in aquaculture.

In the prevention and control of TPD, effective strategies remain limited, with current practices predominantly relying on antibiotics or chemical disinfectants (Jia et al., 2023). However, promising insights emerge from studies investigating alternative interventions for managing *V. parahaemolyticus*-induced vibriosis in *L. vannamei*. These interventions include fish-derived bacteriocins (Lv et al., 2017), vaccine development (Madsari et al., 2022), plasma-activated water (Zhang et al., 2024a), and various plant-derived extracts, such as neem (*Azadirachta indica*) and oregano (*Lippia berlandieri*) aqueous extracts (Morales-Covarrubias et al., 2016), rose myrtle (*Rhodomyrtus tomentosa*) seed extract (Dang et al., 2019), *Pandanus tectorius* fruit extract (Anirudhan et al., 2021), *Psidium guajava* leaf extract (Dewi et al., 2021), *Morinda citrifolia* fruit extract (Moh et al., 2024), *Annona glabra* extract (Thi Truc Linh et al., 2024), and Kiam wood (*Cotylelobium lanceotatum*) extract (Amin et al., 2025). Traditional Chinese medicine formulations (Zhai and Li, 2019; Guo et al., 2025) and natural products such as artemisinin (Liu et al., 2022), isoquinoline alkaloids (Bussabong et al., 2021), and macroalgal phytochemicals (Vargas Cárdenas et al., 2024) have also demonstrated potential. Among these, natural antimicrobial agents, are particularly promising due to their chemical diversity and structural complexity, which may reduce resistance risks while maintaining ecological and food safety standards. Furthermore, targeting bacterial virulence factors with natural products, rather than bactericidal or bacteriostatic approaches, offers a strategic advantage in mitigating selection pressure and curbing resistance evolution. For example, taxifolin and epigallocatechin-3-gallate (EGCG) were shown to interact with the binary PirA/B toxins produced by Vp_{AHPND} (Ahmed et al., 2023). An antimicrobial mixture (a blend of organic acids, citrus, and olive extracts) was recently reported to transcriptionally silence multiple virulence determinants in a Vp_{TPD} strain and conferred robust protection to post-larvae of *L. vannamei* (Stef et al., 2025). Collectively, these findings highlight viable pathways for developing eco-friendly, antibiotic-independent strategies to combat TPD.

Gallic acid (GA; 3,4,5-trihydroxybenzoic acid), a plant-derived phenolic compound, is widely distributed in plants as a secondary metabolite. In the last decade, GA has emerged as a promising broad-spectrum antimicrobial agent with documented efficacy against clinically and environmentally relevant pathogens, including both Gram-positive and Gram-negative bacteria (Liu et al., 2017; Wang et al., 2017; Kang et al., 2018a; Kang et al., 2018b; Abdella et al., 2024). Notably, GA demonstrated its ability in effectively eradicating mature biofilms formed by mono- or dual-species cultures of Gram-negative *Pseudomonas aeruginosa* and Gram-positive *Staphylococcus aureus* (Gobin et al., 2022), as well as the biofilm formed by *Candida albicans* (Teodoro et al., 2018). Its antimicrobial mechanisms are currently understood to involve membrane destabilization, metabolic inhibition, quorum sensing interference, and biofilm disruption (Abdelaziz et al., 2022; Keyvani-Ghamsari et al., 2023; Sang et al., 2024).

While GA's multifaceted bioactivities, including antibacterial, antifungal, antiviral, antioxidant, and anti-inflammatory properties, have been extensively documented (Wang et al., 2023a), its inhibitory potential against *V. parahaemolyticus* (the major pathogen causing shrimp vibriosis) remains underexplored. This study pioneers the evaluation of GA as a natural biocontrol agent for vibriosis management in shrimp aquaculture, addressing the critical industry need for sustainable, non-antibiotic solutions.

In this study, we investigated the multifaceted antibacterial potential of GA against *V. para*. TS-GE, a pathogenic isolate associated with TPD in *L. vannamei*. We first confirmed the pathogenicity of *V. para*. TS-GE in post-larvae of *L. vannamei* through immersion challenge experiments. Subsequently, we evaluated GA's protective efficacy through *in vitro* antibacterial assays and *in vivo* challenge trials. Mechanistic investigations focused on GA's capacity in compromising the integrity of bacterial cell wall and membrane, inhibiting motility and biofilm formation, and potential interacting with key virulence proteins (VHVP1 and VHVP2) of Vp_{TPD}. Our findings provided a scientific foundation for developing GA-based eco-friendly, resistance-mitigating strategies in the prevention and control of TPD.

2. Materials and methods

2.1. Post-larvae of L. vannamei used in this study

Specific pathogen-free (SPF) 5-day-old post-larvae (PL5) of *L. vannamei*, measuring approximately 5–6 mm in body length, were purchased from Guangzhou Liyang Aquatic Products Technology Co., Ltd. (Guangzhou, China). Prior to being sold by the company, the post-larvae were subjected to pathogen screening using commercially validated qPCR kits (Guangzhou Huafeng Biological Technology Co., Ltd., Guangzhou, China) targeting key shrimp pathogens, including white spot syndrome virus (WSSV), shrimp hemocyte iridescent virus (SHIV), *Enterocytozoon hepatopanaei* (EHP), and *Vibrio parahaemolyticus* causing acute hepatopancreatic necrosis disease (Vp_{AHPND}). Pathogen detection tests were performed via TaqMan probe-based real-time PCR, confirming the absence of these pathogens in the tested post-larvae.

Before initiating the challenge test, the *L. vannamei* post-larvae were acclimated to laboratory conditions for 2 days in 10-L plastic tanks equipped with constant aeration. The post-larvae were maintained at 26℃ in sterile seawater with a salinity of 15 ‰ at a density of approximately 30 individuals/L, and fed twice daily with commercial pelleted shrimp post-larvae feed (2 % of their body weight, *ad libitum*) (Guangdong Evergreen Feed Industry Co., Ltd., Zhanjiang, Guangdong, China).

Upon arrival at the laboratory, 10 post-larvae of *L. vannamei* were randomly selected from the batch and pooled into a single composite

sample for re-confirmation of the absence of three specific *Vibrio* pathogens, Vp_{AHPND}, *Vibrio harveyi*, and Vp_{HLVD} (*Vibrio parahaemolyticus* strains associated with highly lethal *Vibrio* disease), using a series of commercial kits supplied by Findrop Biosafety Technology (Guangzhou) Co., Ltd. (Guangzhou, China). Briefly, DNA was extracted from the pooled sample using the ALFA-SEQ Fast Magnetic Universal DNA Kit (Catalog No. DC304-01). Target pathogen DNA was detected using Lyophilized PCR-fluorescent Probe Reagent kits specific for Vp_{AHPND} (catalog No. TAS02T16S1), *V. harveyi* strains (Catalog No. TAS14T16S1), and Vp_{HLVD} (Catalog No. TAS22T16S). All assays were performed according to the respective kit instructions provided by the manufacturer.

2.2. Bacterial strain used in this study and growth conditions

The bacterial strain used in this study, *Vibrio parahaemolyticus* TS-GE (*V. para*. TS-GE) was isolated from moribund *L. vannamei* shrimps exhibiting typical TPD symptoms and donated by the laboratory at Huanghua Hairen Aquatic Seed Industry Technology Co., Ltd. (Huanghua, China). Following purification, the bacterial strain was preserved at −80℃ in 2216E broth containing 20 % glycerol for long-term storage. The bacteria were revived by streaking them onto the thiosulfate citrate bile salts sucrose (TCBS) agar plates, and subsequently, single colonies were proliferated at 28 °C in Luria-Bertani (LB) medium supplemented with 3 % NaCl.

2.3. Bacterial identification

The genus-level taxonomy of the *V. para*. TS-GE strain employed in this study was determined through 16S rRNA gene sequence analysis. Bacterial genomic DNA was extracted using the Bacterial Genomic DNA Extraction Kit (Catalog No. DP302) manufactured by Tiangen Biotech (Beijing) Co., Ltd. (Beijing, China). The universal primers for amplification of the 16S rRNA gene were 27F (5′-AGAGTTTGATCCTGGCTCAG-3′) and 1492R (5′-GGTTACCTTGTTACGACTT-3′). The PCR protocol was conducted as follows: an initial denaturation step at 95℃ for 5 min, followed by 30 cycles of 94℃ for 30 s, 55℃ for 30 s, and 72℃ for 90 s, then a final extension step at 72℃ for 10 min. The resulting PCR products were sequenced by Sangon Biotech Co., Ltd. (Shanghai, China). The obtained 16S rRNA gene sequence was subjected to BLAST analysis against the NCBI databases. A phylogenetic tree was constructed using MEGA-X software using bootstrap analysis based on the neighbor-joining algorithm with 1000 replicates (Kumar et al., 2018).

2.4. Pathogenicity assessment of V. para. TS-GE on L. vannamei post-larvae

The immersion challenge test was conducted based on the method previously described (Jia et al., 2023) with slight modifications. In brief, acclimated post-larvae (PL7) of *L. vannamei* were randomly assigned to 4 groups, comprising 3 challenged groups and one control group. Each of the challenged groups consisted of 3 replicates, and each replicate contained 30 post-larvae maintained in 1 L of seawater within a 2-L glass jar (measuring 13.5 cm × 16.8 cm × 14.4 cm). The post-larvae in the challenged groups were exposed to seawater containing pure cultures of *V. para.* TS-GE at different final concentrations. Meanwhile, the post-larvae in the control group were kept in sterile seawater.

To prepare pure bacterial suspensions, stocked bacterial suspensions were streaked onto TCBS agar plates. A single colony was randomly selected and sub-cultured in LB liquid medium at 28℃ overnight, with continuous shaking at 120 rpm. The bacterial culture was then centrifuged at 6,000 rpm for 10 min. The resulting pellet was washed and re-suspended three times in sterile seawater. The bacterial density was adjusted to an optical density at 600 nm (OD_{600}) of 1.0 using a spectrophotometer, which was approximately equivalent to a bacterial concentration of 1×10^9 CFU/mL (Zou et al., 2020). Subsequently, the bacterial suspension was subjected to serial 10-fold dilutions in sterile seawater to achieve 3 target concentrations (10^7, 10^6, and 10^5 CFU/mL). These diluted bacterial suspensions were then used for the immersion challenge tests. The exact bacterial concentrations were further confirmed using the plate count dilution method. For the *V. para*. TS-GE strain, the final bacterial densities in 3 challenged groups were 2.82×10^7, 2.82×10^6, and 2.82×10^5 CFU/mL, respectively.

During the immersion challenge test, mortalities were recorded at 2-hour intervals across a 32-hour duration. The median lethal concentration (LC_{50}) of the bacterial strain was determined. Dead and moribund post-larvae were promptly removed from the rearing containers. The collected diseased post-larvae were utilized for DNA extraction and subsequent identification of the presence of the virulent genes (*vhvp1* and *vhvp2*) responsible for TPD, as previously reported by Liu et al. (2023). This identification was conducted employing a commercially available Highly Pathogenic *Vibrio* (HLV) Nucleic Acid Detection Kit (Lyophilized Type/TaqMan Fluorescent Probe Method) manufactured by Guangzhou Huafeng Biological Technology Co., Ltd., Guangzhou, China (Catalog No. SC-26J2C-II).

2.5. In vitro antibiotic susceptibility assay

The antibiotic susceptibility of the tested pathogenic bacterial strain *V. para*. TS-GE was evaluated against 12 commonly used antibiotics using the Kirby-Bauer standard disc diffusion method. These antibiotics target various bacterial processes, including cell wall synthesis (Amoxicillin, Cefoperazone, Penicillin G, and Vancomycin), protein synthesis (Chloramphenicol, Clindamycin, Erythromycin, Gentamicin, Kanamycin, Streptomycin), DNA synthesis (Norfloxacin), and cell membrane integrity (Polymyxin B).

In brief, bacterial cultures grown overnight in LB medium at 37 °C were centrifuged at 6,000 rpm for 5 min to pellet the cells. The resulting pellets were washed 3 times with phosphate-buffered saline (PBS), re-suspended in PBS, and adjusted to a concentration of 1.0×10^8 CFU/mL. A 100 μL aliquot of the bacterial suspension was evenly spread onto the surface of 90-mm LB agar plates, which were then allowed to dry at room temperature. Commercial standard antibiotic paper discs (6 mm in diameter, supplied by Hangzhou Microbiological Reagents Co., Ltd., Hangzhou, China) were applied onto the solidified agar surface using a disc dispenser. The plates were first incubated at 4 °C for 30 min for antibiotic diffusion, followed by incubation at 37 °C for 24 h. The diameters of the resulting inhibition zones were measured. The assay was performed in triplicates. Results were categorized as susceptible, moderately susceptible, or resistant based on the interpretative standards provided by the manufacture.

2.6. Antibacterial activities of GA against the tested Vibrio strain

High-purity GA powder (purity ≥ 98.0 %) was purchased from Solarbio Science & Technology Co., Ltd., Beijing, China (Catalog No. SG8040). GA was dissolved in distilled water to prepare a 10 mg/mL stock solution, which was then sterilized by filtration through a 0.22-μm membrane filter and diluted with sterile water to the desired working concentrations. A preliminary agar well diffusion assay was performed to verify the inhibitory effect of GA on the growth of the pathogenic *Vibrio* strain used in this study. The results of the agar well diffusion assay demonstrated that GA could inhibit the growth of *V. para*. TS-GE. Specifically, 125 μg of GA (1.25 mg/mL, 100 μL/well) produced inhibition zones with an average size of 12.88 ± 0.33 mm against *V. para*. TS-GE. These inhibition zones were comparable to those generated by 50 μg of chloramphenicol (0.5 mg/mL, 100 μL/well), which resulted in inhibition zones of 12.62 ± 0.38 mm against *V. para*. TS-GE.

The minimal inhibitory concentration (MIC) and minimum bactericidal concentration (MBC) of both GA and chloramphenicol against *V. para.* TS-GE were determined using a resazurin-based micro-broth dilution method as described by Elshikh et al. (2016). Briefly, overnight

cultures of *V. para.* TS-GE were adjusted to a concentration of 1.5×10^5 CFU/mL using LB medium. A 100-μL aliquot of bacterial suspension was added to each well of a 96-well plate. Subsequently, 100 μL of GA solution was added to achieve final GA concentrations ranging from 8000 μg/mL down to 15.625 μg/mL through a series of two-fold dilutions (i.e., 8000, 4000, 2000, 1000, 500, 250, 125, 62.5, 31.25, and 15.625 μg/mL). For chloramphenicol, final concentrations ranging from 250 μg/mL to 1.953 μg/mL (specifically, 250, 125, 62.5, 31.25, 15.625, 7.813, 3.906, and 1.953 μg/mL) were employed. The positive growth control well consisted of 200 μL of bacterial suspension, while the negative growth control well contained 200 μL of LB medium. After thorough mixing, the plate was incubated at 37 °C for 20 h. Then, 30 μL of a 0.015 % resazurin solution was added to each well, and the plate was incubated for an additional 4 h. The metabolic activity of viable bacterial cells can reduce the blue resazurin to pink resorufin. A purple color in the well indicated the absence of bacterial growth, whereas a pink color indicated bacterial growth. After the incubation period, MICs were recorded at the lowest concentration displaying unchanged purple color. This experiment was repeated 3 times, with 3 replicate wells set up for each concentration in each experiment. To determine the MBC, the contents of wells with concentrations higher than the MIC value were directly plated onto 2216E agar plates and incubated at 37 °C for 48 h. The lowest concentration that showed no bacterial growth on the solid medium was defined as the MBC.

2.7. The checkerboard assays

The synergistic interaction between GA and the antibiotic chloramphenicol (CAP) was evaluated using the checkerboard assay and performed on 96-well plates. Based on the determined MIC values of GA and CAP against the tested *Vibrio* strain, concentrations were prepared at multiple levels both above and below the MIC. Specifically, concentrations above the MIC were set at 4×, 2×, and 1 × MIC, while a two-fold dilution series starting from 1/2 × MIC down to 1/32 × MIC were used for concentrations below the MIC. Both GA and CAP were diluted in LB liquid medium to prepare aqueous solutions. The bacteriostatic effects of various combinations of GA and CAP on *V. para.* TS-GE were then assessed using the microdilution method, as previously described for the determination of MIC.

Briefly, overnight cultures of the *V. para.* TS-GE strain were grown in LB liquid medium and adjusted to 1.5×10^5 CFU/mL using the same medium. A 100-μL aliquot of the bacterial suspension was added to each well of a 96-well plate. Subsequently, 50 μL each of GA and CAP solutions were added to each well to achieve various combinations of the two substances. After a 20-hour incubation at 37 °C, 30 μL of a 0.015 % resazurin solution was added to each well, and the plate was incubated for an additional 4 h. Wells containing only LB medium served as the negative control, whereas wells containing bacterial suspension without the addition of either GA or CAP were designated as the positive control. The fractional inhibitory concentration (FIC) index was calculated according to the following formula:

$$FIC_{GA} = (\text{MIC of GA in the presence of CAP}) / (\text{MIC of GA alone})$$

$$FIC_{CAP} = (\text{MIC of CAP in the presence of GA}) / (\text{MIC of CAP alone})$$

$$\text{FIC index} = FIC_{GA} + FIC_{CAP}$$

The bacteriostatic interactions were interpreted as: synergy (FIC index < 0.5), partial synergy (FIC index from 0.5 to 0.75), additive effect (FIC index from 0.76 to 1.0), indifference (FIC index > 1.0 to 4.0), and antagonism (FIC index > 4.0) (Asok et al., 2004).

2.8. Protective effects of GA on post-larvae challenged by V. para. TS-GE

We initially conducted an experiment to evaluate the potential toxicity of GA on post-larvae (PL7) of *L. vannamei*. Based on the previously determined MIC value of GA against the tested *Vibrio* strain, specifically 1000 μg/mL for *V. para.* TS-GE, we prepared the 1 × MIC concentration (1000 μg/mL) and a 1/5 × MIC concentration (200 μg/mL). The post-larvae were exposed to these GA concentrations. Subsequently, the LC_{50} of GA for the post-larvae was determined at 12 h, 24 h, 36 h, and 48 h post-exposure. Our results demonstrated that a GA concentration of ≤ 200 μg/mL exerted no significant influence on the survival of post-larvae. Based on these findings, we conducted an experiment to evaluate the protective efficacy of GA against the challenges posed by *V. para.* TS-GE on 7-day-old post-larvae of *L. vannamei*.

In this experiment, post-larvae were randomly assigned to 4 experimental groups. The control group ($Group_{control}$) was maintained in sterile seawater without bacterial challenge or GA treatment. The GA group ($Group_{GA}$) received GA at a final concentration of 200 μg/mL (equivalent to 1/5 × MIC against *V. para.* TS-GE). The challenged group ($Group_{Vibrio}$) was subjected to bacterial challenges of *V. para.* TS-GE at a density of 1.26×10^6 CFU/mL. The co-treatment group ($Group_{Vibrio+GA}$) were simultaneously exposed to both *V. para.* TS-GE (1.26×10^6 CFU/mL) and GA (200 μg/mL). Each group had three replicates, with 20 post-larvae in each replicate. The methods for data recording and sampling followed the procedures described above. Frozen sections were prepared from dead post-larvae as described by Cervellione et al. (2017).

2.9. Re-isolation of Vibrio bacteria from post-larvae

Dead or moribund post-larvae of *L. vannamei*, collected from $Group_{Vibrio}$ were used in their entirety (including the stomach, hepatopancreas, and intestines) for sample collection. Initially, bacteria adhering to the exterior surface of the collected post-larvae were thoroughly removed. This was achieved by rinsing the post-larvae with a pre-cooled 1 % benzalkonium chloride solution for 30 s, followed by 3 successive washes in pre-cooled sterile seawater, each lasting 30 s, as described by Niu et al. (2012). Re-isolation of dominant bacteria was performed according to (Yu et al., 2022). Briefly, the post-larvae were fully homogenized in sterile PBS buffer (pH 7.2). The homogenized liquid was then inoculated onto TCBS agar plates and incubated at 28 °C. Dominant colonies were sub-cloned through 3 rounds of re-streaking. The purified bacterial strains obtained were further cultivated in LB liquid medium. Molecular identification of these strains was conducted by amplifying and sequencing the 16S rRNA gene.

2.10. Whole genome sequencing of V. para. TS-GE

The total DNA of the *V. para.* TS-GE strain was extracted from pure cultures using a commercial TIANamp Bacteria DNA Kit (Tiangen, China). The whole genome was sequenced at Tianjin Novogene Bioinformatic Technology Co., Ltd. (Tianjin, China). Short-read sequencing was conducted on the Illumina Hiseq 2500 platform and long-read sequencing was performed using the Oxford Nanopore Technologies MinION platform. Short-read genome assembly was performed with SPAdes v.3.10.1 (Bankevich et al., 2012). The closed, complete genomes were obtained through a hybrid assembly strategy that combined short-read and long-read sequences using Unicycler (Wick et al., 2017). Based on the sequencing data, a whole genome-based taxonomic analysis was performed and the GBDP tree (whole-genome sequence-based) was constructed using the Type (Strain) Genome Server (TYGS), a free bioinformatics platform available under https://tygs.dsmz.de, to further confirm the taxonomic classification of the *V. para.* TS-GE strain. Functional annotation of the *V. para.* TS-GE strain was performed using the RAST-SEED server (Rapid Annotation Subsystem Technology) (https://rast.nmmpdr.org).

2.11. Screening for virulence and antibiotic resistance genes in V. para. TS-GE

Using ABRicate (v1.0.1) we screened antimicrobial resistance genes

(ARGs) and virulence factors (Virulence Factor Database, VFDB) in the whole genome of *V. para.* TS-GE. For the screening of *vhvp*1 and *vhvp*2 genes, we constructed a local database, which included the *vhvp*1 gene sequence (GenBank: OQ378179.1) and 4 nucleotide sequences of the *vhvp*2 gene encoding SpvB/TcaC *N*-terminal, SpvB, TcdB_toxin_midN, and TcdB_toxin_midC from the vp-HL-201910 plasmid pHLC_201910 (NCBI GenBank Accession number: CP152366) (Zhang et al., 2024b).

2.12. Multilocus sequence typing (MLST) and pangenome analyses

A total of 789 assembled genomic sequences of *V. parahaemolyticus* strains were retrieved from the NCBI database (accessed on July 30, 2025). MLST loci were profiled *in silico* using the online tool (https://pubmlst.org/). The MLST scheme for *V. parahaemolyticus* targeted internal sequences of 7 housekeeping gene loci distributed across both chromosomes of *V. parahaemolyticus* (*rec*A, *dna*E, *gyr*B, *dtd*S, *pnt*A, *pyr*C, and *tna*A) (González-Escalona et al., 2008). A final dataset comprising 480 strains was retained for comprehensive MLST analysis, including the *V. para.* TS-GE strain used in this study. Each strain in the dataset was annotated with documented metadata including geographic origin, isolation date, host source, and confirmed MLST type (detailed information, including the RefSeq Assembly Accession number, MLST types, isolation location, source, and date, are provided in Supplemental File S1. This dataset of 480 *V. parahaemolyticus* strains were further used for pangenome analysis. For each genome, the GFF3 files were generated by Prokka (Seemann, 2014) and these files were subsequently employed in the pangenome analysis conducted with Roary v3.12.0 (Page et al., 2015). The phylogenetic tree was constructed using Roary and FastTree based on core genomes and the results obtained from Roary were visualized using an online server (http://jameshadfield.github.io/phandango/#/).

2.13. The influence of GA on the bacterial cell wall and cell membrane

The effects of GA on the cell wall of the tested *Vibrio* strain were assessed by measuring the activity of extracellular alkaline phosphatase (AKP) (Yu et al., 2024). A commercial AKP assay kit (Jiancheng Bioengineering Institute, Nanjing, China) was employed for this quantification, following the manufacturer's instructions. Briefly, bacterial suspensions with a concentration of 1×10^5 CFU/mL were prepared in sterile PBS and used as indicator suspensions. In 12-mL shaking tubes, 3 mL of each indicator suspension was mixed with 3 mL of a GA solution, which was also prepared in sterile PBS, to achieve final GA concentrations of 1/4 × MIC, 1/2 × MIC, 1 × MIC, and 2 × MIC. A control group was established by mixing the indicator suspension with an equal volume of sterile PBS. The experiment was conducted in triplicate. The bacterial cultures were incubated at 28℃ in a shaking incubator set at 120 rpm. At time points of 0, 2, 4, 6, and 8 h, 1-mL samples were taken from each tube. These samples were centrifuged at 4℃ and 6,000 rpm for 10 min, and the supernatants were collected for the measurement of absorbance at a wavelength of 520 nm (OD_{520}). The AKP contents were then calculated and expressed as King units per 100 mL. Additionally, the effects of GA on the cell membranes of the tested *Vibrio* strain were assessed by measuring the absorbance of the supernatants obtained at the 4-hour time point at a wavelength of 260 nm (OD_{260}).

2.14. Inhibitory effects of GA on biofilm formation and biofilm dispersal

The antibiofilm activity of GA against the tested *Vibrio* strain was evaluated using the crystal violet assay, employing a modified version of the protocol outlined by Liu and Wang (2022). In brief, overnight bacterial cultures were harvested and diluted to 1×10^6 CFU/mL in LB medium. For the biofilm formation inhibition assay, 200 μL of the bacterial suspension was dispensed into each well of transparent, flat-bottomed 96-well polystyrene plates. Subsequently, 100 μL of GA solutions at varying concentrations was added to each well to achieve final concentrations equivalent to 2×, 1×, 0.5×, and 0.25 × MIC specific to the *V. para.* TS-GE strain. Wells containing 200 μL of bacterial suspension and 100 μL of LB medium served as the control. The plates were then incubated statically at 28 °C for 24 h. Following incubation, the supernatant in each well was gently aspirated, and the wells were rinsed 2–3 times with sterile PBS to remove suspended bacteria.

Biofilm quantifications were conducted using the crystal violet staining method. Briefly, each well was fixed with 200 μL of methanol for 15 min, followed by aspiration of the methanol and addition of 200 μL of crystal violet (0.1 % w/v) to stain the biofilms. The plate was incubated at room temperature for 20 min, after which the crystal violet solution was carefully aspirated, and the wells were rinsed with sterile distilled water to remove unbound crystal violet and air-dried. Finally, 200 μL of 33 % glacial acetic acid solution was added to each well to dissolve the crystal violet, and after 15 min, the absorbance was measured at 570 nm (OD_{570}) using 33 % (v/v) glacial acetic acid solution as the blank control. The inhibition rate (%) of biofilm formation was calculated using the formula:

Inhibition rate (%) $= 100\ \% \times (D_{control} - D_{GA})/D_{control}$, where $D_{control}$ and D_{GA} are the OD_{570} values measured in the absence and presence of GA, respectively. All experiments were conducted in triplicates.

The biofilm dispersal assay was conducted as previously described (Faleye, et al., 2021) with minor modifications. As described above, the tested *Vibrio* strain was seeded into the 96-well plate (200 μL per well at the density of 1×10^6 CFU/mL in LB medium) in the absence of GA and incubated at 28 °C for 24 h without shaking to establish biofilms. After incubation, the medium was aspirated from each well, and non-adherent bacterial cells were removed by washing the wells three times using sterile PBS. Different concentrations of GA in LB medium (corresponding to 2×, 1×, 0.5×, and 0.25 × MIC specific to the bacterial strain) were added to the wells of 96-well plates and incubated for another 24 h at 28 °C. Then, crystal violet staining was performed and OD_{570} were determined. Results are presented from three independent assays.

2.15. Swimming motility assays

The motility of the *V. para.* TS-GE strain was assessed by measuring the diameter of the bacterial circles after inoculation on swimming plates. Briefly, overnight bacterial cultures were adjusted to a concentration of 1×10^5 CFU/mL in LB liquid medium. A 2-μL aliquot of the resulting bacterial suspension was spotted onto swimming plates, which were prepared using LB medium containing 0.3 % (w/v) agar supplemented with varying concentrations of GA (0.25×, 0.5×, 1×, 2 × MIC). Plates without GA served as the control. To ensure technical replicability, the process of spotting a 2-μL aliquot of the bacterial suspension onto the swimming plates was repeated three times for each condition. The plates were incubated at 28 °C for 24 h. After incubation, the diameter of the turbid area, which resulted from bacterial migration from the initial inoculation site, was measured. The motility inhibition rate was calculated using the formula (Qiao et al., 2021):

Inhibition rate (%) $= 100\ \% \times (D_{control} - D_{GA})/D_{control}$, where $D_{control}$ and D_{GA} represent the motility zone diameter (in millimeters) measured in the absence and presence of GA, respectively.

2.16. Molecular docking (MD) analysis

We performed MD analysis to investigate the impacts of GA on the previously reported key virulence factors of *V. parahaemolyticus* associated with TPD. Specifically, we focused on *Vibrio* high virulent protein (VHVP)-1 and VHVP-2, which were encoded by genes located on plasmids and considered to be the key virulence factors to cause TPD (Liu et al., 2023). By elucidating how GA interacts with VHVP1 and VHVP2 may provide valuable insights into the potential antibacterial mechanisms of GA.

MD analysis was performed according to our previously established protocol (Ye et al., 2025). In brief, the protein structures of VHVP1 and

VHVP2 were predicted using the I-TASSER (Iterative Threading ASSEmbly Refinement) web interface at https://zhanggroup.org/I-TASSER/ (accessed on June 11, 2025). Structure model with the highest confidence score was selected for subsequent docking analysis. Ligand binding pockets within these proteins were identified using the DogSiteScorer online tool at https://proteins.plus/ (accessed on June 15, 2025). For the preparation of protein receptors, polar hydrogens were added, Gasteiger charges were computed, and AD4 atom types were assigned using AutoDock Tools (v1.5.7). The 3-dementional structure of GA (CHEBI:30778) in mol2 format was retrieved from the Chemical Entities of Biological Interest (chEBI) database at https://www.ebi.ac.uk/chebi/ (accessed on June 15, 2025) and converted to the.pdbqt format using OpenBabel (v.2.4.1). MD analysis was conducted using AutoDock Vina (v.1.2.3), with the proteins as rigid receptors and GA as a flexible ligand. Docking results were visualized using Pymol software (v.3.0.4), the online server Protein-Ligand Interaction Profiler (https://plip-tool.biotec.tu-dresden.de/plip-web/plip/index) and LigPlot+ (v.2.2.8).

2.17. Statistical analysis

Data obtained from different groups were analyzed via one-way analysis of variance (ANOVA) using SPSS 22 (Chicago, IL, USA). Initially, the normality of the data was assessed using the Shapiro-Wilk test, and the homogeneity of variance was evaluated using Levene's test (with a significance level set at 0.05). When the *P*-value from Levene's test was greater than 0.05 and the data met the normality assumption, Duncan's multiple range test was employed to identify differences among the means. Otherwise, Dunnett's T3 post-hoc analysis was conducted instead. Data in this study are presented as the mean ± standard deviation (SD). A *P*-value of less than 0.05 was set as the threshold for significance. LC_{50} was calculated utilizing the Probit analysis procedure in SPSS based on the mortality of post-larvae. The comparison of survival rate among the challenged and control groups was analyzed through the Kaplan-Meier survival (Log-rank value) analysis test.

3. Results

3.1. Absence of known Vibrio pathogens in the post-larvae used in this study

Results of molecular detection assays confirmed the absence of 3 known *Vibrio* pathogens (Vp_{AHPND}, *Vibrio harveyi*, and Vp_{HLVD}) in the post-larvae of *L. vannamei* used in the present study (Supplemental

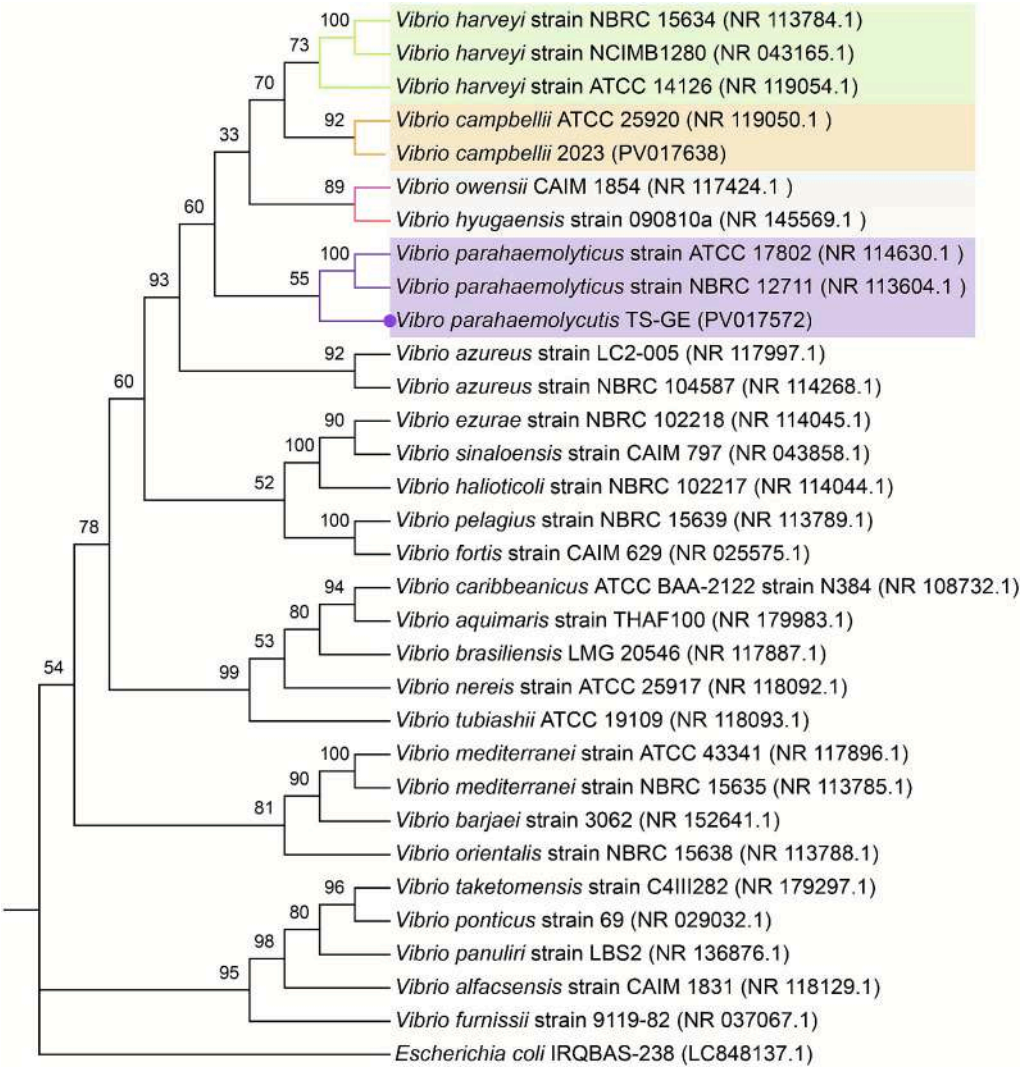

Fig. 1. Phylogenetic tree constructed using the neighbor-joining method based on 16S rRNA gene sequence of the tested bacterial strain. Bootstrap values expressed as percentages (n = 1000 replicates) are shown above nodes. NCBI accession numbers for the 16S rRNA gene sequences are provided in parentheses following each strain name.

Fig. S1).

3.2. Molecular identification of the tested Vibrio strain

Analysis of the 16S rRNA gene sequence demonstrated that the tested bacterial strain (*V. para*. TS-GE) belonged to the genus *V. parahaemolyticus*, with a sequence similarity exceeding 99.9 % (Fig. 1).

3.3. Experimentally reproducing TPD in post-larvae of L. Vannamei

Results from the immersion challenge tests revealed that the post-larvae of *L. vannamei* used in this study exhibited high susceptibility to infection by the tested *Vibrio* strain. Throughout the 32-hour experimental duration, no mortality was observed in the control (unchallenged) group. However, the post-larvae exposed to the *V. para.* TS-GE strain exhibited reduced mobility and appetite loss as early as 6 h post-infection (hpi). As the exposure duration extended, an increasing proportion of post-larvae sank to the bottom of the tank. These moribund post-larvae displayed typical symptoms of TPD, characterized by a colorless hepatopancreas and a transparent body appearance due to their empty digestive tracts. Our results confirmed that the *V. para.* TS-GE strain reproduced the TPD symptoms in the experimental post-larvae of *L. vannamei*. The immersion challenge tests further revealed that the *V. para.* TS-GE strain exhibited high virulence towards *L. vannamei* post-larvae (Supplemental Table S1). At a final bacterial concentration of 2.82×10^7 CFU/mL, the *V. para.* TS-GE strain induced complete mortality (100 %) in post-larvae within 24 hpi (Fig. 2A). The 24-hour LC_{50} value for the *V. para.* TS-GE strain was determined to be 4.72×10^4 CFU/mL. Moreover, commercial kit testing for virulent genes causing TPD yielded positive results in moribund post-larvae samples (Figs. 2B, 2C). These findings confirmed that the *V. para.* TS-GE strain was a highly virulent infectious agent capable of inducing TPD in experimental post-larvae of *L. vannamei*.

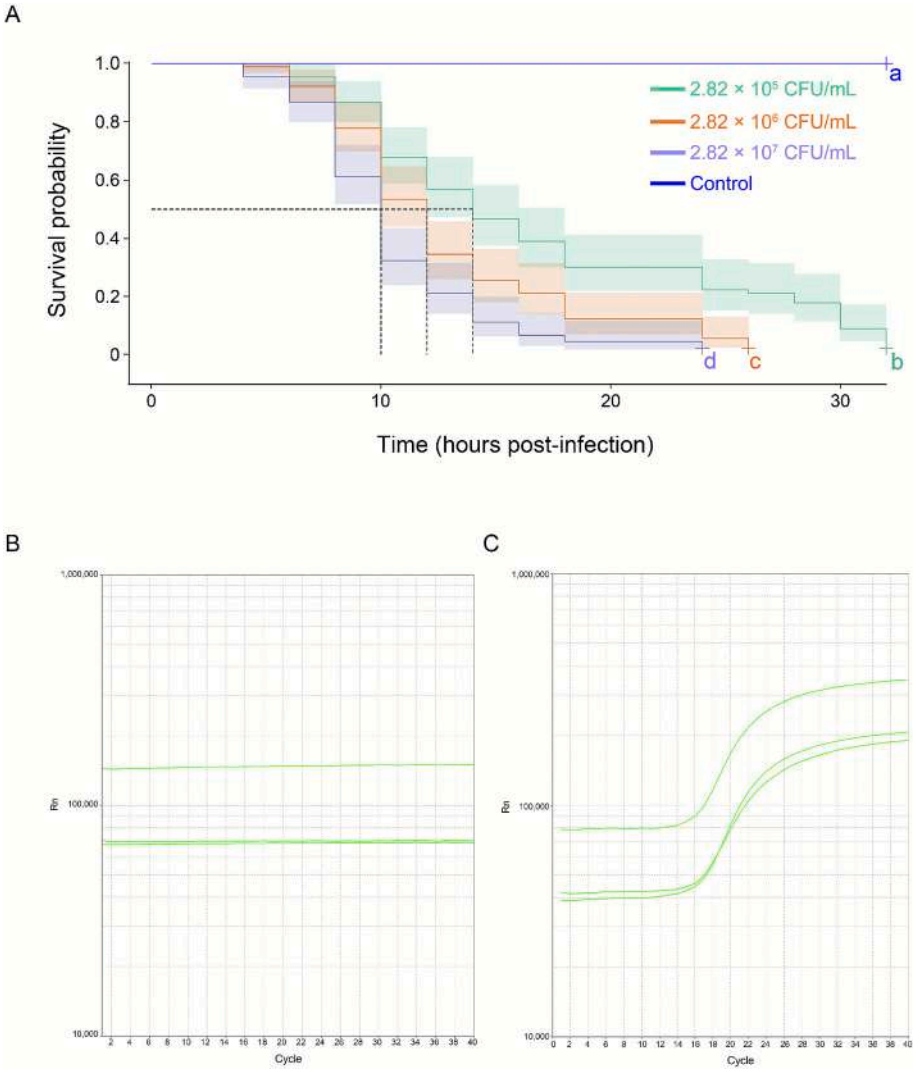

Fig. 2. Experimental validation of the *Vibrio parahaemolyticus* TS-GE strain as a virulent pathogen for post-larvae of *Litopenaeus vannamei*. A. Survival probability of *L. vannamei* post-larvae following exposure to different concentrations of *V. parahaemolyticus* TS-GE. The immersion challenge test consisted of 4 groups, including 3 groups challenged with the tested *Vibrio* strain and one unchallenged control group. Kaplan-Meier survival curves were generated and the log-rank test was performed to compare survival curves among the groups followed by the Holm-Sidak's multiple comparison test. Significant differences ($P < 0.05$) in survival curves were detected among all groups, with different lowercase letters indicating significant differences at the $P < 0.05$ level. B and C. The amplification plots for detection of virulent genes in moribund post-larvae of *L. vannamei* from the immersion challenge test. Post-larvae were collected from the control group rearing in sterile seawater (B) or from groups challenged with *V. parahaemolyticus* TS-GE (C). A straight or slightly sloping curve, lacking an S-shaped amplification curve, indicates a negative sample. Conversely, a test sample with a cycle threshold (Ct) value ≤ 38 and an S-shaped amplification curve is considered positive. Our results confirmed that the moribund post-larvae collected during the immersion challenge test were positive for virulent genes causing TPD.

3.4. Antibiotic profiles of the tested bacterial strain

Our results revealed that the *V. para.* TS-GE, displayed a multiple antibiotic resistance index of 33.33 %. Specifically, it was susceptible to cefoperazone, chloramphenicol, and gentamicin, while demonstrating resistance to penicillin G, vancomycin, clindamycin, and streptomycin (Table 1).

3.5. Inhibitory effects of GA on the growth of the tested Vibrio strain

The *in vitro* antibacterial experiment demonstrated that GA exhibited growth-inhibitory activity against *V. para.* TS-GE. The MIC value of GA was determined to be 1000 μg/mL for *V. para.* TS-GE and the MBC value was twice the respective MIC value. Furthermore, growth curve analysis confirmed that GA prevented the growth of *V. para.* TS-GE at the concentration of 1 × MIC (Supplemental Fig. S2).

To explore whether the antibacterial efficacy of GA could be enhanced in combination with chloramphenicol (CAP), an antibiotic to which *V. para.* TS-GE was susceptible, a checkerboard assay was performed. The results indicated that the GA-CAP combination remarkably improved the inhibition of bacterial growth compared to either compound alone (Table 2). The observed interactions were classified as partial synergistic.

3.6. Protective effects of GA against infections of V. para. TS-GE on post-larvae

We evaluated the acute toxicity of GA in *L. vannamei* post-larvae by determining time-dependent LC_{50} values at 12, 24, 36, and 48 h exposure intervals. The LC_{50} decreased from 943.6 μg/mL (95 % CI: 865.2–1044.1) at 12 h to 745.8 μg/mL (682.6–816.2) at 24 h, and further to 594.8 μg/mL (543.4–667.1) at 36 h. By 48 h, the LC_{50} plateaued at 588.0 μg/mL (537.1–660.1), with only a negligible 1 % decline from the 36-h value, suggesting that GA toxicity approached its maximum threshold under the tested concentration conditions.

During the 48-h exposure period, post-larvae exposed to GA exhibited no observable behavioral abnormalities, including hyperactivity, jumping, or repetitive collisions with container walls. Notably, post-larvae exposed to ≤ 200 μg/mL GA exhibited survival rates statistically comparable to those of the control group (sterile seawater, 0 % mortality; $P > 0.05$). These results collectively indicated that GA concentrations ≤ 200 μg/mL exerted no significant acute toxicity on *L. vannamei* post-larvae under the tested experimental conditions (Supplemental Fig. S3).

Table 1
Susceptibility of the tested *Vibrio* strain to 12 commonly used antibiotics.

Antibiotics	*Vibrio parahaemolyticus* TS-GE	
(Potency per disc)	ZOI[a] (mm)	Sensitivity
Inhibitors of cell wall synthesis		
Amoxicillin (20 μg)	16.18 ± 0.95	I
Cefoperazone (75 μg)	25.15 ± 0.45	S
Penicillin G (10 U)	12.88 ± 0.46	R
Vancomycin (30 μg)	≈ 0.00	R
Inhibitors of protein synthesis		
Chloramphenicol (30 μg)	22.64 ± 1.06	S
Clindamycin (2 μg)	≈ 0.00	R
Erythromycin (15 μg)	13.51 ± 0.69	I
Gentamicin (10 μg)	16.02 ± 0.42	S
Kanamycin (30 μg)	14.90 ± 0.84	I
Streptomycin (10 μg)	11.29 ± 0.06	R
Inhibitor of DNA synthesis		
Norfloxacin (10 μg)	15.60 ± 0.06	I
Disruptor of cell membrane		
Polymyxin B (300 IU)	10.72 ± 0.29	I

[a] ZOI, zone of inhibition; diameter measured in millimeters (mm). The results of antibiotic susceptibility tests are categorized as R (resistant), I (intermediate), or S (susceptible).

Table 2
Combined bacteriostatic effects of gallic acid and chloramphenicol against *Vibrio parahaemolyticus* TS-GE.

Compound	MIC[a] (μg/mL)		FIC[b] index	Effect
	Single	Combined		
GA (gallic acid)	1000	500	0.5312	Partial synergy
CAP (chloramphenicol)	62.5	1.95		

[a] MIC, minimum inhibitory concentration; [b] FIC, fractional inhibitory concentration.

The protective effects of GA against infections by the pathogenic *V. para. TS-GE* were assessed in post-larvae of *L. vannamei* via 48-hour immersion challenge tests (Supplemental Table S2). During the whole experimental period, no mortality was observed in the control group (0/40). Minimal mortality was recorded in $Group_{GA}$ (treated with 200 μg/mL of GA, 2/60). In pathogen-challenged groups (final concentration 1.06×10^6 CFU/mL of *V. para.* TS-GE), the first peak in mortality was observed between 6 hpi and 8 hpi. By 32 hpi, all post-larvae challenged with *V. para.* TS-GE succumbed (100 % mortality) (Fig. 3A). The presence of GA during the bacterial challenge delayed the onset of the mortality peak to 16–18 hpi, with cumulative mortality stabilized at 18.3 % until the end of the experiment (48 hpi). Our results indicated that GA effectively protected post-larvae against infections by the pathogenic strain *V. para.* TS-GE, significantly ($P < 0.01$) enhancing their survival rates (Fig. 3B).

Furthermore, typical clinical signs were observed in the post-larvae challenged with the pathogenic strain, including an empty digestive tract and a colorless hepatopancreas. Histopathological examination revealed that the epithelial cells of the hepatopancreatic tubules and midgut in post-larvae from the control group were well organized and tightly packed, maintaining intact structural integrity. In contrast, infected post-larvae subjected to the immersion bioassay exhibited marked pathological changes. At 24 hpi, post-larvae exposed to *V. para.* TS-GE displayed extensive necrosis and sloughing of epithelial cells in both the hepatopancreatic tubules and midgut. Notably, the presence of GA was found to mitigate histopathological damages in post-larvae challenged with pathogenic bacteria. In the hepatopancreatic tubules, GA helped preserve epithelial cell integrity and reduce the extent of necrosis. Concurrently, the midgut epithelial cells in GA-treated post-larvae displayed a restored normal structure, characterized by orderly organization and intact adhesion to the basement membrane (Fig. 3C).

3.7. Re-isolation of dominant bacterial strains from moribund post-larvae

16S rRNA gene sequencing revealed that the predominant bacterial colonies isolated from moribund *L. vannamei* post-larvae in the challenge tests were identical to the *V. para.* TS-GE strain, establishing *V. para.* TS-GE as the etiological agent of the observed mortality in *L. vannamei* post-larvae.

3.8. Whole genome sequencing and pangenome analysis

Sequencing data revealed that the complete genome of *V. para.* TS-GE consisted of 2 circular chromosomes (3,497,252 bp and 1,916,833 bp) with a (G + C) % of 45.1 % (Figs. 4A, 4B) and 3 plasmids (69,744 bp, 60,716 bp, and 60,512 bp) (Figs. 4E, 4F, 4G). The sequence of the plasmid with a length of 69,744 bp was identical to the *V. parahaemolyticus* strain vp-HL-202006 plasmid pHLC-202006 (GenBank: CP150906.1). The whole-genome sequence-based GBDP tree further confirmed that *V. para.* TS-GE belonged to species *V. parahaemolyticus* (Supplemental **Fig. S4**).

The coded biological features of the genome were revealed using RAST (Figs. 4C, 4D). The results showed that the larger and smaller chromosomes of *V. para. TS-GE* possessed 162 (11.1 %) and 48 (12.6 %)

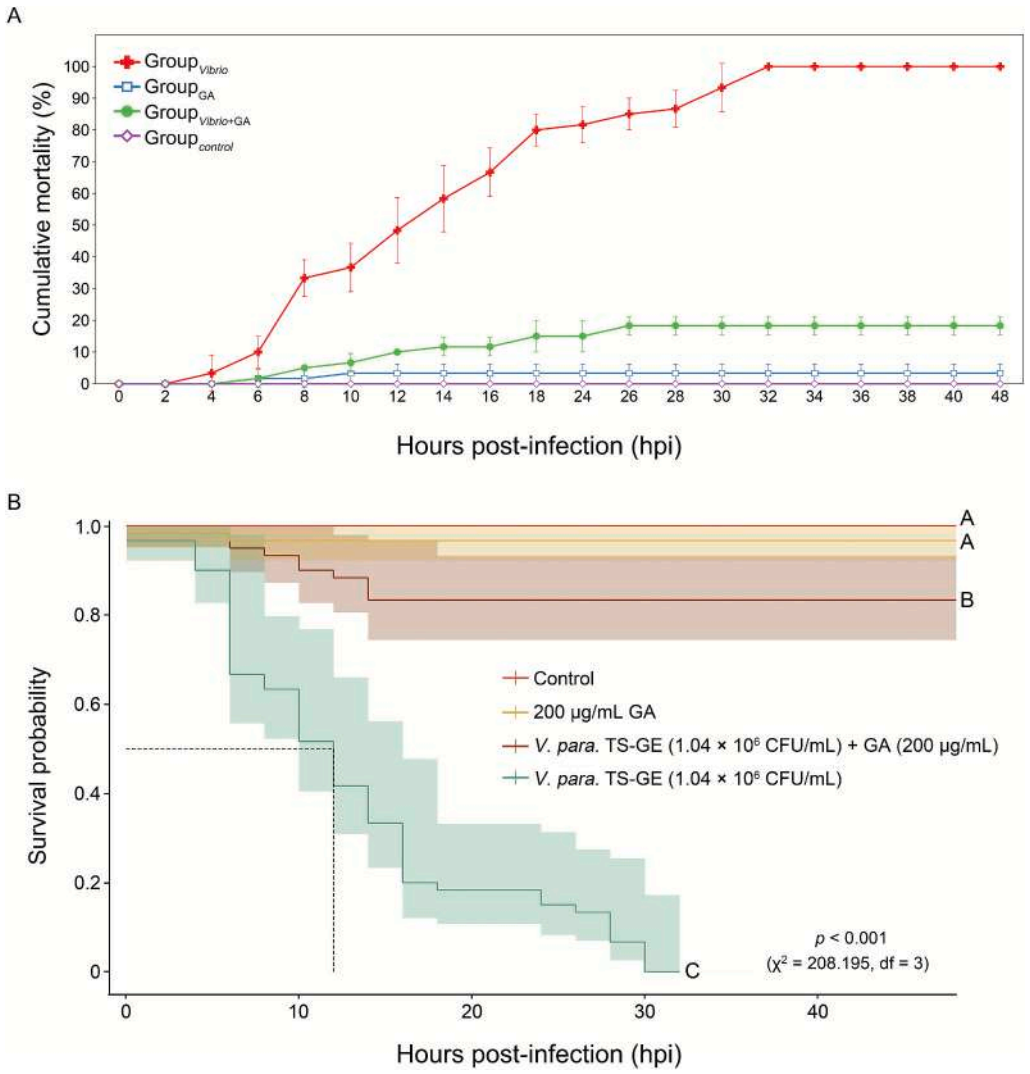

Fig. 3. Protective effects of gallic acid (GA) against the infection of *Vibrio parahaemolyticus* TS-GE in *Litopenaeus vannamei* post-larvae. A. Cumulative mortality of *L. vannamei* post-larvae. Post-larvae were allocated to 4 groups (for each group, n = 20 per replicate, 3 replicates). Group$_{Vibrio}$, immersed in 1.04 × 10^6 CFU/mL of *V. parahaemolyticus* TS-GE. Group$_{GA}$, immersed in 200 μg/mL of GA. Group$_{Vibrio+GA}$, co-exposure to *V. parahaemolyticus* TS-GE and GA (same concentrations as above). Group$_{control}$, immersed in sterile seawater. Cumulative mortality is presented as the mean ± standard deviation (SD) of data from replicates. B. Mitigated mortality in *L. vannamei* post-larvae challenged with pathogenic *Vibrio* strain in the presence of GA. Kaplan-Meier survival curves were generated and the log-rank test was performed to compare different groups followed by the Holm-Sidak's multiple comparison test. Different uppercase letters indicate significant difference at the $P < 0.01$ level. C. Histological sections of the hepatopancreas and midgut in *L. vannamei* post-larvae. All the samples were collected at 24 h post infection. Scale bars = 50 μm. Severe damages were observed in the hepatopancreatic and intestinal tissues in post-larvae collected from Group$_{Vibrio}$ (as indicated by yellow arrows). Histopathological analysis revealed atrophy and deformation of the hepatopancreatic tubules, accompanied by internal plasmacytoid changes. The stellate lumens enlarged, with concurrent deformation of the stellate structures. Severe necrosis and shedding of the hepatopancreatic tubules were observed. In the corresponding midgut sections, damages to the epithelial cell structures and marked cell shedding were visible. Tissue debris were present within the gut, and the integrity of the intestinal tissue structure was compromised. In the tissue sections of post-larvae in the absence of the *Vibrio* strain (as indicated by red arrows in Group$_{control}$ and Group$_{GA}$) and in sections of post-larvae co-exposed to the *Vibrio* strain and gallic acid (as indicated by green arrows in Group$_{Vibrio+GA}$), the hepatopancreatic tubule structures were relatively intact, exhibiting distinct stellate shapes. The hepatocyte structures were basically complete and evenly distributed. Examination of the mid-gut sections revealed that the intestinal epithelial cells were orderly arranged with food residues visible inside. No obvious pathological changes were observed in these sections. Our results showed that gallic acid alleviated pathological symptoms induced by the pathogenic *Vibrio* strain, promoting the restoration of tissue structures toward a normal state. (For interpretation of the references to colour in this figure legend, the reader is referred to the web version of this article.)

genes involved in 3 subsystem categories (virulence, disease and defense, stress response, and motility and chemotaxis), indicating the enhanced adaptive and pathogenic capabilities of *V. para.* TS-GE (detailed information is listed in Supplemental Table S3).

The ABRicate analysis revealed that *V. para.* TS-GE harbored a broad repertoire of virulence factors. The larger chromosome (3,497,252 bp) contained 39 genes encoding structural components, effectors, translocators, chaperones, and regulatory proteins involved in the type III secretion system (T3SS), while the smaller one (1,916,031 bp) carried a single T3SS effector gene and the thermolabile hemolysin gene (tlh), also known as lecithin-dependent hemolysin gene (ldh). Additionally, the 69,744-bp plasmid contained one copy of the TPD-associated toxin genes *vhvp1* and *vhvp2*.

Screening results for ARGs revealed that the larger chromosome contained 3 ARGs associated with potential resistance to quinolones and tetracyclines, whereas the smaller chromosome harbored a single ARG linked to potential beta-lactams resistance in the *V. para.* TS-GE strain. The above-mentioned findings on virulence factors and ARGs are

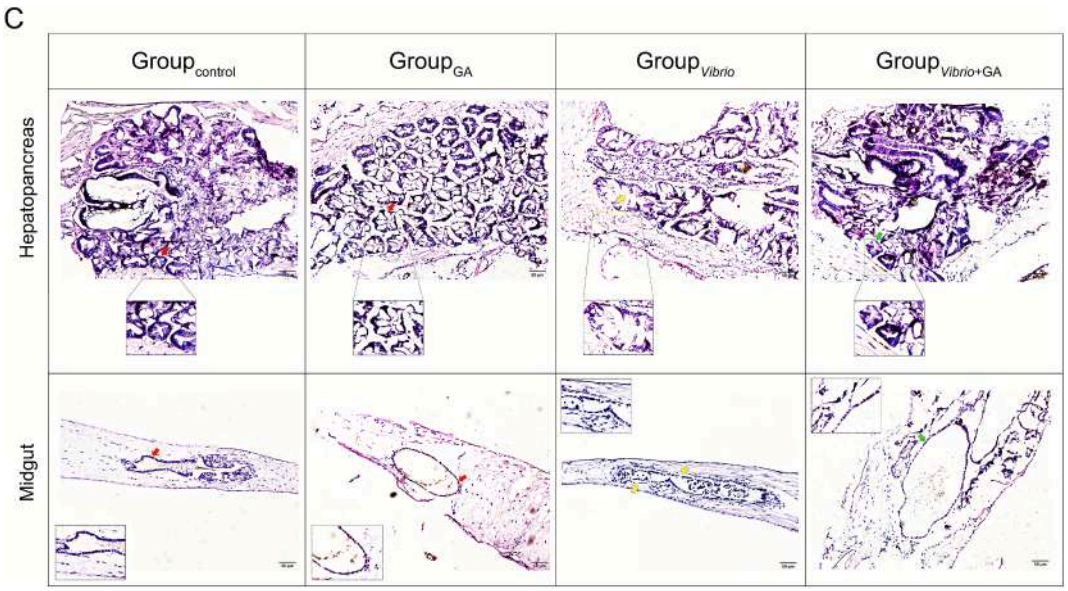

Fig. 3. (*continued*).

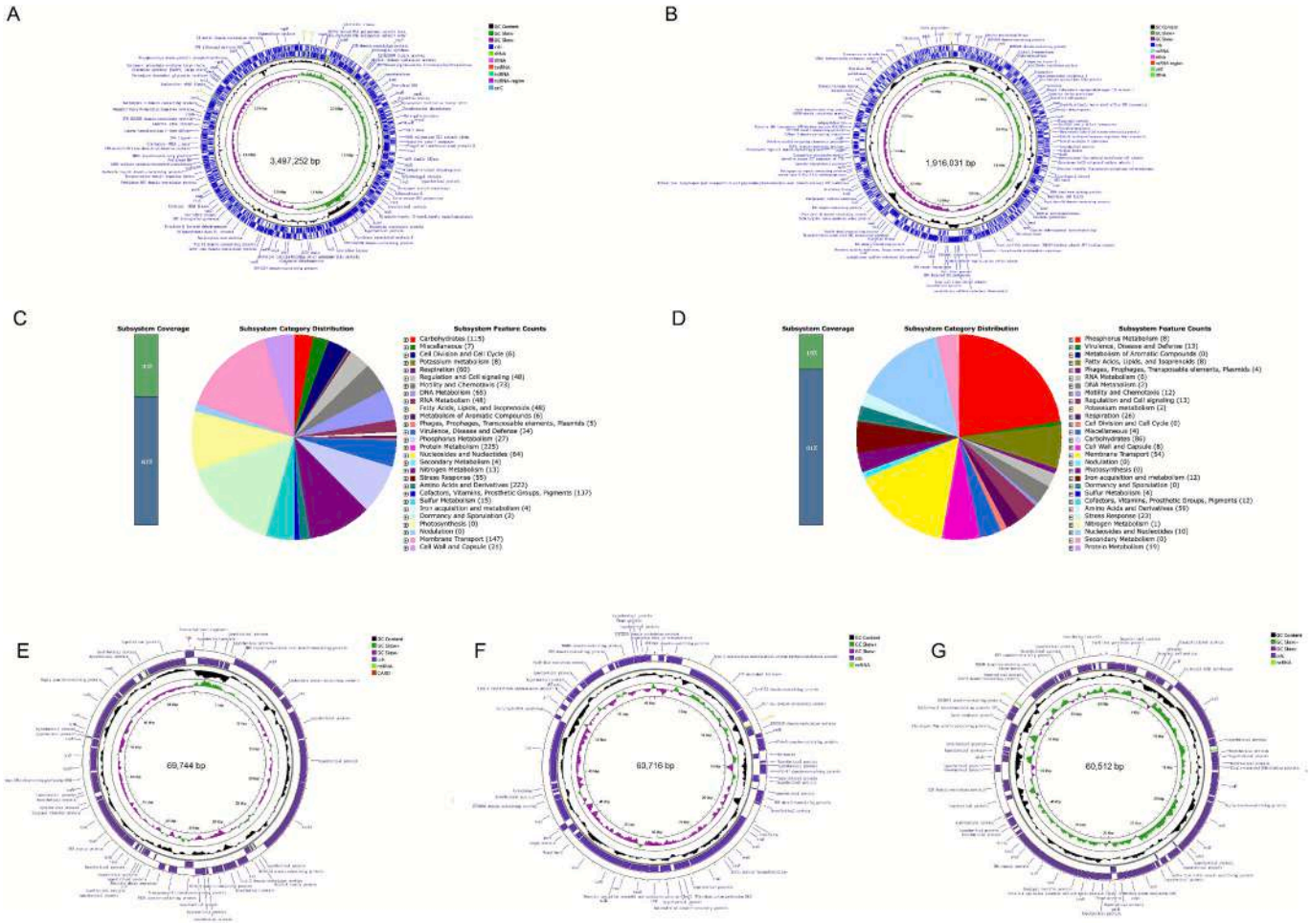

Fig. 4. Circular maps and genomic features of the *Vibrio parahaemolyticus* TS-GE genome. Circular maps of two chromosomes (A, B) and three plasmids (E, F, G) were visualized using the Proksee server (https://proksee.ca). Starting from the outermost ring: Ring 1, Bakta annotation (+); Ring 2, Bakta annotation (−); Backbone; Ring 4, GC content; Ring 5, GC skew (G-C)/(G + C). The size of chromosomes and plasmids is shown in the center of the circle. C and D. The larger (3,497,252 bp) and smaller (1,916,031 bp) chromosomes, respectively, annotated using RAST-SEED server (https://rast.nmmpdr.org).

presented in the Supplementary File S2.

Pangenome analysis of 480 *V. parahaemolyticus* strains unveiled substantial genetic heterogeneity with a highly dynamic accessory genome complementing a conserved core genome (Fig. 5A). Roary analysis revealed a pangenome of 43,633 genes, comprising 3,433 core genes (7.87 % of total; conserved across all strains) and 40,200 accessory genes (92.1 % of total). The accessory genome was stratified into 347 soft-core genes,1,278 shell genes, and 38,575 cloud genes (< 15 % prevalence, accounting for 88.4 % of the pangenome) (Fig. 5B). These findings underscored the open nature of the *V. parahaemolyticus* pangenome, reflecting its dynamic evolutionary adaptability. A phylogenetic tree was constructed to resolve the evolutionary relationships among the 480 *V. parahaemolyticus* strains analyzed, revealing clustering by isolation sources or geographic origins (Fig. 5C). Notably, strains isolated from *L. vannamei* and human clinical samples formed distinct clades. Shrimp-derived strains exhibited extensive intermingling with those derived from other seafood, crayfish, water, and environment. This pattern suggested that shared ecological niches (such as coastal aquacultural systems or estuarine habitats) may facilitate genetic exchange, reinforcing the bacterium's cross-host adaptability.

3.9. MLST analysis

We analyzed the genomes of 480 *V. parahaemolyticus* strains isolated from clinical, environmental, and animal-associated samples collected from multiple geographic regions. *In silico* MLST analysis revealed the presence of 131 unique sequence types (STs) among these isolates. Over the past two decades, an increasing number of *V. parahaemolyticus* strains have undergone whole-genome sequencing and a growing variety of STs have been identified (Fig. 6A).

Among *V. parahaemolyticus* isolates obtained from shrimp, seafood, and red swamp crayfish (*Procambarus clarkii*), the most prevalent STs were ST163, ST308, and ST1166, respectively. In contrast, isolates from human clinical cases, environmental sources, and other origins predominantly belonged to ST3. Human-derived isolates demonstrated limited STs diversity, with ST3 predominating (55.06 % of the isolates). In contrast, isolates from shrimp, seafood, and crayfish exhibited a more heterogenous ST distribution pattern (Fig. 6B). Furthermore, source-specific partitioning of STs was observed, whereby isolates from the same origin predominantly represented a restricted subset of STs (Fig. 6C), indicating a potential association between specific STs (genotype) and their sources (ecological niche).

Specifically, among the 61 *V. parahaemolyticus* isolates sourced from *L. vannamei*, 26 distinct STs were identified. ST1166 and ST2621 were the most prevalent, each constituting 9.84 % of the isolates. Notably, the *V. para.* TS-GE strain employed in the present study was of ST2621, one of the most prevalent ST types within this population. ST413 and ST1925 followed closely, with both representing 8.2 % of the isolates. Subsequently, ST970 ranked third, accounting for 6.56 % of the isolates. Together, these five STs accounted for 42.62 % of the total isolates from *L. vannamei*.

In terms of sample sources, 267 strains were derived from human clinical samples, 103 strains from shrimp (including 61 strains from *L. vannamei*, which was the second most abundant source), and 41 strains from various types of seafood. Regarding geographic origin, 319 strains (66.46 %) were isolated from samples collected in China, followed by Canada (9.38 %), Thailand (6.67 %), and the United States (5.83 %). The remaining strains were distributed globally across 16

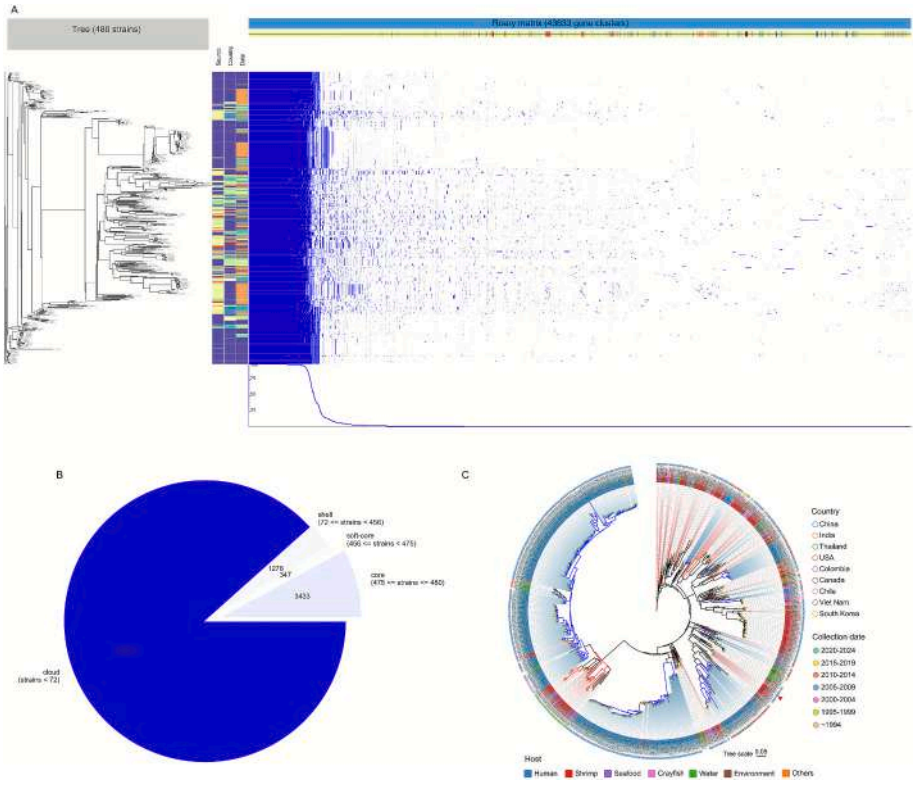

Fig. 5. Pangenome analysis of 480 *Vibrio parahaemolyticus* strains using Roary. A. The gene presence and absence matrix displaying genomic comparisons across the 480 *V. parahaemolyticus* strains, where the blue and white stripes indicate the presence and absence of genes, respectively. B. The pie chart showing the distribution of genes to the core, the soft core, the shell, and the cloud genes of the *V. parahaemolyticus* strains. Based on strain-specific prevalence thresholds, core genes were defined as those detected in ≥ 99 % of the 480 *V. parahaemolyticus* strains. The accessory genome was subdivided into soft-core genes (present in 95 % ≤ prevalence < 99 % of strains), shell genes (present in 15 % ≤ prevalence < 95 % of strains), and cloud genes (present in prevalence < 15 % of strains). C. Phylogenetic tree built on the gene information produced by Roary. Isolates from *Litopenaeus vannamei* and human samples are labeled in red and blue, respectively. (For interpretation of the references to colour in this figure legend, the reader is referred to the web version of this article.)

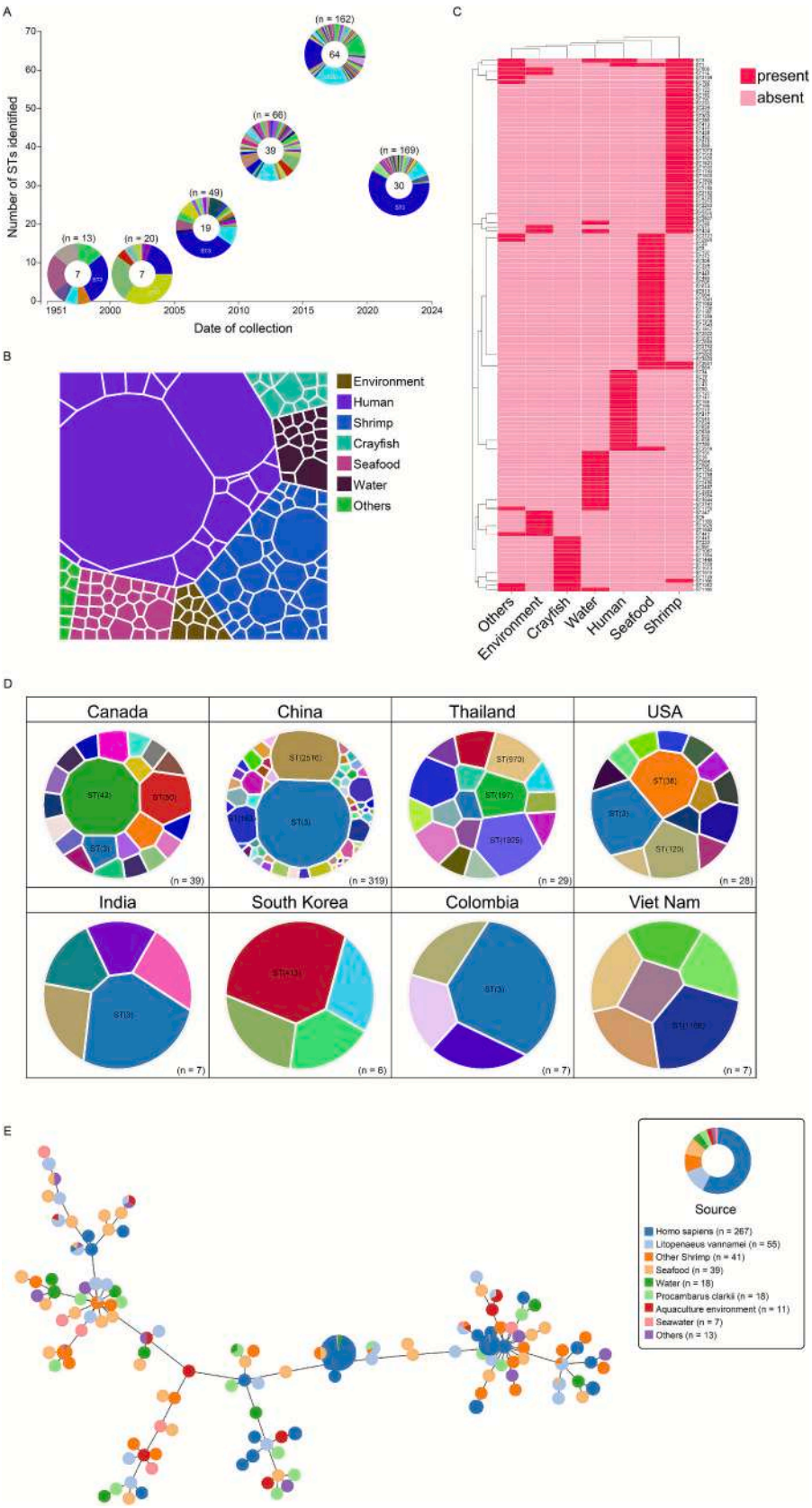

(caption on next page)

Fig. 6. Results of the comprehensive MLST analysis. A. Number of sequence types (STs) identified in *Vibrio parahaemolyticus* isolates. Each pie represents the total isolated strains and STs distribution within a specific time frame. The "n" above each pie indicates the strain count for that period. The numerical value at the center of each pie shows the total number of identified STs in the corresponding strains. White-marked STs within the pies are the most frequently observed among the strains isolated during those respective time periods. B. Source-based STs distribution of *V. parahaemolyticus*. "Shrimp" encompasses *Litopenaeus vannamei* and other shrimp species. "Environment" includes the aquacultural environment and other environmental settings. "Water" covers seawater and other water types. C. A binary graph shows the STs distribution of *V. parahaemolyticus* across different sources. D. Country-based STs distribution of *V. parahaemolyticus*. The "n" in the bottom-right corner indicates the number of *V. parahaemolyticus* strains isolated in that country. The prevalent STs are labeled within the pie. E. The goeBURST minimum spanning tree for the 131 STs obtained from the combination of all allele types of the 7 MLST loci (*rec*A, *dna*E, *gyr*B, *dtd*S, *pnt*A, *pyr*C, and *tna*A) using the PHYLOViZ online server, indicating the genetic relationships between the 480 isolates analyzed.

countries. Within the same country, a larger number of isolated *V. parahaemolyticus* strains tended to be associated with a greater diversity of identified STs. Consistently, the highest diversity of STs was observed among *V. parahaemolyticus* strains isolated in China (Fig. 6D). The gene network analysis revealed that strains from various sources were intertwined (Fig. 6E). While the majority strains isolated from humans clustered together and formed a relatively closely connected gene network, there was a mix of strains from seafood, shrimp, crayfish, and aquaculture settings with those from human samples. This mixing suggested possible ways the *V. parahaemolyticus* strains may spread within these different sources.

3.10. Investigation on the antibacterial mechanisms of GA against *V. parahaemolyticus*

AKP is predominantly localized in the periplasmic space of bacteria, situated between the cell wall and cytoplasmic membrane. In the absence of GA, extracellular AKP activity remained stable over time. However, co-incubation with varying concentrations of GA induced a significant, dose-dependent increase in extracellular AKP activity within 8 h, indicating enhanced cell wall permeability (Fig. 7A). Concurrently, a significant elevation in absorbance at 260 nm was observed in bacterial cultures exposed to GA at concentrations ranging from 1/2 × to 2 × MIC, indicative of the release of intercellular substances, such as DNA or RNA, into the extracellular milieu (Fig. 7B). These findings demonstrated that GA increased the permeability of both the cell wall and cytoplasmic membrane of the tested bacteria in a concentration- and time-dependent manner, facilitating the leakage of intracellular components.

GA significantly inhibited swimming motility of *V. para.* TS-GE ($P < 0.01$), as evidenced by reduced swimming diameters (Figs. 7C, 7D). At sub-inhibitory concentrations (1/4 × and 1/2 × MIC), GA decreased swimming motility diameters of *V. para.* TS-GE by 29.23 % and 41.74 %, respectively. GA exhibited dose-dependent inhibition of biofilm formation (Figs. 7E, 7F). At 1/4 × MIC, biofilm formation was suppressed by 40.93 ± 5.84 %. Additionally, GA at 250 μg/mL significantly disrupted ($P < 0.05$) preformed biofilms of *V. para.* TS-GE (Supplemental Fig. S5). These findings suggested that GA exhibited efficacy in both inhibiting biofilm formation and dispersing established biofilms.

In silico molecular docking simulations indicated the interactions between GA and the virulent VHVP2 and VHVP1. As shown in Fig. 8, in the molecular docking simulation, residues Asn65, Asp294, Phe296, Thr307, Arg309, and Thr350 of the virulent VHVP2 formed hydrogen bonds with GA. Additionally, several other residues contributed to hydrophobic interactions between them. This combined interaction profile resulted in a favorable binding affinity of −7.8 kcal/mol. VHVP1 was predicted to be a homo-pentameric protein. There were four binding pockets predicted by DogSite3 (Supplemental **Table S4**). Results from molecular docking analyses indicated that GA was able to bind to two of them with a favorable binding affinity around −6.3 kcal/mol (Fig. 9).

4. Discussion

In the current study, we evaluated the protective efficacy of GA against Vp_{TPD} infection in *L. vannamei* post-larvae.

The *V. para.* TS-GE strain used in this study was confirmed as *V. parahaemolyticus* at the genus level through 16S rRNA sequencing. This strain reproduced typical TPD manifestations and was successfully re-isolated from moribund post-larvae following experimental infection. At a density of 2.82×10^7 CFU/mL, this strain induced 100 % mortality in post-larvae within 24 hpi. These results collectively confirmed *V. para.* TS-GE as a Vp_{TPD} strain, a highly virulent *V. parahaemolyticus* isolate capable of triggering TPD in *L. vannamei* post-larvae.

The *V. para.* TS-GE strain exhibited resistance to 4 major antibiotic classes: β-lactams (penicillin G), glycopeptides (vancomycin), aminoglycosides (streptomycin), and lincosamides (clindamycin). Its MAR index of 0.33 exceeded the 0.2 threshold (Krumperman 1983), indicating its origin from high-risk antibiotic exposure sources (Kurdi Al-Dulaimi et al., 2019). While quinolones have historically retained potent activity against *V. parahaemolyticus* isolates, with resistance reported in only 4.1 % (3/74) of isolates (Jin et al., 2021), our study detected intermediate resistance to norfloxacin in *V. para.* TS-GE. This finding suggested evolving susceptibility patterns under prolonged selective pressure, underscoring the urgent need for prudent antibiotic stewardship in aquaculture to curb the emergence of multidrug-resistant *Vibrio* pathogens.

In our investigation, GA demonstrated a MIC of 1000 μg/mL against the *V. para.* TS-GE strain. While direct comparisons with *Vibrio* spp. remain limited in literature, the observed MIC value falls within the broad range documented for GA against Gram-negative bacteria, suggesting strain-specific susceptibility patterns rather than genus-level consistency. For instance, exceptionally low MIC values of GA have been reported for *Acinetobacter baumannii* (4.88 μg/mL) (Alturki et al., 2024) and *Klebsiella pneumoniae* (9.75 μg/mL) (Pinho et al., 2014), whereas substantially higher values were recorded for *Pseudomonas aeruginosa* (500 μg/mL) and *Escherichia coli* (1500 μg/mL) (Borges et al., 2013), *Shigella flexneri* (2000 μg/mL) (Kang et al., 2018a), and *Ralstonia solanacearum* (3000 μg/mL) (Sowndarya et al., 2020). Furthermore, both inter- and intra-species variations in MIC values were pronounced. *Escherichia coli* HM615 and HM251 strains required 1250 μg/mL (Cota and Patil, 2023), while *Yersinia enterocolitica* BNCC 108930 necessitated 2500 μg/mL (Tian et al., 2022). This heterogeneity was further corroborated by an average MIC of 1670 μg/mL (from 1320 to 2110 μg/mL) against 30 multidrug-resistant *A. baumannii* isolates (Sherif et al., 2021). These findings underscored the variable antibacterial efficacy of GA against Gram-negative pathogens, likely attributable to microbial genetic diversity, metabolic pathway variations, and strain-specific virulence determinants. In the current study, the *in vitro* growth-inhibitory effect of GA on *V. para.* TS-GE (associated with TPD) renders it a promising candidate for developing novel strategies to prevent and control TPD outbreaks.

We further explored the synergistic potential of GA with conventional antibiotics against *V. para.* TS-GE. The checkerboard assay revealed a partial synergistic interaction between GA and chloramphenicol, enabling a 2-fold reduction in GA MIC and a 32-fold reduction in chloramphenicol MIC, while maintaining antibacterial efficacy against the tested *Vibrio* strain. This dosage-sparing effect held critical implications for TPD treatment optimization, as it may delay antibiotic resistance emergence through reduced selective pressure.

GA's antibiotic-potentiating effects have been consistently validated across diverse pathogens. For instance, GA enhanced the antimicrobial efficacy of penicillin G against methicillin-resistant *Staphylococcus*

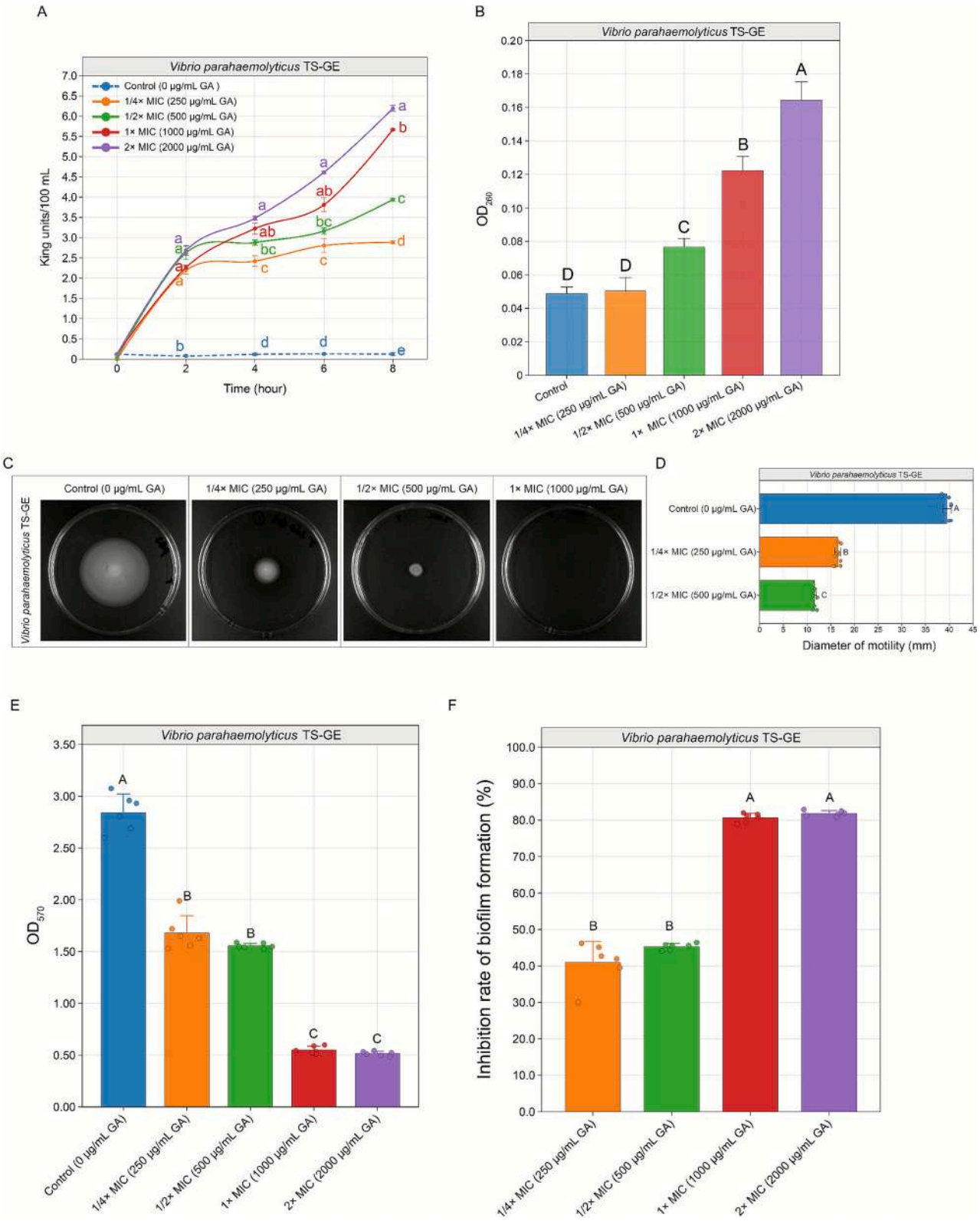

Fig. 7. Antibacterial mechanisms of gallic acid against *Vibrio parahaemolyticus* TS-GE. A and B. Effects of gallic acid (GA) on the structural integrity of bacterial cell walls and cell membranes. A. Extracellular alkaline phosphatase (AKP) activities. At the same time point, different lowercase letters indicate significant differences ($P < 0.05$). B. Absorbance at 260 nm (OD_{260}) in bacterial cultures following exposure to GA. Different uppercase letters indicate significant difference at the $P < 0.01$ level. C and D. Inhibitory effects of GA on swimming motility of *V. parahaemolyticus* TS-GE. C. Representative images of swimming motility for *V. parahaemolyticus* TS-GE on LB agar plates supplemented with GA at the indicated concentration. D. Diameters of migration in the swimming assay. Error bars represent means ± SD, with n = 9 biological replicates. Different uppercase letters indicate significant difference at the $P < 0.01$ level. E and F. Inhibitory effects of GA on the biofilm-forming capacity of the *V. parahaemolyticus* TS-GE strain. Error bars represent the mean ± SD of 6 replicates. Different uppercase letters indicate significant differences ($P < 0.01$).

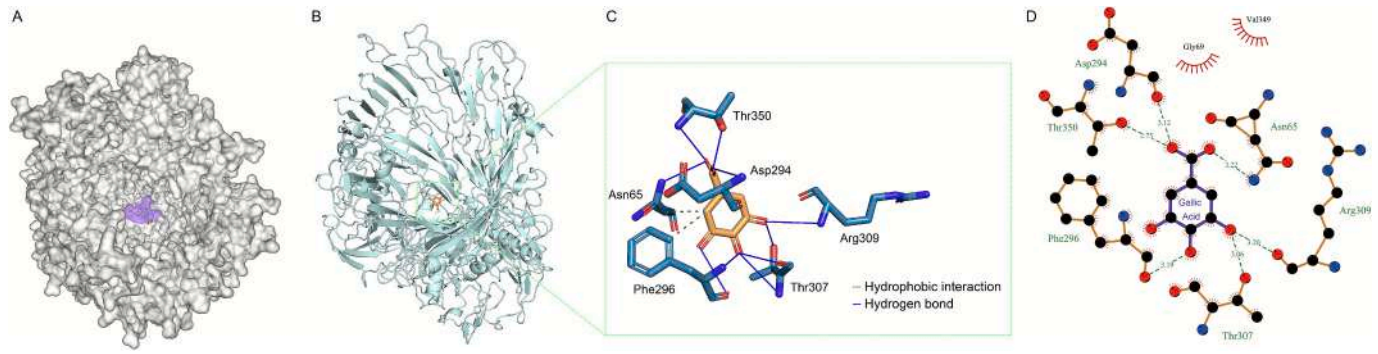

Fig. 8. Molecular docking results of gallic acid and the virulent protein VHVP2. A. The surface area of VHVP2 showing its binding with gallic acid (GA). The binding pocket was predicted using DogSiteScorer where the protein bound to GA. B and C. Close-up 3D views of the *in silico* molecular docking results conducted via AutoDock Vina. The ligand, GA, is depicted in orange. D. 2D diagram showing the interactions between the protein and GA. Dashed green lines indicate hydrogen bonds, while semi-circles represent hydrophobic interactions. (For interpretation of the references to colour in this figure legend, the reader is referred to the web version of this article.)

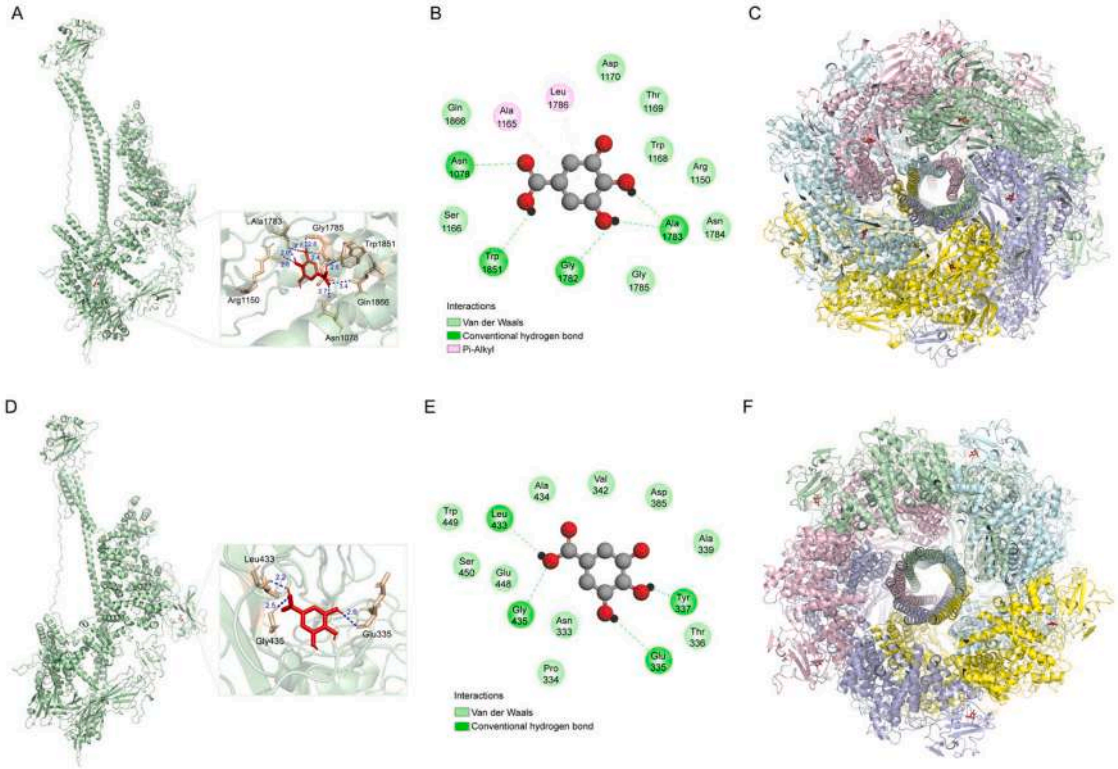

Fig. 9. Molecular docking analyses of gallic acid binding to the virulent protein VHVP1. A and D. The detailed 3D visualization of the molecular docking complexes between the VHVP1 monomer and gallic acid (GA), generated using AutoDock Vina. The ligand, GA, is depicted in red. The calculated binding affinities for these docking poses were −6.3 kcal/mol (A) and −6.0 kcal/mol (D), respectively. B and E. The 2D interaction diagrams illustrating the interactions between GA and the VHVP1 monomer. C and F. The binding modes of GA to each of the five subunits of the homo-pentameric VHVP1. (For interpretation of the references to colour in this figure legend, the reader is referred to the web version of this article.)

Aureus (MRSA), resulting in a ≥ 5-fold reduction in MIC (Jiamboonsri et al., 2011). When paired with tulathromycin, GA exhibited additive to weak synergistic activity against *Mannheimia haemolytica* and *Pasteurella multocida*, reinforcing its role as an antibiotic adjuvant (Rajamanickam et al., 2018). Co-administration of GA with tetracycline or ciprofloxacin significantly augmented their activities against *Staphylococcus aureus*, resulting in reduced MIC values (Macêdo et al., 2022). Even GA derivatives demonstrated synergistic potential. Alkyl gallates potentiated oxacillin activity against MRSA (Shibata et al., 2009). Methyl gallate combined with sub–MIC marbofloxacin effectively inhibited the adhesion and invasion of *Salmonella Typhimurium* (Birhanu et al., 2018). These findings underscored GA's dual-action potential for sustainable TPD management, enhancing antibiotic efficacy at subtherapeutic doses while mitigating resistance through reduced selection pressure.

Immersion challenge with the *V. para.* TS-GE strain successfully reproduced TPD symptoms in *L. vannamei* post-larvae. Notably, GA at 1/5 × MIC significantly reduced cumulative mortality ($P < 0.05$), establishing its *in vivo* efficacy against TPD. While structural analogs of GA have demonstrated activities against *Vibrio* pathogens in previous reports, direct evidence of GA's inhibitory effects on *V. parahaemolyticus* remained lacking until this study. Previous studies revealed that pyrogallol (1,2,3-trihydroxybenzene) potently inhibited *in vitro* growth of *V.*

parahaemolyticus (Tinh et al., 2016). Catechol (1,2-benzenediol), the main constituent of rambutan (*Nephelium lappaceum* L.) peel extracts (Jantapaso and Mittraparp-Arthorn, 2022), demonstrated *in vitro* inhibitory effects on the growth of *V. parahaemolyticus* CAIM 170 (Phuong et al., 2020). Moreover, these extracts also reduced biofilm formation, swimming motility, and virulence gene expression in *V. campbellii* HY01, a strain associated with luminous vibriosis (Pattano et al., 2025). Protocatechuic aldehyde dose-dependently inhibited the biofilm formation and motility of *V. parahaemolyticus* ATCC17802 (Liu and Wang, 2022). Another well-characterized polyphenol, epigallocatechin gallate (EGCG), further exemplified this activity pattern, demonstrating multifaceted antibacterial effects against *V. parahaemolyticus* 17802, including inhibition of bacterial growth, disruption of cell membrane integrity, suppression of biofilm formation, and attenuation of swimming motility (Wang et al., 2022). Consistent with these findings, our mechanistic analyses revealed that GA employed a similar multi-target strategy against *V. para.* TS-GE, including membrane disruption, biofilm inhibition, and motility suppression. Since the co-application of antibiofilm and antimicrobial agents was shown to exert synergistic bactericidal effects (Darouiche et al., 2009), we proposed that GA, a compound with dual antibiofilm and antibacterial activities against *V. para.* TS-GE, could effectively suppress bacterial proliferation and biofilm formation, thereby offering an alternative strategy for controlling TPD.

Our immersion challenge test revealed that GA significantly reduced mortality in post-larvae challenged with *V. para*. TS-GE at a sub-MIC concentration of 200 μg/mL (corresponding to 1/5 × MIC). While GA may interfere with bacterial adhesion and colonization in the post-larval intestinal tracts through inhibiting biofilm formation, GA was not able to fully suppress bacterial growth at this concentration. Therefore, the above-mentioned strategies may not fully explain GA's potent protective activities against the infection of *V. para*. TS-GE. We hypothesized that GA may additionally attenuate key virulence factors in the *V. para*. TS-GE strain, thereby enhancing its antibacterial efficacy.

To evaluate this hypothesis, we performed molecular docking analyses. In accordance with a prior study that employed molecular docking to identify key bacterial proteins interacting with GA, binding affinities ≤ -5.0 kcal/mol were considered favorable for protein–ligand interactions, whereas values ≤ -7.0 kcal/mol (indicating high-affinity interactions due to their larger absolute magnitudes) were regarded as potent (Duan et al., 2023). Our results demonstrated that GA formed a high-affinity complex with VHVP2 (binding energy: −7.8 kcal/mol), exceeding the potent threshold (≤ −7.0 kcal/mol). GA also interacted favorably with VHVP1, showing binding affinities ≤ -6.0 kcal/mol. These findings provided insights into the potential interactions between GA and two critical virulence proteins, VHVP1 and VHVP2. The strong binding affinity of GA to VHVP2, the essential virulent protein for Vp_{TPD} strains (Zhang et al., 2024b), suggested that GA may interfere with its function, thereby attenuating the pathogenicity in *L.* vannamei post-larvae. At present, the functional implications of these interactions remain undefined. Specifically, it is yet to be determined whether GA binding modulates protein stability, alters pathogenic activity, or disrupts host-pathogen interaction dynamics. Comprehensive experimental validation is essential to elucidate these underlying mechanisms.

Notably, acute toxicity assessments in *L. vannamei* post-larvae demonstrated that GA exhibited much lower toxicity (48-hour LC_{50}: 588 μg/mL) compared to multiple conventional aquaculture stressors. Specifically, GA demonstrated up to 3 orders of magnitude lower acute toxicity than heavy metals (96-hour LC_{50} values: Hg 1.23 μg/mL, Cd 2.49 μg/mL, Cu 37 μg/mL, Pb 134 μg/mL) (Frias-Espericueta et al., 2001,2003) and arsenicum (96-hour LC_{50} range: 6.23–12.29 μg/mL) (Valentino-Álvarez et al., 2013). GA exhibited a 19-fold higher safety margin than the conventional disinfectant polyhexamethylene biguanide (PHMB; 48-hour LC_{50}: 10.77 μg/mL) (Jia et al., 2023). It exhibited an extreme safety margin compared to neonicotinoid pesticides. For example, clothianidin induced significantly lower survival rates in post-larvae at an exposure concentration of 8.31 μg/L (Luo et al., 2024). Moreover, GA's 48-hour LC_{50} exceeded the reported values for inorganic nitrogen compounds (ammonia-N, nitrite −N, and nitrate −N) in post-larvae of *L. vannamei* under various sanities (Frías-Espericueta et al., 2000; Valencia-Castañeda et al., 2018). The low toxicity of GA towards post-larvae of *L. vannamei*, coupled with its demonstrated antibacterial efficacy against *V. para.* TS-GE, further strengthens its candidacy as a safe and effective alternative to conventional antibiotics for the prevention and control of TPD.

Additionally, whole-genome sequencing of the *V. para.* TS-GE strain has advanced our understanding of its virulence mechanisms and genetic evolution.

The *V. para*. TS-GE strain utilized in this study was absent of the virulence genes *tdh* (thermostable direct hemolysin) and *trh* (thermostable-related hemolysin) in both chromosomes and plasmids, suggesting that it was non– or low-pathogenic in humans (Singhapol and Tinrat, 2020). However, it was highly virulent in post-larvae of *L. vannamei*, demonstrating a 24-hour LC_{50} of 4.72×10^4 CFU/mL in our study. Genomic characterization revealed 3 key virulence determinants. The smaller chromosome harbored *tlh*, encoding an extracellular phospholipase-like toxin (Shinoda et al., 1991), which is a well-established biomarker for pathogenic *Vibrio* strains. The larger chromosome contained 38 genes encoding T3SS effectors, which mediate host-pathogen interactions. A plasmid carried *vhvp1* and *vhvp2*, key genes associated with TPD. A prior study reported that the tlh-positive Vp_{TPD} strain Vp-JS20200428004-2 induced a 24-hour LC_{50} of 9.84×10^5 CFU/mL in *L. vannamei* post-larvae (Zou et al., 2020). However, this strain lacked information on T3SS effectors or plasmid-borne virulence genes. We suggested the concurrent presence of multiple virulence factors enhanced the virulence of *V. para.* TS-GE, emphasizing the interplay between conserved and horizontally acquired determinants in shaping virulence among different Vp_{TPD} strains.

The pangenome analysis of 480 *V. parahaemolyticus* strains revealed 3,433 core genes, a figure comparable to the 3,523 core genes reported by (Wang et al., 2023b). Notably, the proportion of accessory genes, particularly cloud genes, expanded as more strains were included into the pangenome, suggesting their potential roles in environmental adaption of *V. parahaemolyticus* strains. Phylogenetic analysis revealed extensive genetic admixture among *V. parahaemolyticus* strains from aquacultural environments, a pattern consistent with prior reports of inter-niche gene flow in water-borne pathogens (Kaushik et al., 2019). Our results further implied that aquaculture ecosystems served as reservoirs for pathogen evolution and the dissemination of antibiotic resistance, which could lead to severe challenges for disease control in the shrimp farming sector. One of the most concerning potential issues is the horizontal cross-species transfer of ARGs (Gao et al., 2022). This transfer could undermine the efficacy of commonly used antibiotics (Sotomayor et al., 2019). Another critical aspect was the potential genetic recombination among different strains (Li et al., 2018; Gunasekara et al., 2023), which may facilitate the emergence of novel pathogens with enhanced virulence or broader host ranges. As a result, it could trigger more sever outbreaks in shrimp farms. Considering these concerns, monitoring ARGs in both shrimp and environmental samples would be essential for effective resistance surveillance. Overall, these results further underscored the urgency of developing antibiotic alternatives to mitigate the spread of resistance and ensure the sustainability of the shrimp industry.

In the MLST analysis, source-specific ST clustering was observed, likely reflecting host-adaptive evolution, where niche-specific selection pressures drive the expansion of certain ST lineages. We also identified a high proportion of singleton STs (93 out of 131) which aligned with prior findings, where 57.4 % of the 61 STs identified across 132 *V. parahaemolyticus* isolates (from clinical and oyster sources) were represented by only one isolate (Miller et al., 2021). The prevalence of singleton STs suggested ongoing genotype turnover, which may arise from horizontal gene transfer (HGT) introducing novel genetic variants

or environmental fluctuations selectively favoring transient clones. Together, these observations emphasized the dynamic interplay between genetic diversity and ecological pressures in shaping the population structure of *V. parahaemolyticus*.

Our study demonstrated that GA provided a cost-effective prophylactic strategy for controlling TPD in *L. vannamei* aquaculture. Based on the wholesale market price, GA application at a concentration of 200 μg/mL costs USD 20–50 per treatment cycle in standard production ponds (20–50 m^3, volumes representative of medium-scale nursery systems for post-larvae rearing). This cost-efficiency is particularly advantageous for large-scale operations, as the dosage regimen maintains disease control efficacy while remaining economically sustainable.

Despite promising results, our study has limitations. First, laboratory conditions may not fully reflect real-world shrimp farming environments. Field trials are needed to assess GA's practical efficacy. Second, while multiple anti-pathogenic mechanisms were proposed, GA's overall action profile remains incomplete. Additional research may prioritize host immune modulation and quorum-sensing disruption. Third, long-term impacts on shrimp fitness and ecosystem health require evaluation to ensure sustainable aquaculture deployment. Multi-site, large-scale trials across diverse shrimp species and farming systems will be critical for validating GA's efficacy against Vp_{TPD} infections.

5. Conclusion

This study confirmed *V. para*. TS-GE as a virulent shrimp pathogen causing TPD. Genomic analyses revealed its virulence determinants, including genes encoding T3SS components, thermolabile hemolysin, and TPD-associated toxins (VHVP1 and VHVP2), alongside multidrug resistance genes. Roary analysis demonstrated extensive strain-specific variations within *V. parahaemolyticus* strains. MLST classified *V. para*. TS-GE as ST2621, the dominant ST detected in shrimp-derived isolates, while phylogenetic clustering indicated shared genetic pools among aquatic hosts and environments, suggesting potential cross-niche transmission. GA demonstrated antibacterial activity against *V. para*. TS-GE, disrupted bacterial integrity, inhibited motility, and suppressed biofilm formation. Molecular docking simulations further demonstrated GA's binding to VHVP1 and VHVP2 toxins with favorable affinity. *In vivo*, GA (200 μg/mL) reduced *V. para*. TS-GE induced mortality to 18.3 % while preserving hepatopancreatic and midgut tissue architecture. These findings position GA as a promising non-antibiotic for alternative TPD management in aquaculture, with field validation and dosage optimization as priority next steps.

6. Authors' contributions

MHY and BZ conceived and designed the experiments; QNH performed the immersion challenge tests, histological examinations, and the antibacterial mechanistic investigations; MHY, CM, and FJ performed molecular docking simulations; MHY and BZ performed the comparative genomic analysis. MHY, QNH, and BZ drafted the manuscript. All authors read and approved the final manuscript.

CRediT authorship contribution statement

Man-Hong Ye: Writing – review & editing, Writing – original draft, Validation, Supervision, Software, Methodology, Investigation, Funding acquisition, Conceptualization. **Qian-Nan Han:** Writing – original draft, Software, Methodology, Investigation, Formal analysis, Data curation. **Chuang Meng:** Validation, Software, Resources, Methodology, Investigation, Funding acquisition, Data curation. **Feng Ji:** Visualization, Validation, Software, Resources, Methodology, Investigation, Formal analysis, Data curation. **Bin Zhou:** Writing – review & editing, Writing – original draft, Validation, Supervision, Software, Resources, Project administration, Methodology, Investigation, Funding acquisition, Formal analysis, Conceptualization.

Funding

This work was supported by the National Science Foundation of China (grant number W2421047); the Open Project Program of Jiangsu Key Laboratory of Zoonosis (grant number R2110); and Yangzhou Innovation Capability Enhancement Fund/Program (grant number YZ2023245).

Declaration of competing interest

The authors declare the following financial interests/personal relationships which may be considered as potential competing interests: Manhong Ye reports financial support was provided by National Natural Science Foundation of China. Manhong Ye reports administrative support was provided by Yangzhou Bureau of Science and Technology. If there are other authors, they declare that they have no known competing financial interests or personal relationships that could have appeared to influence the work reported in this paper.

Appendix A. Supplementary data

Supplementary data to this article can be found online at https://doi.org/10.1016/j.jip.2025.108499.

Data availability

The 16S rRNA sequence and whole-genome sequence of the *Vibrio parahaemolyticus* TS-GE strain obtained in this study have been uploaded to NCBI under the accession number of PV017572 and SAMN50649144 (Biosample), respectively.

References

Abdelaziz, N.A., Elkhatib, W.F., Sherif, M.M., Abourehab, M.A.S., Al-Rashood, S.T., Eldehna, W.M., Mostafa, N.M., Elleboudy, N.S., 2022. *In silico* docking, resistance modulation and biofilm gene expression in multidrug-resistant *Acinetobacter baumannii* via cinnamic and gallic acids. Antibiotics 11, 870. https://doi.org/10.3390/antibiotics11070870.

Abdella, M., Lahiri, C., Abdullah, I., Anwar, A., 2024. Antibacterial evaluation of gallic acid and its derivatives against a panel of multi-drug resistant bacteria. Med. Chem. 20, 130–139. https://doi.org/10.2174/1573406419666230823104300.

Ahmed, J., Navabshan, I., Unnikrishnan, S., Radhakrishnan, L., Vasagam, K.P.K., Ramalingam, K., 2023. *In silico* and *in vitro* investigation of phytochemicals against shrimp AHPND syndrome causing PirA/B toxins of *Vibrio parahaemolyticus*. Appl. Biochem. Biotechnol. 195, 7176–7196. https://doi.org/10.1007/s12010-023-04458-1.

Alturki, M.S., Al Khzem, A.H., Gomaa, M.S., Tawfeeq, N., Alhamadah, M.H., Alshehri, F. M., Alzahrani, R., Alghamdi, H., 2024. Gallic acid: a potent metabolite targeting shikimate kinase in *Acinetobacter baumannii*. Metabolites 14, 727. https://doi.org/10.3390/metabo14120727.

Amalina, N.Z., Santha, S., Zulperi, D., Amal, M.N.A., Yusof, M.T., Zamri-Saad, M., Ina-Salwany, M.Y., 2019. Prevalence, antimicrobial susceptibility and plasmid profiling of *Vibrio* spp. isolated from cultured groupers in peninsular Malaysia. BMC Microbiol. 19, 251. https://doi.org/10.1186/s12866-019-1624-2.

Amin, M., Buatong, J., Temdee, W., Rahmalia, S.A., Prihandana, G., Benjakul, S., 2025. Kiam wood, *Cotylelobium lanceotatum*, extract as a natural antimicrobial agent: protecting Pacific white shrimp, *Penaeus vannamei*, against vibriosis. Sci. Rep. 15, 13296. https://doi.org/10.1038/s41598-025-96013-7.

Anirudhan, A., Okomoda, V.T., Mimi Iryani, M.T., Andriani, Y., Abd Wahid, M.E., Tan, M.P., Danish-Daniel, M., Wong, L.L., Tengku-Muhammad, T.S., Mok, W.J., Sorgeloos, P., Sung, Y.Y., 2021. *Pandanus tectorius* fruit extract promotes Hsp70 accumulation, immune-related genes expression and *Vibrio parahaemolyticus* tolerance in the white-leg shrimp *Penaeus vannamei*. Fish Shellfish Immunol. 109, 97–105. https://doi.org/10.1016/j.fsi.2020.12.011.

Asok, K.K., Mazumdar, K., Dutta, N.K., Karak, P., Dastidar, S.G., Ray, R., 2004. Evaluation of synergism between the aminoglycoside antibiotic streptomycin and the cardiovascular agent amlodipine. Biol. Pharm. Bull. 27, 1116–1120. https://doi.org/10.1248/bpb.27.1116.

Bankevich, A., Nurk, S., Antipov, D., Gurevich, A.A., Dvorkin, M., Kulikov, A.S., Lesin, V. M., Nikolenko, S.I., Pham, S., Prjibelski, A.D., Pyshkin, A.V., Sirotkin, A.V., Vyahhi, N., Tesler, G., Alekseyev, M.A., Pevzner, P.A., 2012. SPAdes: a new genome assembly algorithm and its applications to single-cell sequencing. J. Comput. Biol. 19, 455–477. https://doi.org/10.1089/cmb.2012.0021.

Birhanu, B.T., Park, N.H., Lee, S.J., Hossain, M.A., Park, S.C., 2018. Inhibition of *Salmonella Typhimurium* adhesion, invasion, and intracellular survival via treatment

with methyl gallate alone and in combination with marbofloxacin. Vet. Res. 49, 101. https://doi.org/10.1186/s13567-018-0597-8.
Borges, A., Ferreira, C., Saavedra, M.J., Simões, M., 2013. Antibacterial activity and mode of action of ferulic and gallic acids against pathogenic bacteria. Microb. Drug Resist. 19, 256–265. https://doi.org/10.1089/mdr.2012.0244.
Bussabong, P., Rairat, T., Chuchird, N., Keetanon, A., Phansawat, P., Cherdkeattipol, K., Pichitkul, P., Kraitavin, W., 2021. Effects of isoquinoline alkaloids from *Macleaya cordata* on growth performance, survival, immune response, and resistance to *Vibrio parahaemolyticus* infection of Pacific white shrimp (*Litopenaeus vannamei*). PLoS One 16, e0251343. https://doi.org/10.1371/journal.pone.0251343.
Cervellione, F., McGurk, C., Berger Eriksen, T., Van den Broeck, W., 2017. Use of computer-assisted image analysis for semi-quantitative histology of the hepatopancreas in whiteleg shrimp *Penaeus vannamei* (Boone). J. Fish Dis. 40, 1223–1234. https://doi.org/10.1111/jfd.12599.
Chi, W., Zou, Y., Qiu, T., Shi, W., Tang, L., Xu, M., Wu, H., Luan, X., 2024. Horizontal gene transfer plays a crucial role in the development of antibiotic resistance in an antibiotic-free shrimp farming system. J. Hazard. Mater. 476, 135150. https://doi.org/10.1016/j.jhazmat.2024.135150.
Cota, D., Patil, D., 2023. Antibacterial potential of ellagic acid and gallic acid against IBD bacterial isolates and cytotoxicity against colorectal cancer. Nat. Prod. Res. 37, 1998–2002. https://doi.org/10.1080/14786419.2022.2111560.
Dang, L.T., Nguyen, H.T., Hoang, H.H., Lai, H.N.T., Nguyen, H.T., 2019. Efficacy of rose myrtle *Rhodomyrtus tomentosa* seed extract against acute hepatopancreatic necrosis disease in Pacific whiteleg shrimp *Penaeus vannamei*. J. Aquat. Anim. Health 31, 311–319. https://doi.org/10.1002/aah.10080.
Darouiche, R.O., Mansouri, M.D., Gawande, P.V., Madhyastha, S., 2009. Antimicrobial and antibiofilm efficacy of triclosan and DispersinB® combination. J. Antimicrob. Chemoth. 64, 88–93. https://doi.org/10.1093/jac/dkp158.
Dewi, N.R., Huang, H.T., Wu, Y.S., Liao, Z.H., Lin, Y.J., Lee, P.T., Nan, F.H., 2021. Guava (*Psidium guajava*) leaf extract enhances immunity, growth, and resistance against *Vibrio parahaemolyticus* in white shrimp *Penaeus vannamei*. Fish Shellfish Immun. 118, 1–10. https://doi.org/10.1016/j.fsi.2021.08.017.
Duan, Y., Zhao, L.J., Zhou, Y.H., Zhou, Q.Z., Fang, A.Q., Huang, Y.T., Ma, Y., Wang, Z., Lu, Y.T., Dai, Y.P., Li, S.X., Li, J., 2023. UPLC-Q-TOF-MS, network analysis, and molecular docking to investigate the effect and active ingredients of tea-seed oil against bacterial pathogens. Front. Pharmacol. 14, 1225515. https://doi.org/10.3389/fphar.2023.1225515.
Elshikh, M., Ahmed, S., Funston, S., Dunlop, P., McGaw, M., Marchant, R., Banat, I.M., 2016. Resazurin-based 96-well plate microdilution method for the determination of minimum inhibitory concentration of biosurfactants. Biotechnol. Lett 38, 1015–1019. https://doi.org/10.1007/s10529-016-2079-2.
Faleye, O.S., Sathiyamoorthi, E., Lee, J.H., Lee, J., 2021. Inhibitory effects of cinnamaldehyde derivatives on biofilm formation and virulence factors in *Vibrio* species. Pharmaceutics 13, 2176. https://doi.org/10.3390/pharmaceutics13122176.
Food and Agriculture Organization of the United Nations, 2022. The state of world fisheries and aquaculture. FAO, Rome.
Frías-Espericueta, M.G., Harfush-Melendez, M., Páez-Osuna, F., 2000. Effects of ammonia on mortality and feeding of postlarvae shrimp *Litopenaeus vannamei*. Bull. Environ. Contam. Toxicol. 65, 98–103. https://doi.org/10.1007/s0012800100.
Frias-Espericueta, M.G., Voltolina, D., Osuna-López, J.I., 2001. Acute toxicity of cadmium, mercury, and lead to whiteleg shrimp (*Litopenaeus vannamei*) postlarvae. Bull. Environ. Contam. Toxicol. 67, 580–586. https://doi.org/10.1007/s001280163.
Frías-Espericueta, M.G., Voltolina, D., Osuna-López, J.I., 2003. Acute toxicity of copper, zinc, iron, and manganese and of the mixtures copper-zinc and iron-manganese to whiteleg shrimp *Litopenaeus vannamei* postlarvae. Bull. Environ. Contam. Toxicol. 71, 68–74. https://doi.org/10.1007/s00128-003-0132-z.
Gao, Q., Ma, X., Wang, Z., Chen, H., Luo, Y., Wu, B., Qi, S., Lin, M., Tian, J., Qiao, Y., Grossart, H.P., Xu, W., Huang, L., 2022. Seasonal variation, virulence gene and antibiotic resistance of *Vibrio* in a semi-enclosed bay with mariculture (Dongshan Bay, Southern China). Mar. Pollut. Bull. 184, 114112. https://doi.org/10.1016/j.marpolbul.2022.114112.
Gobin, M., Proust, R., Lack, S., Duciel, L., Des Courtils, C., Pauthe, E., Gand, A., Seyer, D., 2022. A combination of the natural molecules gallic acid and carvacrol eradicates *P. aeruginosa* and *S. aureus* mature biofilms. Int. J. Mol. Sci. 23, 7118. https://doi.org/10.3390/ijms23137118.
González-Escalona, N., Martinez-Urtaza, J., Romero, J., Espejo, R.T., Jaykus, L.A., DePaola, A., 2008. Determination of molecular phylogenetics of *Vibrio parahaemolyticus* strains by multilocus sequence typing. J. Bacteriol. 190, 2831–2840. https://doi.org/10.1128/jb.01808-07.
Gunasekara, C.W.R., Rajapaksha, L., Wimalasena, S., 2023. Comparative analysis unravels genetic recombination events of *Vibrio parahaemolyticus recA* gene. Infect. Genet. Evol. 107, 105396. https://doi.org/10.1016/j.meegid.2022.105396.
Guo, Z., Wang, L., Zhou, J., Tong, Y., Zhang, J., Guan, M., Yu, M., Hu, T., Wei, Y., 2025. The effects of the sanhuanglianqiao mixture on *Vibrio parahaemolyticus* infection in *Penaeus vannamei*. Microb. Pathog. 206, 107735. https://doi.org/10.1016/j.micpath.2025.107735.
Hossain, A., Habibullah-Al-Mamun, M., Nagano, I., Masunaga, S., Kitazawa, D., Matsuda, H., 2022. Antibiotics, antibiotic-resistant bacteria, and resistance genes in aquaculture: risks, current concern, and future thinking. Environ. Sci. Pollut. Res. Int. 29, 11054–11075. https://doi.org/10.1007/s11356-021-17825-4.
Hu, Q., Chen, L., 2016. Virulence and antibiotic and heavy metal resistance of *Vibrio parahaemolyticus* isolated from crustaceans and shellfish in Shanghai China. J. Food Prot. 79, 1371–1377. https://doi.org/10.4315/0362-028x.Jfp-16-031.
Jantapaso, H., Mittraparp-Arthorn, P., 2022. Phytochemical composition and bioactivities of aqueous extract of rambutan (*Nephelium lappaceum* L. cv Rong Rian). Peel. Antioxidants 11, 956. https://doi.org/10.3390/antiox11050956.
Jia, T., Xu, T., Xia, J., Liu, S., Li, W., Xu, R., Zhang, K.J., Q.,, 2023. Clinical protective effects of polyhexamethylene biguanide hydrochloride (PHMB) against *Vibrio parahaemolyticus* causing translucent post-larvae disease (Vp_{TPD}) in *Penaeus vannamei*. J. Invertebr. Pathol. 201, 108002. https://doi.org/10.1016/j.jip.2023.108002.
Jiamboonsri, P., Pithayanukul, P., Bavovada, R., Chomnawang, M.T., 2011. The inhibitory potential of Thai mango seed kernel extract against methicillin-resistant *Staphylococcus aureus*. Molecules 16, 6255–6270. https://doi.org/10.3390/molecules16086255.
Jin, J., Zhou, Y., Zhang, Z., Wang, H., Hou, W., Wang, H., Li, R., Zhou, M., 2021. Characteristics of antimicrobial-resistant *Vibrio parahaemolyticus* strains and identification of related antimicrobial resistance gene mutations. Foodborne Pathog. Dis. 18, 873–879. https://doi.org/10.1089/fpd.2020.2911.
Kang, J., Liu, L., Liu, M., Wu, X., Li, J., 2018a. Antibacterial activity of gallic acid against *Shigella flexneri* and its effect on biofilm formation by repressing mdoH gene expression. Food Control 94, 147–154. https://doi.org/10.1016/j.foodcont.2018.07.011.
Kang, J., Li, Q., Liu, L., Jin, W., Wang, J., Sun, Y., 2018b. The specific effect of gallic acid on *Escherichia coli* biofilm formation by regulating pgaABCD genes expression. Appl. Microbiol. Biotechnol. 102, 1837–1846. https://doi.org/10.1007/s00253-017-8709-3.
Kaushik, M., Kumar, S., Kapoor, R.K., Gulati, P., 2019. Integrons and antibiotic resistance genes in water-borne pathogens: threat detection and risk assessment. J. Med. Microbiol. 68, 679–692. https://doi.org/10.1099/jmm.0.000972.
Keyvani-Ghamsari, S., Rahimi, M., Khorsandi, K., 2023. An update on the potential mechanism of gallic acid as an antibacterial and anticancer agent. Food Sci. Nutr. 11, 5856–5872. https://doi.org/10.1002/fsn3.3615.
Krumperman, P.H., 1983. Multiple antibiotic resistance indexing of *Escherichia coli* to identify high-risk sources of fecal contamination of foods. Appl. Environ. Microbiol. 46, 165–170. https://doi.org/10.1128/aem.46.1.165-170.1983.
Kumar, S., Stecher, G., Li, M., Knyaz, C., Tamura, K., 2018. MEGA X: Molecular evolutionary genetics analysis across computing platforms. Mol. Biol. Evol. 35, 1547–1549. https://doi.org/10.1093/molbev/msy096.
Lee, C.T., Chen, I.T., Yang, Y.T., Ko, T.P., Huang, Y.T., Huang, J.Y., Huang, M.F., Lin, S. J., Chen, C.Y., Lin, S.S., Lightner, D.V., Wang, H.C., Wang, A.H., Wang, H.C., Hor, L. I., Lo, C.F., 2015. The opportunistic marine pathogen *Vibrio parahaemolyticus* becomes virulent by acquiring a plasmid that expresses a deadly toxin. PNAS 112, 10798–10803. https://doi.org/10.1073/pnas.1503129112.
Li, P., Xin, W., Kang, L., Chen, Z., Guo, C., Gao, S., Yang, H., Ji, B., Yan, Y., Wang, H., Zhou, D., Yang, W., Wang, J., 2018. Genetic and population analyses of *Vibrio parahaemolyticus* isolates from three major coastal regions in China. Future Microbiol. 13, 1261–1269. https://doi.org/10.2217/fmb-2018-0060.
Liu, H., Chen, G., Li, L., Lin, Z., Tan, B., Dong, X., Yang, Q., Chi, S., Zhang, S., Zhou, X., 2022. Supplementing artemisinin positively influences growth, antioxidant capacity, immune response, gut health and disease resistance against *Vibrio parahaemolyticus* in *Litopenaeus vannamei* fed cottonseed protein concentrate meal diets. Fish Shellfish Immunol. 131, 105–118. https://doi.org/10.1016/j.fsi.2022.09.055.
Liu, M., Wu, X., Li, J., Liu, L., Zhang, R., Shao, D., Du, X., 2017. The specific anti-biofilm effect of gallic acid on *Staphylococcus aureus* by regulating the expression of the ica operon. Food Control 73, 613–618. https://doi.org/10.1016/j.foodcont.2016.09.015.
Liu, S., Wang, W., Jia, T., Xin, L., Xu, T.T., Wang, C., Xie, G., Luo, K., Li, J., Kong, J., Zhang, Q., 2023. *Vibrio parahaemolyticus* becomes lethal to post-larvae shrimp via acquiring novel virulence factors. Microbiol. Spectr. 11, e0049223. https://doi.org/10.1128/spectrum.00492-23.
Liu, Y., Wang, L., 2022. Antibiofilm effect and mechanism of protocatechuic aldehyde against *Vibrio parahaemolyticus*. Front. Microbiol. 13, 1060506. https://doi.org/10.3389/fmicb.2022.1060506.
Luo, Z., Lin, Z.Y., Li, Z.F., Fu, Z.Q., Han, F.L., Li, E.C., 2024. Developmental toxicity of the neonicotinoid pesticide clothianidin to the larvae of the crustacean decapoda *Penaeus Vannamei*. J. Hazard. Mater. 474, 134787. https://doi.org/10.1016/j.jhazmat.2024.134787.
Lv, X., Du, J., Jie, Y., Zhang, B., Bai, F., Zhao, H., Li, J., 2017. Purification and antibacterial mechanism of fish-borne bacteriocin and its application in shrimp (*Penaeus vannamei*) for inhibiting *Vibrio parahaemolyticus*. World J. Microbiol. Biotechnol. 33, 156. https://doi.org/10.1007/s11274-017-2320-8.
Kurdi Al-Dulaimi, M., 2019. Multiple antibiotic resistance (MAR), plasmid profiles, and DNA polymorphisms among *Vibrio vulnificus* isolates. Antibiotics 8, 68. https://doi.org/10.3390/antibiotics8020068.
Macêdo, N.S., Barbosa, C., Bezerra, A.H., Silveira, Z.S., da Silva, L., Coutinho, H.D.M., Dashti, S., Kim, B., da Cunha, F.A.B., da Silva, M.V., 2022. Evaluation of ellagic acid and gallic acid as efflux pump inhibitors in strains of *Staphylococcus aureus*. Biol. Open. 11, bio059434. https://doi.org/10.1242/bio.059434.
Madsari, N., Maskaew, S., Obchoei, S., Kwankaew, P., Senghoi, W., Utarabhand, P., Runsaeng, P., 2022. Determination of the efficacy of using a serine protease gene as a DNA vaccine to protect against *Vibrio parahaemolyticus* infection in *Litopenaeus vannamei*. Dev. Comp. Immunol. 135, 104459. https://doi.org/10.1016/j.dci.2022.104459.
Miller, J.J., Weimer, B.C., Timme, R., Lüdeke, C.H.M., Pettengill, J.B., Bandoy, D. D., Weis, A.M., Kaufman, J., Huang, B.C., Payne, J., Strain, E., Jones, J.L., 2021. Phylogenetic and biogeographic patterns of *Vibrio parahaemolyticus* strains from north America inferred from whole-genome sequence data. Appl. Environ. Microbiol. 87, e01403-20. doi:10.1128/aem.01403-20.
Moh, J.H.Z., Okomoda, V.T., Mohamad, N., Waiho, K., Noorbaiduri, S., Sung, Y.Y., Manan, H., Fazhan, H., Ma, H., Abualreesh, M.H., Ikhwanuddin, M., 2024. *Morinda citrifolia* fruit extract enhances the resistance of *Penaeus vannamei* to *Vibrio*

parahaemolyticus infection. Sci. Rep. 14, 5668. https://doi.org/10.1038/s41598-024-56173-4.
Morales-Covarrubias, M.S., García-Aguilar, N., Bolan-Mejía, M.D., Puello-Cruz, A.C., 2016. Evaluation of medicinal plants and colloidal silver efficiency against *Vibrio parahaemolyticus* infection in *Litopenaeus vannamei* cultured at low salinity. Dis. Aquat. Organ. 122, 57–65. https://doi.org/10.3354/dao03060.
Niu, Y., Defoirdt, T., Rekecki, A., De Schryver, P., Van den Broeck, W., Dong, S., Sorgeloos, P., Boon, N., Bossier, P., 2012. A method for the specific detection of resident bacteria in brine shrimp larvae. J. Microbiol. Methods 89, 33–37. https://doi.org/10.1016/j.mimet.2012.02.004.
Okeke, E.S., Chukwudozie, K.I., Nyaruaba, R., Ita, R.E., Oladipo, A., Ejeromedoghene, O., Atakpa, E.O., Agu, C.V., Okoye, C.O., 2022. Antibiotic resistance in aquaculture and aquatic organisms: a review of current nanotechnology applications for sustainable management. Environ. Sci. Pollut. Res. Int. 29, 69241–69274. https://doi.org/10.1007/s11356-022-22319-y.
Onohuean, H., Agwu, E., Nwodo, U.U., 2022. Systematic review and meta-analysis of environmental *Vibrio* species - antibiotic resistance. Heliyon 8, e08845. https://doi.org/10.1016/j.heliyon.2022.e08845.
Page, A.J., Cummins, C.A., Hunt, M., Wong, V.K., Reuter, S., Holden, M.T., Fookes, M., Falush, D., Keane, J.A., Parkhill, J., 2015. Roary: rapid large-scale prokaryote pan genome analysis. Bioinformatics 31, 3691–3693. https://doi.org/10.1093/bioinformatics/btv421.
Pattano, J., Jintasakul, V., Jantapaso, H., Mittraparp-Arthorn, P., 2025. Inhibition of quorum sensing, biofilm formation, and virulence-related characteristics in shrimp pathogenic *Vibrio campbellii* by rambutan (*Nephelium lappaceum* L. cv. Rong Rian) peel extract. Microb. Pathog. 205, 107702. https://doi.org/10.1016/j.micpath.2025.107702.
Phiwsaiya, K., Charoensapsri, W., Taengphu, S., Dong, H.T., Sangsuriya, P., Nguyen, G.T. T., Pham, H.Q., Amparyup, P., Sritunyalucksana, K., Taengchaiyaphum, S., Chaivisuthangkura, P., Longyant, S., Sithigorngul, P., Senapin, S., 2017. A natural *Vibrio parahaemolyticus* $\Delta pirA^{Vp}pirB^{Vp+}$ mutant kills shrimp but produces neither Pir^{Vp} toxins nor acute hepatopancreatic necrosis disease lesions. Appl. Environ. Microbiol. 83. https://doi.org/10.1128/aem.00680-17.
Phuong, N.N.M., Le, T.T., Van Camp, J., Raes, K., 2020. Evaluation of antimicrobial activity of rambutan (*Nephelium lappaceum* L.) peel extracts. Int. J. Food Microbiol. 321, 108539. https://doi.org/10.1016/j.ijfoodmicro.2020.108539.
Pinho, E., Ferreira, I.C., Barros, L., Carvalho, A.M., Soares, G., Henriques, M., 2014. Antibacterial potential of northeastern Portugal wild plant extracts and respective phenolic compounds. Biomed Res. Int. 2014, 814590. https://doi.org/10.1155/2014/814590.
Qiao, Y., Jia, R., Luo, Y., Feng, L., 2021. The inhibitory effect of *Ulva fasciata* on culturability, motility, and biofilm formation of *Vibrio parahaemolyticus* ATCC17802. Int. Microbiol. 24, 301–310. https://doi.org/10.1007/s10123-021-00165-1.
Rajamanickam, K., Yang, J., Sakharkar, M.K., 2018. Gallic acid potentiates the antimicrobial activity of tulathromycin against two key bovine respiratory disease (BRD) causing-pathogens. Front. Pharmacol. 9, 1486. https://doi.org/10.3389/fphar.2018.01486.
Sang, H., Jin, H., Song, P., Xu, W., Wang, F., 2024. Gallic acid exerts antibiofilm activity by inhibiting methicillin-resistant *Staphylococcus aureus* adhesion. Sci. Rep. 14, 17220. https://doi.org/10.1038/s41598-024-68279-w.
Seemann, T., 2014. Prokka: rapid prokaryotic genome annotation. Bioinformatics 30, 2068–2069. https://doi.org/10.1093/bioinformatics/btu153.
Sherif, M.M., Elkhatib, W.F., Khalaf, W.S., Elleboudy, N.S., Abdelaziz, N.A., 2021. Multidrug resistant *Acinetobacter baumannii* biofilms: evaluation of phenotypic-genotypic association and susceptibility to cinnamic and gallic acids. Front. Microbiol. 12, 716627. https://doi.org/10.3389/fmicb.2021.716627.
Shibata, H., Nakano, T., Parvez, M.A., Furukawa, Y., Tomoishi, A., Niimi, S., Arakaki, N., Higuti, T., 2009. Triple combinations of lower and longer alkyl gallates and oxacillin improve antibiotic synergy against methicillin-resistant *Staphylococcus aureus*. Antimicrob. Agents Ch. 53, 2218–2220. https://doi.org/10.1128/aac.00829-08.
Shinoda, S., Matsuoka, H., Tsuchie, T., Miyoshi, S., Yamamoto, S., Taniguchi, H., Mizuguchi, Y., 1991. Purification and characterization of a lecithin-dependent haemolysin from *Escherichia coli* transformed by a *Vibrio parahaemolyticus* gene. J. Gen. Microbiol. 137, 2705–2711. https://doi.org/10.1099/00221287-137-12-2705.
Singhapol, C., Tinrat, S., 2020. Virulence genes analysis of *Vibrio parahaemolyticus* and anti-vibrio activity of the citrus extracts. Curr. Microbiol. 77, 1390–1398. https://doi.org/10.1007/s00284-020-01941-4.
Sotomayor, M.A., Reyes, J.K., Restrepo, L., Domínguez-Borbor, C., Maldonado, M., Bayot, B., 2019. Efficacy assessment of commercially available natural products and antibiotics, commonly used for mitigation of pathogenic *Vibrio* outbreaks in Ecuadorian *Penaeus* (*Litopenaeus*) *vannamei* hatcheries. PLoS One 14 (1), e0210478. https://doi.org/10.1371/journal.pone.0210478.
Sowndarya, J., Rubini, D., Sinsinwar, S., Senthilkumar, M., Nithyanand, P., Vadivel, V., 2020. Gallic acid an agricultural byproduct modulates the biofilm matrix exopolysaccharides of the phytopathogen *Ralstonia solanacearum*. Curr. Microbiol. 77, 3339–3354. https://doi.org/10.1007/s00284-020-02141-w.
Stef, L., Pet, I., Popescu, C.A., Dumitrescu, G., Ciochina, L.P., Iancu, T., Cretescu, I., Corcionivoschi, N., Balta, I., 2025. The role of natural antimicrobials in reducing the virulence of *Vibrio parahaemolyticus* TPD in shrimp gut and hepatopancreas primary cells and in a post-larvae challenge trial. Int. J. Mol. Sci. 26. https://doi.org/10.3390/ijms26146557.
Teodoro, G.R., Gontijo, A.V.L., Salvador, M.J., Tanaka, M.H., Brighenti, F.L., Delbem, A. C.B., Delbem, Á., 2018. Effects of acetone fraction from *Buchenavia tomentosa* aqueous extract and gallic acid on *Candida albicans* biofilms and virulence factors. Front. Microbiol. 9, 647. https://doi.org/10.3389/fmicb.2018.00647.
Thi Truc Linh, N., Thi Hai Ha, P., Van Day, P., Thi Thuy Hai, L., Huyen Vu, S., Trong Nghia, N., Thanh Dung, T., Quoc Phu, T., Mong Huyen, H., Do-Hyung, K., Thanh Luan, N., 2024. Efficacy of *Annona glabra* extract against acute hepatopancreatic necrosis disease in white-leg shrimp (*Penaeus vannamei*). J. Invertebr. Pathol. 205, 108142. doi:10.1016/j.jip.2024.108142.
Thornber, K., Verner-Jeffreys, D., Hinchliffe, S., Rahman, M.M., Bass, D., Tyler, C.R., 2020. Evaluating antimicrobial resistance in the global shrimp industry. Rev. Aquac. 12, 966–986. https://doi.org/10.1111/raq.12367.
Tian, L., Fu, J., Wu, M., Liao, S., Jia, X., Wang, J., Yang, S., Liu, Z., Liu, Z., Xue, Z., Wang, Y., Li, H., Gong, G., 2022. Evaluation of gallic acid on membrane damage of *Yersinia enterocolitica* and its application as a food preservative in pork. Int. J. Food Microbiol. 374, 109720. https://doi.org/10.1016/j.ijfoodmicro.2022.109720.
Tinh, T.H., Nuidate, T., Vuddhakul, V., Rodkhum, C., 2016. Antibacterial activity of pyrogallol, a polyphenol compound against *Vibrio parahaemolyticus* isolated from the central region of Thailand. Procedia Chem. 18, 162–168. https://doi.org/10.1016/j.proche.2016.01.025.
Valencia-Castañeda, G., Frías-Espericueta, M.G., Vanegas-Pérez, R.C., Pérez-Ramírez, J. A., Chávez-Sánchez, M.C., Páez-Osuna, F., 2018. Acute toxicity of ammonia, nitrite and nitrate to shrimp *Litopenaeus vannamei* postlarvae in low-salinity water. Bull. Environ. Contam. Toxicol. 101, 229–234. https://doi.org/10.1007/s00128-018-2355-z.
Valentino-Álvarez, J.A., Núñez-Nogueira, G., Fernández-Bringas, L., 2013. Acute toxicity of arsenic under different temperatures and salinity conditions on the white shrimp *Litopenaeus vannamei*. Biol. Trace Elem. Res. 152, 350–357. https://doi.org/10.1007/s12011-013-9635-6.
Vargas Cárdenas, J., Chávez Pérez, J., Martínez Ordinola, N., Soto Rodríguez, I., Brito, L. O., Peixoto, S.R.M., Galvez, A.O., 2024. Phytochemical screening and antibacterial assessment of two macroalgae *Ulva papenfussi* and *Ulva nematoidea* (Chlorophyta) against the bacterium *Vibrio parahaemolyticus*. Food Sci. Technol. Int. 30, 352–360. https://doi.org/10.1177/10820132231165540.
Wang, D., Fletcher, G.C., Gagic, D., On, S.L.W., Palmer, J.S., Flint, S.H., 2023a. Comparative genome identification of accessory genes associated with strong biofilm formation in *Vibrio parahaemolyticus*. Food Res. Int. 166, 112605. https://doi.org/10.1016/j.foodres.2023.112605.
Wang, H., Zou, H., Wang, Y., Jin, J., Wang, H., Zhou, M., 2022. Inhibition effect of epigallocatechin gallate on the growth and biofilm formation of *Vibrio parahaemolyticus*. Lett. Appl. Microbiol. 75, 81–88. https://doi.org/10.1111/lam.13712.
Wang, K., Wu, K., Li, N., 2023b. Insect tea originated from ethnic minority regions in southwest China: a review on the types, traditional uses, nutrients, chemistry and pharmacological activities. J. Ethnopharmacol. 309, 116340. https://doi.org/10.1016/j.jep.2023.116340.
Wang, Q., de Oliveira, E.F., Alborzi, S., Bastarrachea, L.J., Tikekar, R.V., 2017. On mechanism behind UV-A light enhanced antibacterial activity of gallic acid and propyl gallate against *Escherichia coli* O157:H7. Sci. Rep. 7, 8325. https://doi.org/10.1038/s41598-017-08449-1.
Wick, R.R., Judd, L.M., Gorrie, C.L., Holt, K.E., 2017. Unicycler: resolving bacterial genome assemblies from short and long sequencing reads. PLoS Comput. Biol. 13, e1005595. https://doi.org/10.1371/journal.pcbi.1005595.
Yang, F., Xu, L., Huang, W., Li, F., 2022. Highly lethal *Vibrio parahaemolyticus* strains cause acute mortality in *Penaeus vannamei* post-larvae. Aquaculture 548, 737605. https://doi.org/10.1016/j.aquaculture.2021.737605.
Yang, F., You, Y., Lai, Q., Xu, L., Li, F., 2023. *Vibrio parahaemolyticus* becomes highly virulent by producing Tc toxins. Aquaculture 576, 739817. https://doi.org/10.1016/j.aquaculture.2023.739817.
Ye, M., Jiang, Y., Han, Q., Li, X., Meng, C., Ji, C., Ji, F., Zhou, B., 2025. Probiotic potential of *Enterococcus lactis* GL3 strain isolated from honeybee (*Apis mellifera* L.) larvae: Insights into its antimicrobial activity against *Paenibacillus larvae*. Vet. Sci. 12, 165. https://doi.org/10.3390/vetsci12020165.
Yu, P., Shan, H., Cheng, Y., Ma, J., Wang, K., Li, H., 2022. Translucent disease outbreak in *Penaeus vannamei* post-larva accompanies the imbalance of pond water and shrimp gut microbiota homeostasis. Aquacult. Rep. 27, 101410. https://doi.org/10.1016/j.aqrep.2022.101410.
Yu, Z., Hong, Y., Zhao, S., Zhou, M., Tan, X., 2024. Antibacterial effect of fermented pomegranate peel polyphenols on *Vibrio alginolyticus* and its mechanism. Biology (basel) 13. https://doi.org/10.3390/biology13110934.
Zhai, Q., Li, J., 2019. Effectiveness of traditional Chinese herbal medicine, San-Huang-San, in combination with enrofloxacin to treat AHPND-causing strain of *Vibrio parahaemolyticus* infection in *Litopenaeus vannamei*. Fish Shellfish Immunol. 87, 360–370. https://doi.org/10.1016/j.fsi.2019.01.008.
Zhang, H., Wei, J., Xv, H., Khan, I., Sun, Q., Zhao, X., Gao, J., Liu, S., Wei, S., 2024a. Bactericidal efficacy of plasma-activated water against *Vibrio parahaemolyticus* on *Litopenaeus vannamei*. Front. Nutr. 11, 1365282. https://doi.org/10.3389/fnut.2024.1365282.
Zhang, Y., Tan, P., Yang, M., 2024b. Characteristics of *vhvp-2* gene distribution and diversity within the *Vibrio* causing translucent post-larvae disease (TPD). J. Invertebr. Pathol. 207, 108228. https://doi.org/10.1016/j.jip.2024.108228.
Zhao, S., Ma, L., Wang, Y., Fu, G., Zhou, J., Li, X., Fang, W., 2018. Antimicrobial resistance and pulsed-field gel electrophoresis typing of *Vibrio parahaemolyticus* isolated from shrimp mariculture environment along the east coast of China. Mar. Pollut. Bull. 136, 164–170. https://doi.org/10.1016/j.marpolbul.2018.09.017.
Zou, Y., Xie, G., Jia, T., Xu, T., Wang, C., Wan, X., Li, Y., Luo, K., Bian, X., Wang, X., Kong, J., Zhang, Q., 2020. Determination of the infectious agent of translucent post-larva disease (TPD) in *Penaeus vannamei*. Pathogens 9. https://doi.org/10.3390/pathogens909074.

Journal of Microbiological Methods 243 (2026) 107439

Contents lists available at ScienceDirect

Journal of Microbiological Methods

journal homepage: www.elsevier.com/locate/jmicmeth

Development and validation of TaqMan-based real-time PCR assays for translucent post larvae disease (TPD) detection in *Penaeus vannamei*

Hung N. Mai, Nguyen Dinh-Hung, Arun K. Dhar *

Aquaculture Pathology Laboratory, School of Animal and Comparative Biomedical Sciences, The University of Arizona, 1117 E Lowell Street, Tucson, AZ 85721, USA

ARTICLE INFO

Keywords:
TPD
Vp_{TPD}
Post-larvae
TaqMan assay
Shrimp

ABSTRACT

Translucent Post larvae Disease (TPD), caused by *Vibrio parahaemolyticus*, has emerged as a critical disease impacting shrimp hatcheries across several Asian countries. This disease severely affects the early larval stages and can lead up to 100 % mortality. Thus, controlling TPD is essential to reduce losses in shrimp hatcheries. Although PCR-based assays have recently been reported for the detection of TPD-causing *V. parahaemolyticus* (Vp_{TPD}), these methods have not yet undergone comprehensive validation in accordance with the Aquatic Animal Health Code of the World Organization for Animal Health (WOAH). In this study, we developed TaqMan real-time PCR assays targeting three candidate virulence genes of Vp_{TPD} (i.e., *vhvp-1, −2,* and *− 3)* following the WOAH guidelines for diagnostic assay development. All three assays demonstrated 100 % diagnostic sensitivity (DSe) and specificity (DSp), with analytical sensitivity (i.e., limit of detection, LOD) of 10 copies per reaction. Experimental challenges were conducted using Vp_{TPD} and Specific Pathogen Free (SPF) *Penaeus vannamei* shrimp. We evaluated the performance of the newly developed assays in comparison to a published protocol. The results confirmed that the newly developed assays reliably detected Vp_{TPD} in infected *P. vannamei*. The availability of a validated real-time PCR assay for detecting Vp_{TPD} will provide a valuable diagnostic tool for screening *P. vannamei* stocks prior to domestic or international movement, thereby supporting biosecurity measures and helping to prevent the spread of disease beyond its current geographic boundary.

1. Introduction

Since 2020, shrimp hatcheries in several Asian countries, beginning with China, have faced a severe disease known as Translucent Postlarvae Disease (TPD). The disease can cause 100 % mortality in the larval stages of *Penaeus vannamei,* characterized by clinical signs of pale or colorless hepatopancreas and digestive tract (Zou et al., 2020). For these clinical signs, the disease is referred as glass post larvae disease (GPD) (Zou et al., 2020). Subsequent report indicate that TPD has also emerged in countries outside China (Dinh-Hung et al., 2025). Recently, *Vibrio parahaemolyticus* carrying the virulent proteins (i.e., VHVP-1, −2, and − 3) has been identified as the causative agent of TPD (Jia et al., 2024; Liu et al., 2023; Yang et al., 2023). These virulent factors have been found to be similar to Tc toxins, a class of insecticidal proteins produced by entomopathogenic bacterium *Photorhabdus luminescens*. Genomic characterization of Vp_{TPD} shows that the Tc toxin-encoding genes are located on a 187,791 bp plasmid, where the lengths of *vhvp-1, −2,* and *− 3* are 7635, 4266, and 1971 bp, respectively (Liu et al., 2023).

Polymerase chain reaction (PCR) has been widely recognized as a powerful diagnostic tool for both aquatic and terrestrial animals. Both conventional PCR and real-time PCR have been recommended as surveillance tools for all notifiable diseases listed by the World Organization for Animal Health (WOAH, formerly known as OIE) (WOAH, 2023). Additionally, real-time PCR is preferable for diagnostics due to its speed, sensitivity, and robustness compared to conventional PCR (WOAH, 2023). However, any PCR-based diagnostic assay must undergo rigorous development and validation in accordance with WOAH guidelines before it can be recommended for disease surveillance or diagnosis (WOAH, 2021). Although TPD is not currently listed as a notifiable disease by WOAH, its impact on the shrimp aquaculture industry highlights the urgent need for the availability of a reliable real-time PCR assay for its detection. Two PCR-based assays were recently published for the detection of TPD (Jia et al., 2024; Liu et al., 2023). Both papers performed part of the workflow of diagnostic assay development (*Stage 1: Analytical Characteristics*: Analytical Sensitivity, Analytical Specificity and Candidate test compared with Standard Test Method [Provisional Recognition, applicable when other comparable methods are available], and (b) *Stage 2: Diagnostic Characteristics*: Diagnostic Sensitivity,

* Corresponding author.
E-mail address: adhar@arizona.edu (A.K. Dhar).

https://doi.org/10.1016/j.mimet.2026.107439
Received 25 July 2025; Received in revised form 27 January 2026; Accepted 19 February 2026
Available online 26 February 2026

Diagnostic Specificity and Cut Off determination), as recommended by the WOAH, but not in its entirety (WOAH, 2021).

In this study, we developed three new TaqMan real-time PCR assays targeting three genes that encode virulence factors for TPD (i.e., *vhvp-1, vhvp-2*, and *vhvp-3*) in accordance with WOAH assay development guidelines. We compared their analytical sensitivity, specificity, and diagnostic accuracy with those of previously published methods. The findings from this study will provide a scientifically validated and reliable detection tool for the diagnosis of Vp_{TPD} in shrimp hatcheries.

2. Materials and methods

2.1. Experimental bioassay to generate a panel of TPD-infected samples

An experimental bioassay was conducted to generate a panel of clinical samples using a *Vibrio parahaemolyticus* isolate causing TPD (Vp_{TPD} AG1 strain), as described by Dinh-Hung et al. (2025). Specific pathogen-free (SPF) shrimp (*Penaeus vannamei)* postlarval stage 15 (PL15) were challenged via immersion with a bacterial inoculum at a concentration of 10^5 CFU/ml for 7 days. TPD infected tissues were collected, the bacteria were re-isolated, and hematoxylin and eosin (H&E) histopathological examination was performed to confirm infection prior to the samples for diagnostic assay development.

2.2. Primer design

The nucleotide sequence of the Vp_{TPD} plasmid (accession no. SRR23329176.4) was retrieved from the NCBI database. Primers and TaqMan probes targeting *vhvp-1, −2,* and *− 3* were designed using Primer Express v.3.0.1 (Thermofisher, USA) with default parameters (Table 1, Fig. 1).

2.3. Analytical specificity

DNA was extracted from Specific Pathogen Free (SPF) *P. vannamei* and *P. vannamei* experimentally infected with $Vp_{TPD,}$ *Enterocytozoon hepatopenaei* (EHP), *Hepatobacter penaei* (NHP), decapod penstylhamaparvovirus 1 (IHHNV), white spot syndrome virus (WSSV), and *V. parahaemolyticus* causing acute hepatopancreatic necrosis disease (Vp_{AHPND}) using DNeasy Blood and Tissue kit (QIAGEN, Germany) following the manufacturer's protocol. The extracted DNA was subjected to singleplex real-time PCR for specificity analysis using three newly developed primer/probe sets (i.e., V1–3) and one previously published set (VHVP) (Jia et al., 2024). DNA quality was evaluated by using A260/280 and A260/230 ratios. The PCR compatibility was evaluated using primers and probes targeting the *EF-1α* gene (Dhar et al., 2024). A total of 10 μl real-time PCR reaction included 2.5 μl of TaqMan Fast Virus 1-step Master Mix (Thermofisher, USA), 1 μl of Primers (0.5 μM each), 0.5 μl of Probe (0.2 μM), 5 μl of molecular biology water, and 1 μl of extracted DNA. The Master Mix is designed for fast, highly sensitive real-time PCR for both DNA and RNA pathogens, even in the presence of PCR inhibitors (https://www.thermofisher.com/order/catalog/product/4444434). The thermal profiles for amplification include 95 °C for 20 s, followed by 40 cycles of 95 °C for 3 s and 60 °C for 30 s. This PCR preparation and conditions were used throughout the study.

2.4. Analytical sensitivity

A 360 bp synthetic DNA fragment (gBlock; Integrated DNA Technologies, USA) containing the binding regions for all four primer/probe sets (V1–V3 and VHVP) was custom synthesized. The gBlock was serially diluted (from 100,000 to 1 copies/μl) using DNA (10 ng/ μl) isolated from SPF *P. vannamei* shrimp. The serially diluted gBlock DNA was used to determine the analytical sensitivity of the primer/probe sets. The assay was performed in triplicate and independently repeated three times over three separate days. Analytical sensitivity was assessed by calculating the limit of detection (LOD) ± standard deviation (SD) and coefficient of variation (CV) among replicates.

2.5. Determining diagnostic specificity and diagnostic sensitivity

The DNA from fifty-nine blind samples was extracted using the DNeasy Blood and Tissue kit (QIAGEN, Germany) following the manufacturer's protocol. The extracted DNA was subjected to the TaqMan real-time PCR for TPD detection using three newly designed and one previously published primers/probes (Table 1). The results were then used to determine the Diagnostic specificity (Dsp) and Diagnostic sensitivity (Dse) of each primer/probe set using Medcalc v23.1.7 (Medcalc software Ltd., Belgium) with a confidence interval of 95 %.

2.6. Statistical analysis

The statistical differences in Ct values obtained from the primer/probe sets in the sensitivity test were determined using one-way ANOVA and the Tukey test (GraphPad Prism v10.4.2, UK).

3. Results

3.1. Generating a panel of TPD-infected tissues samples for assay development

Experimental immersion challenges successfully generated TPD-

Table 1
The nucleotide sequence of the primers and probes used for the detection of *Vibrio parahaemolyticus* causing translucent post larval disease (TPD).

Primers/probes	Sets	Target	Sequence (5′-3′)	Tm (°C)	Amplicon size (bp)	Sources
VHVP-F*	VHVP	*vhvp-2*	ACACCCAATACTCCAAACGAC	58.2	119	Jia et al. (2024)
VHVP-R			AACTCCCGAAATCCGTCAAG	57.9		Jia et al. (2024)
VHVP-probe			6FAM-AGGCATGGACCGTAAAGCTCTCAC-TAMRA	64.7		
V1-qF	V1	*vhvp-1*	AATGTAGCCTCCATATCGGAAATC	58.5	91.0	This study
V1-qR			CGCTATCCACATTATCCAAACCA	58.9		
V1-probe			6FAM-CATCAATTGCTTGCACCTCACATCGC-TAMRA	65.6		
V2-qF	V2	*vhvp-2*	AATCGCCACTCACTCAGATTCA	59.8	76.0	This study
V2-qR			ACGCCCCGCTTTTTTGTT	58.8		
V2-probe			6FAM-CAGCTCAGCGTTATCCAGTCGCGA-TAMRA	67.0		
V3-qF	V3	*vhvp-3*	ACTACCGCCACCCTGATGAG	61.3	73	This study
V3-qR			GCGCCACGTGTATCGTACTG	61.5		
V3-probe			6FAM-CAAATACGACACAGACACGCATTACGCATC-TAMRA	66.7		
EF1-F		*EF-1α*	TCGCCGAACTGCTGACCAAGA	60.0	205	Dhar et al. (2024)
EF1-R			TCCTTGATCACACCCACAGC			
EF1-probe			6FAM-GGTTCCCAGCAAGCCTATGT-TAMRA			

* It is noteworthy that the primers and probe described in the paper by Jia et al. (2024) published in the journal Aquaculture are incorrect. Subsequently, these authors reported the correct sequence in a Corrigendum published in the same journal by Jia et al., 2025.

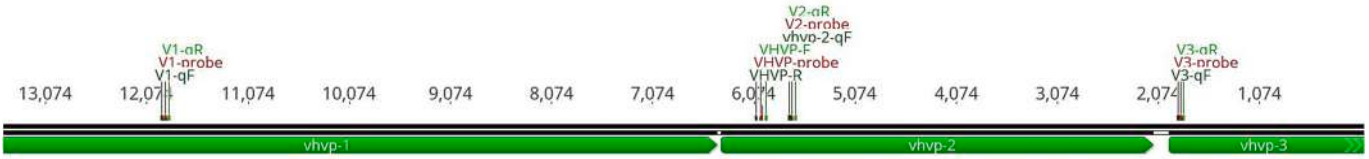

Fig. 1. The location of primers and probes in the plasmid DNA of *Vibrio parahaemolyticus,* the etiologic agent of translucent post larval disease (TPD) in shrimp.

infected tissues. Infected post-larvae exhibited clinical signs such as a pale or colorless hepatopancreas and an empty digestive tract, resulting in a transparent or translucent body, features consistent with naturally infected shrimp exhibiting TPD (Fig. 2A). In contrast, uninfected shrimp showed no gross or histopathological abnormalities in the abdominal region (Fig. 2A, B and D). Histopathological analysis confirmed hepatopancreatic degeneration, including tubular necrosis and epithelial cell sloughing (Fig. 2C and E), consistent with previously reported TPD pathology. Additionally, hemocytic enteritis, a hallmark lesion associated with infection by the Vp_{TPD} AG1 strain, was observed, characterized by intense inflammation and a thickened hemocyte layer in the intestine (boxed area in Fig. 2C), as described in the bacterial characterization study (Dinh-Hung et al., 2025). Moreover, green-pigmented bacterial colonies were re-isolated on TCBS agar, consistent with the typical morphology of *V. parahaemolyticus* (data not shown). The TPD-infected shrimp were taken for developing TaqMan assays targeting three virulence factor genes.

3.2. Determining analytical specificity

All newly developed and previously published primer/probe sets successfully detected Vp_{TPD}, while no amplifications were observed in non-target samples. Additionally, all samples with A260/280 > 1.8 and A260/230 > 1.6 yielded successful amplification signals with the *EF-1α* gene, confirming the quality of the DNA (Fig. 3).

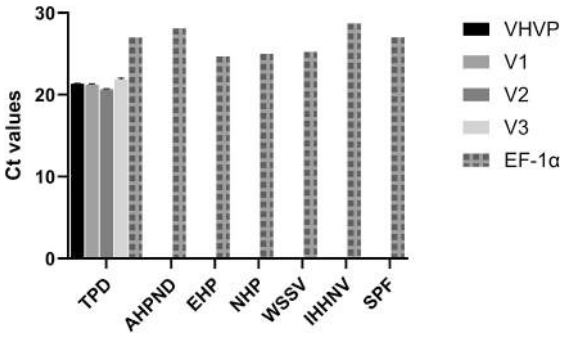

Fig. 3. Analytical specificity of VHVP, V1–3, and EF-1α sets of primers/probes against SPF *Penaeus vannamei*, *P. vannamei* shrimp infected with TPD, and shrimp infected with other pathogens. TPD = Translucent post larvae disease; SPF = Specific pathogen free; AHPND = Acute hepatopancreatic necrosis disease; EHP = *Enterocytozoon hepatopenaei*; NHP = Necrotizing hepatopancreatitis; WSSV = White spot syndrome virus; IHHNV = Decapod penstylhamaparvovirus 1.

3.3. Determining analytical sensitivity

The limit of detection (LOD) of all primers/ probe sets was 10 copies. The amplification profile of serially diluted template gBlock DNA

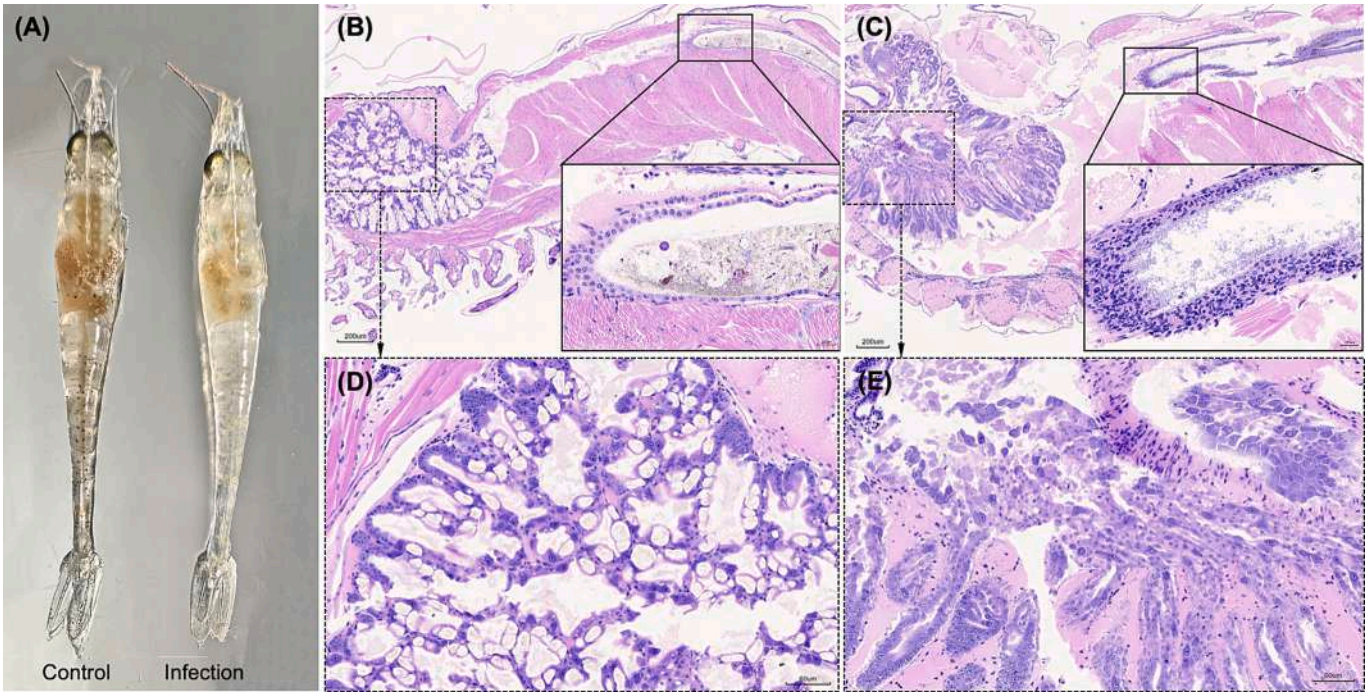

Fig. 2. Gross signs and histopathology of shrimp from bioassay-generated TPD-infected tissues. Infected post-larvae exhibited a pale hepatopancreas and an empty digestive tract, resulting in a translucent body, while uninfected shrimp displayed a darkened hepatopancreas and a well-defined intestine (A). Histologically, uninfected shrimp showed normal hepatopancreatic architecture with intact tubules and abundant lipid deposits (B, D), as well as a well-defined intestine containing digested food (boxed area in B). In contrast, infected shrimp exhibited hepatopancreatic degeneration, including tubular necrosis and epithelial cell sloughing (C, E), along with hemocytic enteritis characterized by intense inflammation and thickened hemocyte layers (boxed area in C), consistent with TPD pathology.

provided consistent linearity, with R-squared values (R^2) of 0.99. The amplification efficiency values (Eff%) ranged from 93.99 to 100.84 for VHVP, 86.81 to 102.41 for V1, 95.43 to 100.61 for V2, and 96.21 to 109.01 for V3 (Fig. 4).

The coefficient of variation (CV%) values of the intra- and inter-assay reproducibility of the VHVP primer/probe set ranged from 0.2 to 2.2 % and 0.2–0.5 %, respectively. For the newly developed primers/probes, intra- and inter-assay CV values ranged as follows: 0.1–1.2 % and 0.5–2.1 % for V1, 0.2–2.0 % and 0.2–0.5 % for V2, and 0.1–2.6 % and 0.4–1.9 % for V3 (Table 2). No statistically significant differences in Ct values were observed for any of the tested primer/probe sets ($p > 0.05$).

3.4. Determining diagnostic characteristics (specificity and sensitivity) of the assay

All tested primer/probe sets demonstrated 100 % diagnostic specificity (DSp) and 100 % diagnostic sensitivity (DSe) (Table 3, Table S1). The results show the assay described here fulfils fitness of assay for its intended purpose.

4. Discussion

The translucent post-larvae disease, also known as glass post larvae disease, has emerged as a new threat to the shrimp industry causing up to 100 % mortality in post larvae of *P. vannamei*. The disease was first officially reported in China in 2020 (Zou et al., 2020) and has recently been reported in a country outside China (Dinh-Hung et al., 2025). *Vibrio parahaemolyticus* has been widely recognized as a causative agent of TPD (Zou et al., 2020). Three genes, *vhvp-1, vhvp-2,* and *vhvp-3* encoding VHVP-1, −2, and − 3 proteins were presumptively identified as virulence factors for TPD (Liu et al., 2023; Yang et al., 2023). Proteomic and genomic analyses revealed that the putatively identified virulence factors are homologous to the Tc toxin complex of *Photorhabdus luminescens* (Liu et al., 2023; Yang et al., 2023).

It has been hypothesized that the presence of all three genes is necessary for pathogenicity of Vp_{TPD} in shrimp post larvae. Therefore, it is prudent that validated assays are developed targeting all three candidate genes to prevent further spread of this economically important and emerging disease in shrimp aquaculture.

In the present study, three newly developed primer/probe sets (i.e., V1, V2, and V3, see Table 1) targeting vhvp-1, −2, and − 3 gene, along with a previously published primer/probe set (VHVP, see Table 1) targeting *vhvp*-2, were tested in screening laboratory challenged Vp_{TPD}-infected *P. vannamei* shrimp. None of the assays showed cross-reactivity with shrimp infected with other pathogens or SPF shrimp, fulfilling a critical requirement for assay validation as outlined by the World Organization for Animal Health (WOAH, 2024, 2018). The newly developed methods also exhibited equivalent sensitivity to the published VHVP assay (Table 2). The new developed methods achieved R^2 values greater than 0.99, indicating high linearity and precision (Bivins et al., 2021) and the assay efficiency (Eff%) for each assay fell within the acceptable range (Nybo, 2011).(Nybo, 2011). Although the Ct values of dilution series of gBlock DNA for the *vhvp*-2 gene for the published method were slightly lower or comparable to the newly developed primer/probe, there were no significant differences between the two sets of primers/probes (See Table 2). This suggests that the newly developed methods are comparable to the published method with respect to the sensitivity.

According to WOAH guidelines, the repeatability of the assay refers to the coefficient of variation (CV) values derived from Ct values among replicates (intra-assay), and the reproducibility refers to the CV values derived from Ct values between assays (inter-assay). Generally, CV values less than 5 % are considered acceptable for intra- and inter-assays (Hays et al., 2022; Moody, 2018)(Hays et al., 2022; Moody, 2018). The newly developed assays showed CV values below this threshold (i.e., > 5 %), suggesting all three newly developed assays are precise and acceptable. The lowest intra-assay CV was for the gene *vhvp*-1 followed by *vhvp*-2 and *vhvp*-3.

The diagnostic accuracy, including diagnostic sensitivity (DSe) and specificity (DSp), is a key requirement for assay validation (WOAH, 2024)(WOAH, 2024). All three primer/probe sets described in this study achieved 100 % DSe and DSp, meeting or exceeding the performance benchmarks for the WOAH-listed pathogens, such as WSSV (Moody et al., 2022)(Moody et al., 2022), YHV (Moody, 2018)(Moody, 2018), and MrNV (Sahul Hameed et al., 2011)(Sahul Hameed et al., 2011).

In summary, three new TaqMan real-time PCR assays were

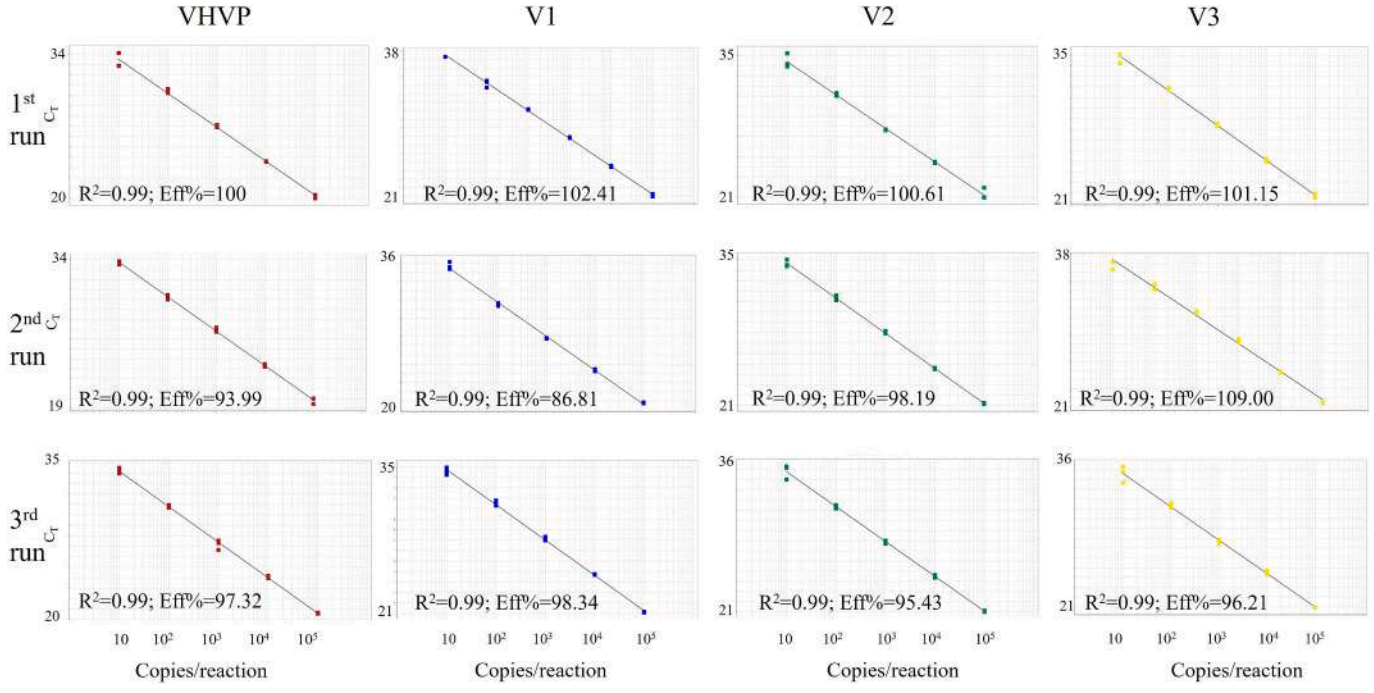

Fig. 4. Analytical sensitivity of VHVP, and V1–3 sets of primers/probes in detecting *Vibrio parahaemolyticus* causing translucent post larval disease (TPD) in shrimp.

Table 2
Analytical sensitivity comparison of primer/probe sets for Vp_{TPD} detection.

Copies/reaction	VHVP			V1			V2			V3		
	Ct Mean	SD	CV (%)	Ct Mean	SD	CV (%)	Ct Mean	SD	CV (%)	Ct Mean	SD	CV (%)
Intra-assay												
1	ND	NA	NA	ND	NA	NA	ND	NA	NA	ND	NA	NA
1	ND	NA	NA	ND	NA	NA	ND	NA	NA	ND	NA	NA
1	ND	NA	NA	ND	NA	NA	ND	NA	NA	ND	NA	NA
10	33.29	0.72	2.17	34.18	0.42	1.24	34.45	0.69	2.01	34.78	0.46	1.32
10	33.73	0.17	0.51	35.65	0.39	1.10	34.64	0.34	0.98	34.47	0.30	0.88
10	34.22	0.27	0.78	34.55	0.34	0.99	34.84	0.70	2.00	34.60	0.84	2.44
100	30.23	0.23	0.76	31.15	0.05	0.16	31.15	0.14	0.43	31.82	0.12	0.37
100	30.40	0.22	0.71	31.46	0.15	0.48	31.35	0.23	0.72	31.60	0.12	0.37
100	30.78	0.14	0.44	31.53	0.23	0.74	31.32	0.17	0.55	31.34	0.22	0.69
1000	27.06	0.12	0.45	27.85	0.06	0.21	27.66	0.05	0.16	28.43	0.11	0.38
1000	26.91	0.22	0.82	27.79	0.05	0.18	28.04	0.12	0.44	28.36	0.19	0.67
1000	27.18	0.46	1.70	28.09	0.19	0.67	27.89	0.16	0.58	27.64	0.20	0.72
10,000	23.58	0.03	0.11	24.50	0.10	0.39	24.41	0.07	0.28	25.04	0.12	0.47
10,000	23.33	0.14	0.58	24.34	0.12	0.48	24.56	0.06	0.24	24.93	0.07	0.30
10,000	24.10	0.12	0.48	24.73	0.03	0.12	24.50	0.13	0.53	24.56	0.20	0.81
100,000	20.19	0.15	0.76	21.06	0.16	0.75	21.29	0.55	2.60	21.69	0.19	0.87
100,000	19.81	0.30	1.54	20.78	0.06	0.29	21.20	0.06	0.29	21.47	0.03	0.15
100,000	20.63	0.05	0.22	21.14	0.03	0.14	21.06	0.06	0.27	20.91	0.02	0.09
Inter-assay												
1	ND	NA	NA	ND	NA	NA	ND	NA	NA	ND	NA	NA
10	33.73	0.45	1.34	34.77	0.74	2.12	34.63	0.15	0.44	34.63	0.15	0.44
100	30.47	0.31	1.00	31.40	0.17	0.55	31.27	0.06	0.18	31.57	0.25	0.80
1000	27.07	0.15	0.56	27.93	0.15	0.55	27.87	0.15	0.55	28.13	0.46	1.64
10,000	23.67	0.40	1.71	24.50	0.20	0.82	24.50	0.10	0.41	24.83	0.21	0.84
100,000	20.20	0.40	1.98	21.00	0.17	0.82	21.20	0.10	0.47	21.37	0.42	1.95

SD = Standard deviation; CV = Coefficient of variation, ND: Not detected; NA: Not applicable.

Table 3
The diagnostic accuracy of tested methods with 95 % confidence intervals (CI) (the numbers in parentheses).

	V1	V2	V3	VHVP
Diagnostic sensitivity (DSe %)	100 (90.3–100)	100 (90.3–100)	100 (90.3–100)	100 (90.3–100)
Diagnostic specificity (DSp %)	100 (85.2–100)	100 (85.2–100)	100 (85.2–100)	100 (85.2–100)

developed for the detection of Vp_{TPD} in shrimp. These new assays demonstrated equivalent specificity, sensitivity, precision and diagnostic accuracy. Additionally, the newly described assay targeting the Vp_{TPD} gene *vhvp-2* is comparable to a TaqMan assay targeting the same gene described by Jia et al. (2024). Considering a confirmatory test for any given disease diagnostics following a WOAH-recommended protocol requires screening a suspected sample by PCR targeting two different genomic regions of the same pathogen, the primer/probe set described here will satisfy the need. Collectively, the availability of validated assays for routine screening of *P. vannamei* stocks will be valuable in assuring disease free status of shrimp stocks for transboundary movement and thereby preventing the spread of TPD in shrimp aquaculture.

Author contribution

HM and AKD conceptualized the study. HM designed the primers/probes and conducted analytical specificity and sensitivity. DHN generated TPD-infected tissues via bioassay, interpreted the histopathology, and conducted diagnostic accuracy testing. HM analyzed the data and wrote the manuscript. HM, DHN, and AKD reviewed and edited the manuscript.

Data statement

All data were provided in this manuscript.

CRediT authorship contribution statement

Hung N. Mai: Writing – original draft, Methodology, Formal analysis, Data curation, Conceptualization. **Nguyen Dinh-Hung:** Writing – review & editing, Investigation, Formal analysis, Data curation, Conceptualization. **Arun K. Dhar:** Writing – review & editing, Supervision, Resources, Project administration, Conceptualization.

Declaration of competing interest

The authors declare the following financial interests/personal relationships which may be considered as potential competing interests:

Arun K. Dhar reports financial support was provided by The University of Arizona. Arun K. Dhar reports a relationship with The University of Arizona that includes: employment. If there are other authors, they declare that they have no known competing financial interests or personal relationships that could have appeared to influence the work reported in this paper.

Acknowledgment

The authors would like to thank Mr. Paul Schofield for conducting the TPD experimental bioassay and providing a blind panel of *Penaeus vannamei* tissue infected with TPD for the diagnostic accuracy test. The bacterial culture of *Vibrio parahaemolyticus* causing TPD was generously provided by Dr. Harris Wright, Shrimp Improvement System (Florida, USA). The authors would like express sincere thanks to Maiya Matthews (MJ) for isolating DNA from TPD-infected shrimp tissue used for the assay development.

Appendix A. Supplementary data

Supplementary data to this article can be found online at https://doi.org/10.1016/j.mimet.2026.107439.

Data availability

Data will be made available on request.

References

Bivins, A., Kaya, D., Bibby, K., Simpson, S.L., Bustin, S.A., Shanks, O.C., Ahmed, W., 2021. Variability in RT-qPCR assay parameters indicates unreliable SARS-CoV-2 RNA quantification for wastewater surveillance. Water Res. 203, 117516. https://doi.org/10.1016/J.WATRES.2021.117516.

Dhar, A.K., Cruz-Flores, R., Mai, H.N., Warg, J., 2024. Comparison of polymerase chain reaction (PCR) assay performance in detecting decapod penstylhamaparvovirus 1 in penaeid shrimp. J. Virol. Methods 323, 114840. https://doi.org/10.1016/J.JVIROMET.2023.114840.

Dinh-Hung, N., Mai, H.N., Matthews, M., Wright, H., Dhar, A.K., 2025. Isolation, characterization, and pathogenicity of a *Vibrio parahaemolyticus* strain causing translucent post-larvae disease in *Penaeus vannamei* outside China. PLoS One 20, e0331862. https://doi.org/10.1371/journal.pone.0331862.

Hays, A., Islam, R., Matys, K., Williams, D., 2022. Best practices in qPCR and dPCR validation in regulated bioanalytical laboratories. AAPS J. 24. https://doi.org/10.1208/s12248-022-00686-1.

Jia, T., Liu, S., Yu, X., Xu, T., Xia, J., Zhao, W., Wang, W., Kong, J., Zhang, Q., 2024. Prevalence investigation of translucent post-larvae disease (TPD) in China. Aquaculture 583, 740583. https://doi.org/10.1016/J.AQUACULTURE.2024.740583.

Liu, S., Wang, W., Jia, T., Xin, L., Xu, T., Wang, C., Xie, G., Luo, K., Li, J., Kong, J., Zhang, Q., Liu, S., Wang, W., Jia, T., Xin, L., Xu, T., Wang, C., Xie, G., Luo, K., Li, J., Kong, J., Zhang, Q., 2023. Vibrio parahaemolyticus becomes lethal to post-larvae shrimp via acquiring novel virulence factors. Microbiol. Spectr. 19, 10.1128 11.

Moody, N., 2018. Template for the Validation Report form for Tests Recommended in the WOAH Aquatic Manual Section 1. Guide for Applicants/Contributors to the Aquatic Manual 1.1. Information to Fill Out in this Form Section 2. General Information 2.1. Information About the Applicant.

Moody, N.J.G., Mohr, P.G., Williams, L.M., Cummins, D.M., Hoad, J., Slater, J., Valdeter, S.T., Colling, A., Singanallur, N.B., Gardner, I.A., Gudkovs, N., Crane, M.S. J., 2022. Performance characteristics of two real-time TaqMan polymerase chain reaction assays for the detection of WSSV in clinically diseased and apparently healthy prawns. Dis. Aquat. Org. 150, 169–182. https://doi.org/10.3354/DAO03687.

Nybo, K., 2011. qPCR efficiency calculations. Biotechniques 51, 401–402. https://doi.org/10.2144/000113776;WGROUP:STRING:PUBLICATION.

Sahul Hameed, A.S., Ravi, M., Farook, M.A., Taju, G., Hernandez-Herrera, R.I., Bonami, J.R., 2011. Screening the post-larvae of *Macrobrachium rosenbergii* for early detection of *Macrobrachium rosenbergii* nodavirus (MrNV) and extra small virus (XSV) by RT–PCR and immunological techniques. Aquaculture 317, 42–47. https://doi.org/10.1016/J.AQUACULTURE.2011.04.022.

WOAH, 2018. Development and optimisation of nucleic acid assays. In: Manual of Diagnostic Tests and Vaccines for Terrestrial Animals, pp. 1–11.

WOAH, 2021. Principles and methods of validation of diagnostic assays for infectious diseases. Chapter 1.1.2. In: OIE Manual of Diagnostic Tests for Aquatic Animals, pp. 1–26.

WOAH, 2023. Aquatic Code Online Access - WOAH - World Organisation for Animal Health. WOAH, Paris, France.

WOAH, 2024. Chapter 1.1.6-validation of diagnostic assays for infectious diseases of terrestrial animals. In: Manual of Diagnostic Tests and Vaccines for Terrestrial Animals, pp. 1–27.

Yang, F., You, Y., Lai, Q., Xu, L., Li, F., 2023. *Vibrio parahaemolyticus* becomes highly virulent by producing Tc toxins. Aquaculture 576, 739817. https://doi.org/10.1016/J.AQUACULTURE.2023.739817.

Zou, Y., Xie, G., Jia, T., Xu, T., Wang, C., Wan, X., Li, Y., Luo, K., Bian, X., Wang, X., Kong, J., Zhang, Q., 2020. Determination of the infectious agent of translucent post-larva disease (Tpd) in *penaeus vannamei*. Pathogens 9, 1–17. https://doi.org/10.3390/pathogens9090741.

Diseases of Crustaceans – **Translucent Post-larvae Disease (TPD)**

Figure 1. Clinical signs of *Penaeus vannamei* affected by translucent post-larvae disease (TPD) / translucent post-larvae vibriosis (TPV) / glass post-larvae disease (GPD). All the samples were at PL7 stage, and body length was about 0.6~0.9 cm. The diseased individuals (indicated by the white arrows) demonstrated syndromes of abnormal hepatopancreas and digestive tract necrosis. The hepatopancreas and digestive tract of the diseased post-larvae were pale and colorless. The bar scales are 10 mm and 2 mm in the figures and the magnified figures, respectively. Source: QL Zhang

General Signs of Disease

Important: affected animals may show one or more of the signs below, but the infection may be present in the absence of any signs, especially during the early phase of infection.

- The diseased shrimps show pale and colorless of hepatopancreas and digestive tract (Figure 1), as well as pale and shrunken body. The affected post-larvae sink to the bottom of rearing tanks because of the decreased swimming capability caused by the disease.
- The disease progresses very quickly, a few individuals initially show clinical signs on the first day, 60% mortality accrues on the second day, and more than 90% mortality may accrue on the third day.

Disease agent

The pathogen of TPD a *Vibrio* spp. causing TPD (V_{TPD}), which carries the *Vibrio* high virulent protein (VHVP)-1 and VHVP-2.

Translucent post-larvae disease

Host range

Crustaceans known to be susceptible to infection with V_{TPD} (RT-PCR and ISH positive) include *Penaeus vannamei, P. chinensis,* and *P. japonicus* (Zou *et al*., 2020; Liu, *et al*., 2023; Jia *et al*., 2024).

Geographical Distribution

TPD occurred in hatcheries in China (2020) and Vietnam (2023) (Zou *et al*., 2020; Vietnam Fisheries Magazine, 2023; Hong Tham, 2024).

Similar Diseases

- Acute hepatopancreatic necrosis disease (AHPND). **Note:** the virulence of V_{TPD} is about 1000 times higher than that of V_{AHPND} (Zou et al., 2020; Yang *et al*., 2021).

Epidemiology

- The disease mostly affects post-larvae at four to seven days old (PL2~PL7), and is highly infectious and lethal
- The morbidity of a diseased population can reach up to 60% in 24h after first observation of clinical signs, and even up to 90–100% in severe cases on the second to third day (Zou *et al*., 2020; Yang *et al*., 2021).
- Horizontal transmission was observed in the hatchery tanks and ponds (Jia *et al*., 2024).

Prevention and Control

- Due to the high lethality and transmission of TPD, it is strongly recommended to stop production, destroy affected stock and thoroughly disinfect all culture facilities as soon as the pathogen enters the culture system.
- When the disease becomes obvious, no chemical medicine or disinfectant has been found that is effective in stopping or slowing down the disease.
- PHMB is generally safe with low toxicity. Animal studies show an oral LD50 exceeding 5,000 mg/kg, classifying it as "practically non-toxic." It causes no skin or eye irritation at proper dilutions and has been approved for use in various medical applications including wound care, surgical disinfection, and even eye drops for treating *Acanthamoeba keratitis*. In aquaculture, PHMB effectively controls harmful bacteria like *Vibrio* species and prevents diseases in aquatic species. The environmental impact appears minimal when used at recommended concentrations.

Translucent post-larvae disease

Histopathology

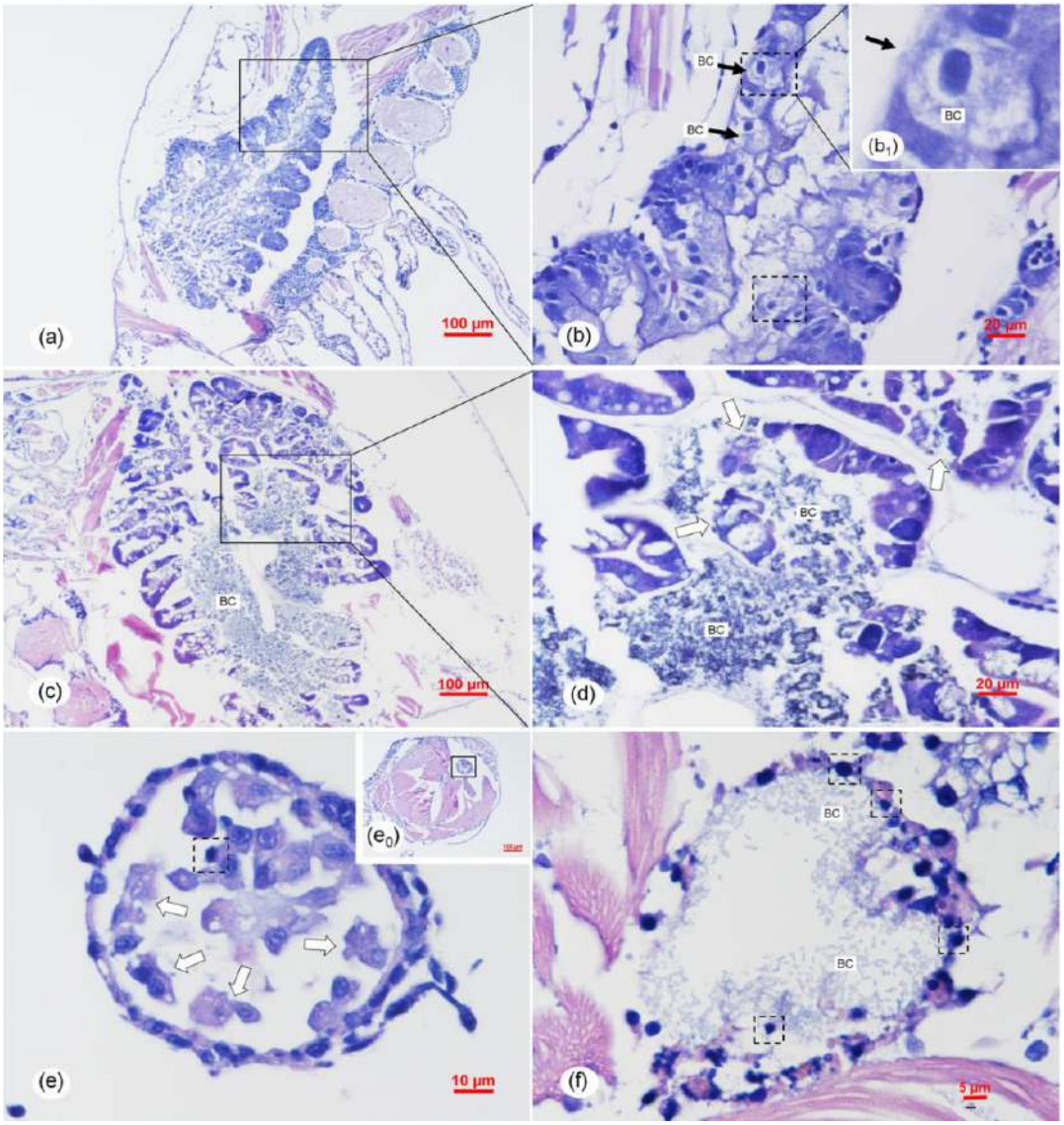

Figure 2. Histological sections of the naturally infected post-larvae in shrimp rearing tanks of post-larvae suffering from TPD. (a, b) Early phase with active destruction of the hepatopancreas. Note the mild necrosis of epithelial cells (ECs) of hepatopancreatic (HP) tubules, especially the ECs in the dotted boxes showing typical dark, smaller, and condensed nuclei. The bacterial colonization (BC) in the early phase of infection were indicted by the black arrows. The arrowed ECs (black arrow) were B-cells with the large vacuoles. (c, d) Acute phase with massive bacterial invasion. There was vast bacterial invasion of the hepatopancreatic tubules in half of the organs, where the bacterial masses and the tubules were destroyed. Note the detachment/sloughing of hepatopancreatic ECs (white arrows). (e, f) Midgut of an affected digestive tract of a naturally infected post-larvae showing necrosis (dotted box) and sloughing (white arrows) of ECs of the digestive tract. Note the mass BC in the tubule lumens of the digest tract at the midgut. (b), (b1), (d), and (e) are the magnified micrographs of the area in the black frames in (a), (b), (c), and (e0), respectively. (a), (b), and (e) show the pathological change in the early phase of infection. (c), (d), and (f) show the pathological change in the acute phase of infection. Scale bars = (a) 100 µm, (b) 20 µm, (c) 100 µm, (d) 20 µm, (e0) 100 µm, (e) 10 µm, and (f) 5 µm.. Source: QL Zhang

Translucent post-larvae disease

Molecular Diagnostics

PCR methods

Molecular diagnostic method was established based on the sequence of VHVP gene. The reported methods include:

- A comman PCR (PCR) (Jia, *et al*., 2024).

Taqman probe based qPCR methods

- Two different taqman probe based qPCR methods for *V*TPD were described in 2024 (Jia *et al*., 2024) and in 2025 (Zhang *et al*., 2025). The TaqMan qPCR targeted the double fragments on the sequence of VHVP gene reported by Zhang *et al*. in 2025 has better specificity and compatibility.

Table 1. Primers and Probe for the abovementioned methods

Methods	Primers/Probe	Sequences (5'-3')	Ta	Target region
TaqMan Qpcr [1]	vhvp_SpvB-F1 vhvp_SpvB-R1 vhvp_SpvB-P1	AGTCGTTTGGAGTATTGGGTG GCCATCAGAGGTGTAGATCAC 6-FAM-TCTTCGAGTGCTGCGACCACTTT-TAMRA	59°C	72 bp
	vhvp_TcdB-F2 vhvp_TcdB-R2 vhvp_TcdB-P2	GTAATCGTTTGGTTAGCACCG ACCAAACCCACGGAACTC VIC-CACGGCCATCCCAGACTCCAT-BHQ1	59°C	77 bp
PCR [2]	VHVP-1-P -F VHVP-1-P -R	GAGGAGAGTGTTGACCGAAATC CTGCGCCAGTAGTAACGATAAG	58°C	362 bp
	VHVP-2-P -F VHVP-2-P -R	GCTGGTCCGGACGGTGCC GTGATACATTAATACTTGTCTACAA	60°C	864 bp
	VHVP-3-P -F VHVP-3-P -R	CCCGTATCACAGAGCGATTT CTTTGGTGTCGGTCGTAGTT	58°C	306 bp
TaqMan qPCR [2]	VHVP-F VHVP-R VHVP-P	AACTCCCGAAATCCGTCAAG ACACCCAATACTCCAAACGAC AGGCATGGACCGTAAAGCTCTCAC	55.7°C	119 bp

[1] The TaqMan qPCR detection method targeted the double fragments on the sequence of VHVP gene (Zhang *et al*., 2025).

[2] The TaqMan qPCR detection method targeted the single virulence gene (Jia *et al*., 2024).

Translucent post-larvae disease

List of Experts:

Dr. Qingli Zhang
Maricultural Organism Diseases Control & Molecular Pathology Laboratory
Yellow Sea Fisheries Research Institute
Chinese Academy of Fishery Sciences
106 Nanjing Road
Qingdao, SD 266071
PR China
zhangql@ysfri.ac.cn

References

Hong Tham. Warning of new disease appearing on white leg shrimp. 2024. https://vietnamagriculture.nongnghiep.vn/warning-of-new-disease-appearing-on-white-leg-shrimp-d364369.html

Jia, T., Xu, T., Xia, J., Liu, S., Li, W., Xu, R.D, Kong J., Zhang, QL. (2023). Clinical protective effects of polyhexamethylene biguanide hydrochloride (PHMB) against *Vibrio parahaemolyticus* causing translucent post-larvae disease (Vp_{TPD}) in *Penaeus vannamei*. Journal of Invertebrate Pathology, 201, 108002.

Jia, T-C., Liu, S., Yu, X-T., Xu, T-T., Xia, J-T., Zhao, W-X., Wang, W., Kong., J., Zhang, Q-L. (2024). Prevalence investigation of translucent post-larvae disease (TPD) in China. Aquaculture, 583, 740583.

Vietnam Fisheries Magazine. Zeigler Vietnam meets with customers on management of transparent post-larvae disease. https://vietfishmagazine.com/news/zeigler-vietnam-meets-with-customers-on-management-of-transparent-postlarvae-disease.html

Wang, Y.G., Yu, Y.X, Liu, X., 2021. Pathogens and histopathological characteristics of shrimp postlarvae bacterial vitrified syndrome (BVS) in the *Litopenaeus vannamei*. Journal of Fisheries of. China 45 (09), 1563–1573.

Yang F, Xu LM, Huang WZ, Li F. Highly lethal *Vibrio parahaemolyticus* strains cause acute mortality in Penaeus vannamei post-larvae. Aquaculture. 2022; 548,737605.

Yang F, You Y, Lai Q, Xu L, Li F. *Vibrio parahaemolyticus* becomes highly virulent by producing Tc toxins. Aquaculture. 2023; 739817.

Zhang Q, Liu S, Yang B, Feng D, Wan X, Zhang X, Xu T, Yu X, Wang W, Xie G. Diagnostic Method for shrimp translucent post-larva disease (TPD). Aquaculture Industry Standard of the People's Republic of China, SC/T 7243-2025. Date of Publication: January 9, 2025.

Zou Y, Xie G, Jia T, Xu T, Wang C, Wan X, Li Y, Luo K, Bian X, Wang X, Kong J, Zhang Q. Determination of the infectious agent of translucent post-larva disease (TPD) in *Penaeus vannamei*. Pathogens. 2020 Sep 10;9(9):741. doi: 10.3390/pathogens9090741. PMID: 32927617; PMCID: PMC7558154.

National Referral Laboratory for Brackishwater Aquatic Animal Diseases
NABL Accredited Laboratory
Aquatic Animal Health and Environment Division
ICAR – Central Institute of Brackishwater Aquaculture
(ISO 9001:2015 certified)
75, Santhome High Road, MRC Nagar, Chennai 600 028, Tamil Nadu, India
www.ciba.res.in